Collagen Ultrastructure in Primary Teeth Affected with Osteogenesis Imperfecta and Dentinogenesis Imperfecta

Submitted in partial fulfilment of the requirements for the Degree of Clinical Doctorate in Dentistry (Paediatric Dentistry) Eastman Dental InstituteUniversity College London

Submited By:

Albatool M J Shinawi

Abstract

The main organic component in dentine is collagen type I, which provides mechanical support and strength. Any cross-linking or genetic mutations occurring during collagen formation can cause incorrect collagen fibril formation. Osteogenesis Imperfecta associated with Dentinogenesis Imperfecta (DI type I) and Dentinogenesis Imperfecta in teeth alone (DI type II) are genetic disorders which may affect the ultrastructure of dentinal collagen fibrils. Very little is known about the possible changes in collagen ultrastructure and impact on physical properties of dentine, particularly in primary teeth.

Aim: Identify the ultrastructure and investigate the mechanical properties of dentinal collagen;

1. Measurement of bulk dentine hardness.
2. Exposure of collagen by applying a demineralisation protocol.
3. Investigation of the differences in collagen ultrastructure between DI types I&II and control primary teeth.

Methods: Primary teeth were categorized in three groups with five teeth per group: Control, DI type I and DI type II. Samples were sectioned and the median hardness was measured by Wallace Indenter and calculated. Samples were prepared using a demineralisation with different agents and deproteinisation techniques in each group; 37% Phosphoric acid for 15 seconds, then 6.5% Sodium Hypochlorite for 5 seconds, and 17% EDTA for 30 minutes to expose collagen networks. Fourier Transform Spectroscopy (FTIR) was used to analyse demineralisation. Exposed collagen fibril ultrastructure was characterised by using Scanning electron microscopy (SEM) and Atomic force microscopy (AFM).

Results: Dentine hardness value significantly decreased in DI types I and II compared to the control group ($P \leq 0.0001$). FTIR showed phosphate peak reduction and amide I peak intensification after demineralisation in all groups with Phosphoric acid, indicating effective demineralisation. In control teeth, fibrils were exposed with uniform arrangement and collagen D-band periodicity was homogenous. In DI type I, collagen fibrils were identified but D-banding periodicity was not clearly visible. The collagen fibrils in DI type II were difficult to identify, due to smear layer formation subsequent to demineralisation. Demineralisation with EDTA was performed on both DI teeth groups to

expose collagen ultrastructure. Collagen fibrils were identified but D-banding periodicity was not clearly visible. Both DI types collagen fibrils demonstrated local swellings in multiple areas.

Conclusion: There was a significant difference in dentine hardness between control and DI primary teeth ($P \leq 0.0001$). On a microscopic level there were differences in collagen structure between the three groups.

Dedication

''All Praise is due to Allah''

This thesis is dedicated to my family for their love and support throughout my life. To my mother (Majda Abdulghafar), all that I am or hope to be I owe to you. And to my father (Mustafa J Shinawi), you have always been my lead and number one admirer. And Thank you both for the prayers and giving me the strength to reach for my goals, for understanding and encouragement to proceed in my path, and for teaching me to believe in God, myself, and in my dreams and I owe you everything. Many thanks to my lovely sisters specially (Thoraia Shinawi), you are my guiding light and my idol throughout this journey and you taught me how to be strong, insistence, and to force my self for the success. And finally, to my little brothers, you are the coolest brothers ever.

Acknowledgments

Three years has passed, I would like to spread my appreciation and sincere gratefulness for lots of people who assisted me through my entire research program both direct and indirectly, I wish for them a continuous success and achievements in the future.

Special thanks for the following people who were the most impact in my experimental work:

My supervisors: **Dr. Laurent Bozec**, primary supervisor, Biomaterials and Tissue Engineering Department, UCL. And **Dr. Susan Parekh,** secondary supervisor, Paediatric Department, EDI, UCL; for their assistance and motivation throughout this study, and mainly for their belief in me. I deem I learned from the greatest.

Dr. Paul Ashley and the rest of the Eastman's Paediatric Department members; for their continuous encouragement throughout this journey.

Dr. Nicola Mordan, Biomaterials and Tissue Engineering Department, UCL; for her help with my experimental work, feedback and inspiration.

Dr. Graham palmer, research technician, Biomaterials and Tissue Engineering Department, UCL; for his constant help and assistance with laboratory related procedures.

The Eastman's Anomalies Team, my colleagues, friends, and fellow researchers.

Adam Strange, You gave me your time, the most helpful gift of all. I extend my sincerest wishes for your future.

Non-stoppable thanks for my friends Shaikha **AlMarhubi, Shaima Sarkhouh,** we have been together from the beginning of this journey; helping, supporting, and being my London family. I am so lucky to have this bonded friendship. Special thanks to my colleagues; **Nikolaos Lygidakis and Elavarasi Kuppusamy. Suha AlQadi, Lama Dakkoury, Abdulfattah Alazma, May AlQahtani, Salwa Ibrahim, Dalal AlSubah, Zoi Tzelepi, Rawan Alkhuwaitem, Aspasia Katsimplali and Dimitra Saliakelli.** You were a maximum support throughout the time of my research and Paediatric dentistry program.

I also would like to acknowledge Ministry of Defence, Saudi Arabia for their sponsorship. My deepest gratitude goes to my colleagues at King Fahad Armed Forces hospital in Jeddah who always encourages and convinces me to pursue my career in Paediatric Dentistry. Last but not least to my beloved friends (Sara, Fatma, Farah, And Suzan) for their encouragement and truthful support to this achievement.

Declaration

I confirm that the work offered in this thesis is completely my own. The substances of this dissertation, to the greatest of my knowledge, has not been beforehand presented in part or in full for a degree of this or any other university or examination board. Information originated from the published and unpublished work of others has been accredited in the text and the related references were included.

List of Figures:

Figure 5-1: SEM images at two different magnifications of demineralised dentinal surface and exposed collagen, showing (A) pre demineralisation and (B) post demineralisation protocol of one control primary tooth sample.

Figure 5-2: Fourier transform infrared (FTIR) spectrum of control primary tooth at pre (red spectra) and post (black spectra) demineralisation.

Figure 5-3: Fourier transform infrared (FTIR) spectra of control primary tooth. Spectra shown in green is at 0 min, prior to acid etching, and light blue spectra is post demineralisation spectra after 15 s. the gradual reduction of phosphate peak is recorded in 5,8,10 toward 15 sec.

Figure 5-4: SEM images of dentinal surface of control tooth after demineralisation with phosphoric acid. (A) without deproteinisation. (B) with deproteinisation by using 6.5% NaOCl for 5 seconds

Figure 5-5: Fourier transform infrared (FTIR) spectra of control primary tooth. Spectra shown in black is at 0 min, prior to acid etching, and blue spectra is post demineralisation. Spectra after 15 s.

Figure 5-6: Fourier transform infrared (FTIR) spectra of DI type I primary tooth. (A)Spectra shown in purple is at 0 min, prior to acid etching, and black spectra is 5 seconds post demineralisation. (B) Spectra shown in blue is at 0 min, prior to acid etching, and red spectra after 15 seconds.

Figure 5-7: Scanning electron microscope (SEM) micro photographs of DI type I primary tooth dentine samples at different acid etching times by 37 % Phosphoric acid. (A) 15 secondes etching, (B) 5 seconds etching time.

Figure 5-8: Fourier transform infrared (FTIR) spectra of DI primary tooth after applying 17% of EDTA. Spectra shown in red is at 0 min, prior to demineralisation, and Green spectra is post demineralisation. (A) Spectra after 30 minutes on DI type I, (B) Spectra after 30 minutes on DI type II.

Figure 5-9: AFM images post demineralisation protocol in DI and Control healthy samples (2.6 um). (A) D-banding periodicity is distorted in DI when it is compared to the control sample (B).

Figure 6-10: Scanning Electron Microscopy (SEM) photo micrographs of demineralised DI sample showing collagen ultrastructure (A) DI type I at high magnifications of 12000x and 35000x, and (B) DI type II at magnification of 12000x and 25000x. The red circles indicates local swellings of collagen fibrils.

Figure 6-11: images at different magnifications of a control sample before demineralisation protocol is implemented.

Figure 6-12: Atomic Force Microscopy (AFM) images at various magnifications of a control samples after demineralisation, and verifying effectiveness of standardized protocol on healthy teeth.

Figure 6-13: AFM images showing collagen fibrils in different magnification DI I. (collagen firbils discontinuity and unusual morphology)

Figure 6-14: AFM images showing collagen fibrils in different magnification DI II. Collagen fibrils and the D-banding periodicity was not clear and spherical substances was on the sample surface as indicated by the circles.

Figure 6-15: Three graphs displaying the count of dentinal tubules number per 20 μm square area in control, DI type I and DI type II.

Figure 6-16: Kruskal Wallis Test Analysis of dentinal tubule number in control, DI type I, and DI type II samples

Figure 6-17 Three graphs presenting dentinal tubules diameter of control (n=1020), DI type I (n=217), and DI type II (n=107).

Figure 6-18: Kruskal Wallis Test Analysis of dentinal tubule diameter in control (Median = 3), DI type I (Median = 1), and DI type II (Median = 3) samples. Noting the similarity of the Medians of control and DI type II samples.

Figure 6-19: Three count graphs presenting collagen fibril diameter of control, DI type I, and DI type II.

Figure 6-20: Measuring the D- band width by taking line profile for each collagen fibril.

Figure 6-21: Comparison between collagen fibrils in control and both DI types in primary teeth.

Figure 6-17: Line profile for Collagen fibrils in bone and dentine (line profile in bone was 66.6 (A), and in dentine is 71.4 (B))

List of Tables:

List Of Abbreviations

α	Alpha
H	Hydrogen
s	Seconds
NH	Amide
C=O	Carbonyl
3D	Three dimensional
AD	Autosomal Dominant
AFM	Atomic force microcopy
ANOVA	Analysis of Variance
AR	Autosomal Recessive
ATR	Attenuated Total Reflection
BMP1	Bone morphogenetic protein 1
BSP	Bone sialoprotein
CRTAP	Cartilage associated protein
COL1A1	Collagen type 1, alpha 1
COL1A2	Collagen type 1, alpha 2
DD	Dentine Dysplasia
DEJ	Dento-enamel junction
DI	Dentinogenesis Imperfecta
DMP1	Dentine matrix protein 1
DPP	Dentine phosphoprotein

DSPP	Dentine sialophosphoprotein
DSP	Dentine sialoprotein
ECM	Extracellular matrix
ECF	Extracellular fluid
EDH	Eastman Dental Hospital
EDTA	Ethylenediaminetetraacetic acid
ER	Endoplasmic reticulum
FKBP10	FK506 binding protein 10, 65 kDa
GAG	Glycosaminoglycan
HA	Hydroxyapatite $Ca_5 (PO_4)_3 (OH)$
KHN	Knoop Hardness Number
LLD	Lower left primary first molar
LLE	Lower left primary second molar
LRD	Lower right primary first molar
LRE	Lower right primary second molar
MCT	Mercury cadmium telluride
mRNA	Messenger ribo-nucleic acid
NaOCl	Sodium hypochlorite
NHS	National Health Service
OI	Osteogenesis Imperfecta
OMIM	Online Mendelian Inheritance in Man
OPN	Osteopontin

PLOD2	Pocollagen-lysine, 2-oxoglutarate 5-dioxygenase 2
RER Rough	Endoplasmic Retuculum
RNA	Ribonucleic acid
SEM	Scanning electron microscopy
SERPINF1	Serpin peptidase inhibitor, clade F, member 1
SMPD3	Sphingomyelin phosphodiesterase 3 SP7 Sp7 transcription factor
SPM	Scanning Probe Microscopy
STD	Standard deviation
TEM	Transmission electron microscopy
ULD	Upper left primary first molar
ULE	Upper left primary second molar
URD	Upper right primary first molar
URE	Upper right primary second molar
UV	Ultraviolet
VHN	Vickers Hardness Number
vol	Volume

Chapter 1 Introduction

1.1 Collagen structure

1.1.1 Definition

Collagen provides mechanical support and strength to tissues and it is constructed as a complex hierarchical arrangement in the extracellular matrix and connective tissue. The human body contains 30% collagen and approximately 90% of the collagen is type I (Di Lullo et al. 2001).

1.1.2 Types of collagen

Numerous collagen types are present in human tissues:

- Fibril forming collagen
- Non-fibril forming collagen
- Fibril-associated collagens with interrupted triple helices (FACITs)
- Network-forming collagens
- Transmembrane collagens
- Endostatin-producing collagens
- Anchoring fibrils
- Beaded-filament-forming collagen

The two largest groups of collagens: are 1) fibril forming and 2) non-fibril forming. The first type includes collagen types I, II and III while the second type includes type IV, VIII and X collagen fibrils.

The morphology of collagen can be altered by the fibril configuration (Kadler, 2007). Collagen structure is composed of three polypeptide chains; one of α2, and two of α1 that build the triple helical structure (Rest and Garrone, 1991a). These polypeptide chains have a repeating system of amino acids; their arrangement is either in Glycine-Proline-X arrangement or Glycine-X-Hydroxyproline, where X indicates any other type of amino acid. The triple helix is made up of the three polypeptides chains that intertwine at the Glycine residue (Rest and Garrone, 1991b). Every Glycine chain has an Hydrogen

atom that attaches to Nitrogen by a peptide bond, that links to the nearby polypeptide by carboxy (C=O) to form the helical structure. The amino acids on each chain repeat at every third position so the chain condenses to form a helical structure. Changing the type of amino acid in the chain will prevent the formation of the triple helix (Kadler et al., 1996).

The majority of the fibril forming collagens consist of collagen type I, then type II and III. Bone, vertebrae, dentine, tendon ligaments and skin are predominantly comprised of collagen type I (Abou Neel et al. 2013). This research will focus on fibrillar collagen (predominantly type I), so will be the main focus of the rest of this thesis.

1.1.3 Collagen synthesis

For type I collagen to be synthesised, procollagen is made by fibroblast-lineage cells that has globular C- and N- propeptides, which form the terminals of the triple helix structure, and formulate the collagen monomer that transforms to collagen fibril by monomer assembly. The structure of type I collagen fibril is made up of polypeptide which form sequenced chains, as shown in figure 1-1.

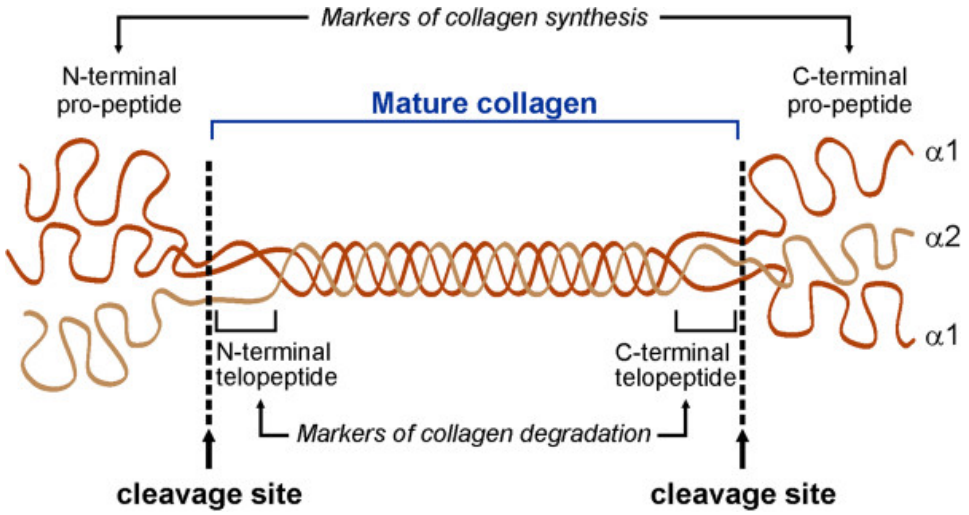

Figure 1-1: Collagen type I Synthesis and Structure of collagen molecule. Pro-collagen is contained of two alpha-1 chains and one alpha-2 chain tangled into a triple helix. Pro-peptide domains at the carboxy-terminals and amino-terminals are cleaved, causing in formation of mature collagen. Fan et al. Tissue Repair (2012)

Procollagen is formed by gathering the three alpha chains (Gelse 2003). Subsequently, procollagen is secreted into the extracellular matrix by a cleavage process and forms tropocollagen. which assemble by cross linkage to create a collagen fibril. The primary stabilisation of the 3D tropocollagen structure is by hydrogen bonding, whilst the covalent bond stabilises the collagen fibril and within the tropocollagen molecules (Figure 1-2).

The arrangement of these molecules in a quarter-staggered arrangement forms the overlapping region called “D-banding periodicity, (the distances between two adjacent D-bands is approximately 67nm) and each D-band represent five tropocollagen molecules (Hodge and Petruska, 1963), as shown in Figure 1-3. This D-period represents the overlap and gap zones (Chapman et al. 1990), where the light bands indicate an overlap area and the dark bands indicate gap areas. More collagen molecules are found in the overlap than the gap regions, as the molecules in the overlap area are strongly saturated, and create a crystalline structure (Wess et al., 1998). Collagen fibrils resemble a cord like structure, and this topological feature is caused by repetition of a coil of the molecules of the collagen and the filament interactions (Bozec et al., 2005).

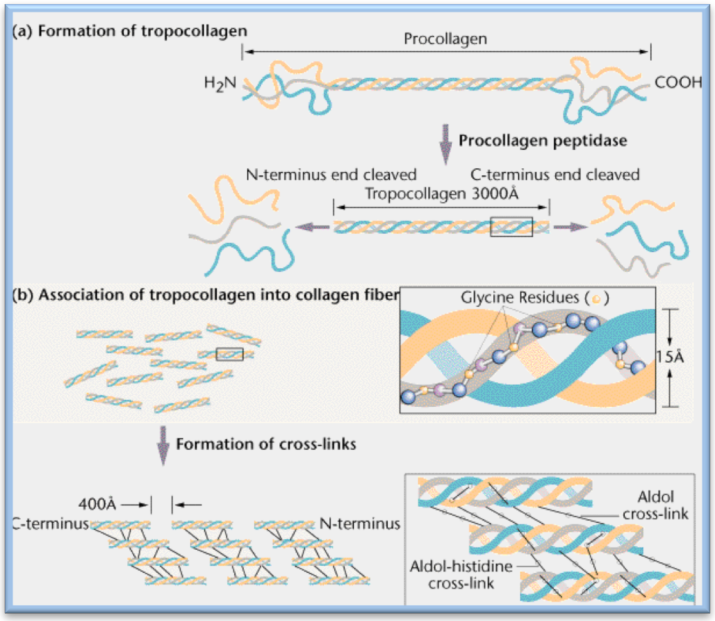

Figure 1-2: Tropocollagen formation and assembly by covalent bond to form collagen fibre (Adapted from Griffiths et al 2000)

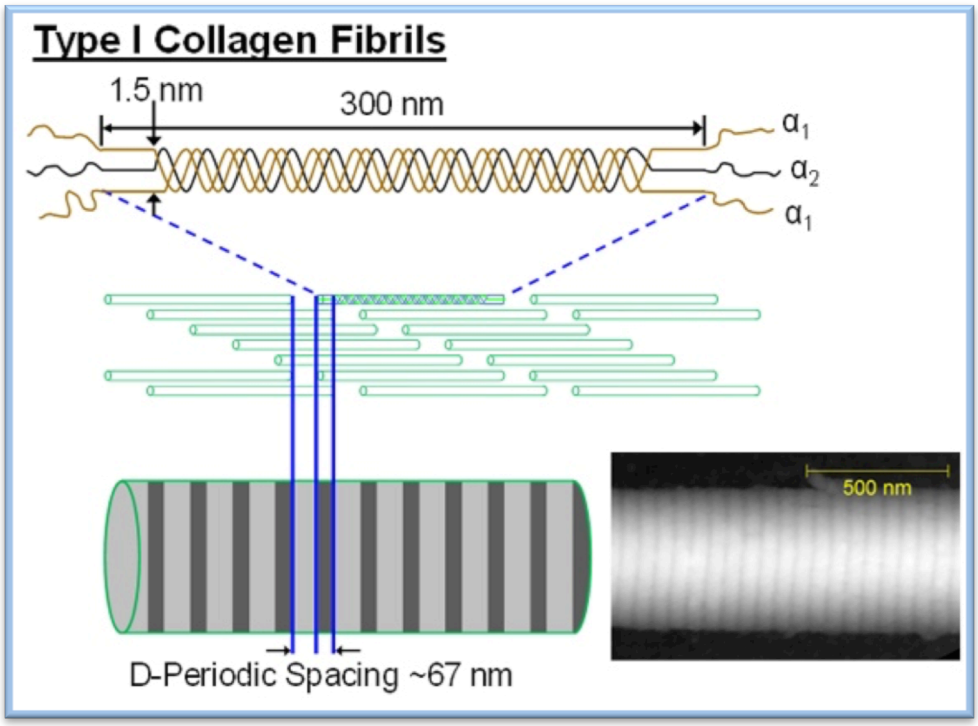

Figure 1-3: Nanoscale of type I collagen fibril in bone tissue showing the alternative gap and overlap zones in D-periodic spacing which is approximately equal to 67 nm. Copyright © 2012 Bone Biology And Mechanics Lab (bbml)

1.1.4 Function of collagen:

Bone, vertebrae, dentine, tendon ligaments and skin are predominantly comprised of collagen type I and non-collagenous proteins (Abou Neel et al. 2013). Collagen provides numerous functional roles in the body. The main function of collagen is mechanical, such as; scaffolding, restoring and morphogenesis (Abou Neel et al. 2013). Force transmission between the bone and the adjacent tissues is one of the collagen functions that is associated with the collagen in tendons and ligaments, as well as joining between muscles and bone to support the movement of the body skeleton.

In mineralised tissues as bone and dentine, collagen is joined with hard substances such as hydroxyapatite. Collagen in these mineralised tissues provides an amount of flexibility, and helps these tissues with resistance to fracture. On the other hand, collagen in skin, blood vessels, cartilage and muscles provides a degree of flexibility. The corneal tissues also contain collagen, but the arrangement of the collagen networks are well aligned in order to enhance the optical characteristic of the tissue and deliver its mechanical stability (Abou Neel et al. 2013).

This research will focus on fibrillar collagen (predominantly type I), as this is the type of collagen found in dentine. There is limited research regarding collagen in primary teeth and in Dentinogenisis imperfecta (DI) teeth. Thus, the main concentration in this research is on dentine in primary teeth in healthy and DI teeth. The composition and collagen configuration of dentine is described in the next section.

1.2 Dentine

The structure of any given human tooth consists of an anatomic crown and one or more roots (Figure 1-4). The internal tooth structure is composed of a pulp chamber surrounded by a relatively tough material known as dentin and an external layer of a very hard material known as enamel (Aiello and Dean, 2002)

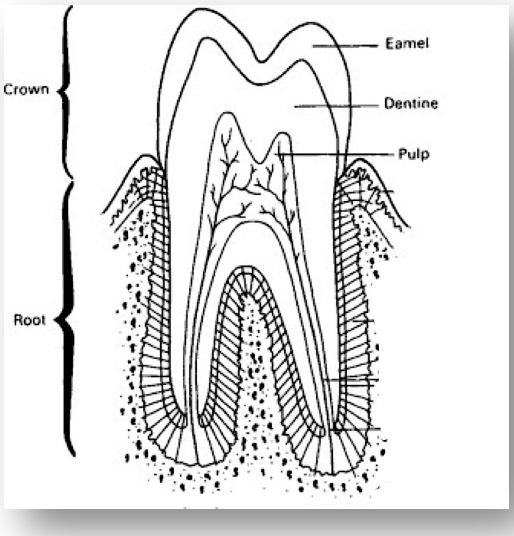

Figure 1-4: Vertical section of tooth, showing the internal structures.
(Courtesy of Aiello and Dean, 2002)

1.2.1 Dentinogenesis

Odonotoblasts originate from the mesenchymal cells of the dental papilla, and are important in dentine formation. They produce a complex arrangement of unmineralised predentine in a process that arises after enamel formation. Dentinogenesis is the process of conversion of the unmineralised predentine into mineralised dentine (Hart & Hart, 2007). The structure of dentine is 20% organic component, 70% inorganic and 10% water. The inorganic component is composed of hydroxyapatite mineral matrix (HA). Of the organic phase, 90% is collagen type I, with dentine phosphoprotein (DPP) the main of the non-collagenous part of the organic matrix, which is about 50%.

Odontoblasts play an important role in dentine formation by secreting type I collagen into the predentine layer, during the bell stage of tooth formation. Odontoblasts secrete the

organic matrix by migration and elongation of the cells towards the centre of the dental papilla, leaving cytoplasmic extensions, known as the odontoblast process. Odontoblasts then increase in their size, migrate and the matrix becomes dominated by parallel oriented type I collagen towards the dentino-enamel junction that forms mineralised dentine that is known as “Primary Dentine” (Barron et al., 2008). The smaller extracellular space results in more tightly packed collagen fibrils that are then mineralized. Secondary dentine forms after completion of root formation. In case of tertiary dentine, it is created when any external stimuli such as caries or trauma disturb the tooth.

1.2.2 Dentine structure

Type I collagen is the major component that found in the organic matrix and type III and V are present in minor amounts, with the remaining 10% of organic matrix is consisting of non-collagenous protein. In addition, the most abundant protein found is dentine sialophosphoprotein (DSPP) that is made of dentine phosphoprotein (DPP) and dentine sialoprotein (DSP).

These non-collagenous proteins are formed by odontoblasts and are important in dentinal mineral deposition regulation (Nanci, 2008). The DSPP molecule has a C-terminal proteolytic cleavage product that is for DPP while the N-terminal proteolytic cleavage product is DSP (MacDougall et al., 1997). Due to the capability of DPP to bind with huge amount of calcium, it has been proposed that DPP plays an important role in the mineralisation of dentine (Milan et al., 2006). Nevertheless, the function of DSP is still not fully understood. It has been suggested that DSP can stimulate the growth of hydroxyapatite as part of a reaction of matrix mineralisation crystals, since they are more dominant in some of dentinal parts (A. Boskey et al., 2000).

One of the non-collagenous proteins found in predentine is Proteoglycan. The main core of it consists of polypeptides that attach to one or multiple glycosaminoglycan (GAG) chains. The main function of proteoglycan is to maintain and stabilize the fibrils of collagen.

1.2.3 Dentine composition

Dentine is composed of three types (as shown in figure 1-5):

1) Primary dentine
2) Secondary dentine
3) Tertiary dentine.

The first type is primary dentine, which forms the majority of the dentine structure. Primary dentine develops during teeth formation, with mantle dentine as the first layer that forms, and is located at the dentine-enamel junction (DEJ). Dentine in this area is less mineralised and contains collagen and non-collagenous proteins.

The formation of secondary dentine starts when the teeth begins to erupt and during formation of the roots. This formation is carried out by the same odontoblasts that formed primary dentine, and they continue in dentine deposition but in slower pace. Secondary dentine formation occurs due to normal physiological factors or different stimulus (Avery, 2002). Histologically, primary dentine can be distinguished from secondary dentine by a demarcation line. This is due to irregularity of the dentinal tubules and the uneven deposition of organic matrix. These changes in dentinal deposition can be observed at the edge of the pulp chamber (Nanci, 2008).

The third type of dentine is tertiary dentine that is known as “reparative” dentine, which is formed as consequence of pathological stimuli, such as caries, attrition or dental treatments. The deposition of dentine only at specific positions by damaged odontoblasts or undifferentiated cells recruited from pulp cells that differentiate to become odonotoblasts as a reaction to injury. The dentine deposition rate depends on the degree of injury. In severe injury, rapid deposition of dentine occurred, and cells become trapped in the newly formed matrix affecting the tubular pattern, resulting in irregular or absent tubules arrangement in tertiary dentine (Mjör, 2009).

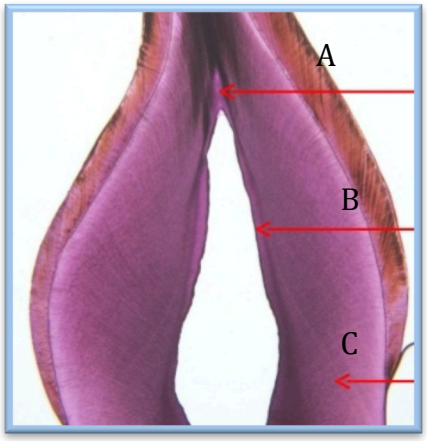

Figure 1-5: Histology of dentine under light microscope, showing types of dentine in longitudinal section of the tooth; A) Tertiary dentine, B) secondary dentine and C) Primary dentine. (M. Islam, 2010)

1.2.4 Histology of dentine

Numerous structures of dentine can be recognized under microscope: dentinal tubules, peritubular and intertubular dentine, interglobular dentine, incremental growth lines and the granular layer of Tomes. The dentinal tubules are formed by odontoblasts processes that run across in canaliculations in the dentine layer from DEJ to the pulp. Dentine tubules are cylindrical and each tubule diameter alters depending on the age of the person. They are approximately 2.5μm in diameter closer to pulp, 1.2μm in the middle of the dentine and 900nm next to DEJ (Nanci, 2008). The number of dentine tubules increases towards the pulp, with approximately 20,000 tubules per mm^2 at the DEJ and around 50,000 per mm^2 in the pulp (Marshall et al., 1997b). Each dentinal tubule is enervated by nerve fibres involved with the odontoblastic process and extracellular fluid (ECF). These microtubular components play a role in providing tooth sensation (Tidmarsh, 1981). The configuration of dentinal tubules can be observed in two curvatures. S shaped curvature that is called primary curvature from outer surface of dentine to dentine around the pulp in the coronal section of the tooth (Avery, 2002) whereas the secondary curvature is wrinkly in texture. This curvature is formed by odontoblasts throughout dentine formation. Figure (1-6)

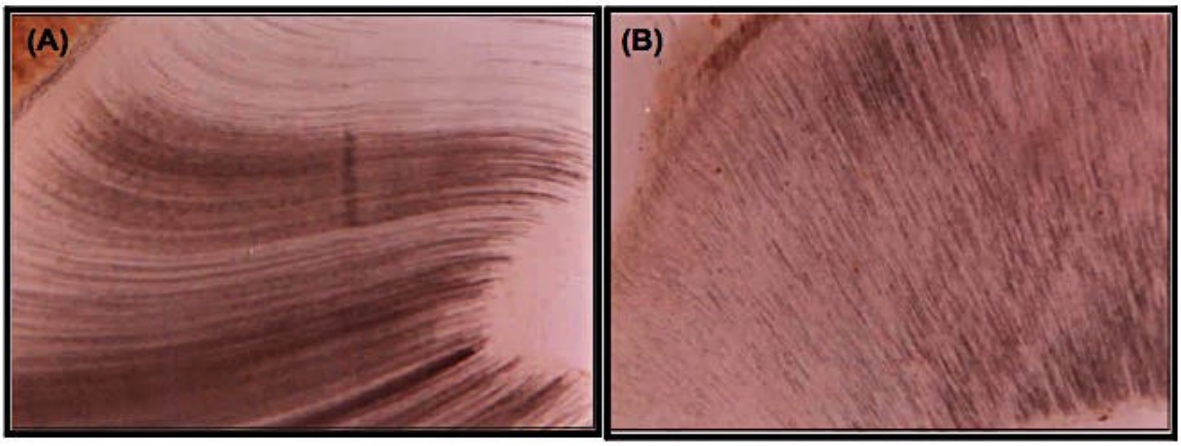

Figure 1-6 Dentinal surface observed under polarized light microscope. (A) the characteristic S – shape curvature of dentinal tubules mode of arrangement in Permanent dentine. (B) dentinal tubules in Primary dentine keep on a straighter path. (Chowdhary & Subba Reddy 2010)

The dentine tubules have a branching scheme depending on the location. The major branches are found more in the root part where they are more numerous than those in the coronal dentine (Nanci, 2008). Each dentinal tubule is engaged by nerve fibers involved with the odontoblastic process and extracellular fluid (ECF). These microtubular components play a role in providing tooth sensation and nutrition (Tidmarsh, 1981).

Peritubular dentine, or intratubular dentine, is the dentine surrounding the dentine tubules. The size of this area is about 1 to 2μm and the quantity volume differs in regard to the location from 3 vol% at DEJ to 60 vol% near to pulp (Gotliv et al., 2006). The composition of peritubular dentine is made of hydroxyapatite about 60 vol% combined with small portion of collagen fiber (GW Marshall et al., 1997). Peritubular dentine has less water and organic substances compared to intertubular dentine. It is suggested that peritubular dentine is formed by non-collagenous and glutamic acid-rich proteins that are a significant inducer for the mineralisation process by encouraging nucleation of the apatite which results in high amount of mineralisation of peritubular dentine (Linde, 1989). In the early phase of dentinogenesis, odontoblasts play an important part in the non-collagenous protein foundation near the end of crown formation, which produces less arranged peritubular dentine in the root area (Weiner et al., 1999).

Inter tubular dentine is found between dentine tubules. The main component is an interlaced network of collagen type I, with the collagen fibrils perpendicular to the dentinal tubules (Kramer, 1951). Intertubular dentine contains about 45 vol% Hydroxyapatite (Marshall et al., 1997), amorphous ground substance containing of non-collagenous proteins and some plasma proteins (Nanci, 2008).

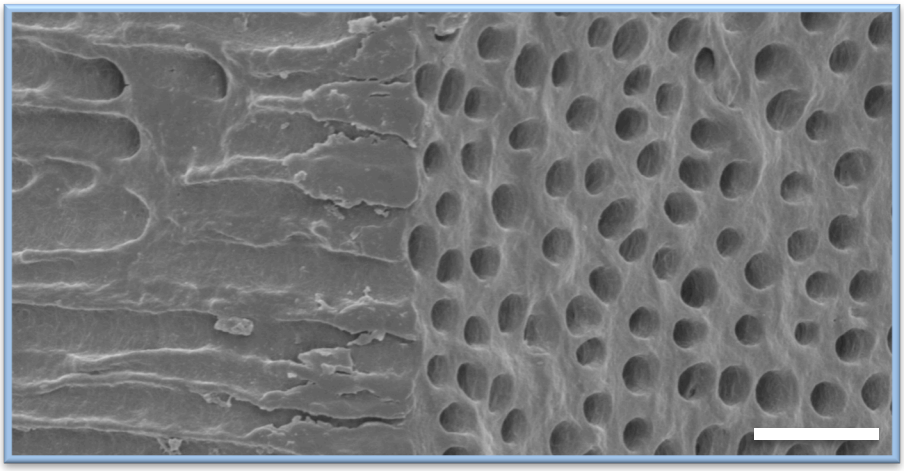

Figure 1- 7: Scanning electron microscope (SEM) images dentine, showing the dentinal tubules in cross section (A) and longitudinal section (B) in primary tooth, scale bar 10 µm. (Courtsy of Ibrahim, 2015)

1.2.5 Physical properties of dentine:

The hardest tissue in the tooth is enamel, followed by dentine, which is harder than cementum. Dentinal tubules make the dentine even harder than bone, because of their arrangement and the composition of the organic matrix in dentine. The dentinal tubule architecture also provides greater tensile and compressive strengths (Marshall, 1993). It is believed that the hardness of dentine is not affected with age (Dalitz, 1962). However, it has been found that the permeability is strongly affected by age, when compared with dentine in young teeth (Tagami et al, 1993). The dentine hardness varies, depending on the location; it is believed that the hardness of deep dentine is reduced compared to superficial dentine. The arrangement of minerals and distribution between the mesh of the collagen in intertubular dentine has a significant role in increasing dentine hardness (Kinney et al, 1999). However, other studies found that the hardness of inner dentine

near to the pulp is constant up to the dentine surface close to DEJ in permanent teeth (Fuentes et al., 2003) and as well as the primary teeth (Mahoney et al., 2006).

Calcium and phosphate levels in dentine play an important role on the hardness. The higher the mineral levels of intertubular and peritubular dentine, the higher the hardness (Hirayanma, 1990). Therefore, the hardness of dentine in permanent teeth is greater than primary teeth (Hosoya et al., 2006; Hosoya et al., 2005). Various studies have proposed that the alterations in the mineralisation in primary and permanent dentine effect the hardness (Johnsen, 1994; Hosoya et al., 2000). This alteration will weaken the bonding strength of adhesion restoration materials. In addition, the porosity of primary dentine reduces the hardness of it. (Sumikawa et al.,1999). Dentine mechanical characteristics are strongly affected with collagen presence in dentine, especially collagen type I (Marshall, 1993).

Methods to measure the hardness of dentine have included; abrasion (Wright et al., 1938; Taketa et al., 1957), pendulum (Karlstrom, 1931), scratching (Burg, 1921; Hodge et al., 1933; Totah, 1942) and indentation (Gustafson et al., 1948; Atkinson et al., 1953; Caldwell et al., 1957; Hodge, 1936; Phillips et al., 1948; Klinger, 1940). For indentation tests, a diamond indenter that has pyramidal configuration is preferred, as the indenter penetrates the specimen surface with a specified load (Marshall, 1993). The short diagonals of the pyramid configuration of the indenter reduce the measurmaent error. Thus, the pyramidal shape indenter penetrates about twice as far into the specimen as the more shallow indenters like Knoop indenter (Knoop et al., 1939; Lysaght et al., 1969; Lesheras, 1981).

1.2.6 Collagen in Dentine:

Dentinal collagen is more intertwined with crossing fibrils than the collagen in bone (Habelitz et al., 2002). The function of collagen in dentine is mainly structural, by embracing the extracellular protein matrix together as a well-designed unit (Silver et al., 2003). A complex network in the spaces between cells, called the extracellular matrix (ECM), holds a variety of collagen and non-collagen proteins, such as proteoglycans and glycoproteins. Induction of the nucleation of hydroxyapatite occurs due to collagen of

dentine that affords nucleation sites (Silver and Landis, 2011).

1.2.7 Ultrastructure of Dentinal Collagen:

In dentine, odontoblasts secrete procollagen arranged into fibres and insert them into the predentine (Leblond, 1989). The structure of each collagen molecule is rod-like in shape, the diameter is ~1.5nm, and the length is about 300 nm. The density of the collagen network increases around the predentine and dentine interface, and decreases in density as they get closer to the odontoblast cells (Avery, 2002). Dental collagen originates from procollagen, odotoblasts synthesize the dentinal collagen which takes place in rough endoplasmic reticulum (RER). The structure of the chain of procollagen contains a main central α segment that has two terminal ends: (C-terminal) indicates Carboxy and (N-terminal) represents amino propeptides. Between these terminal ends, disulphide bonds form and supports the alignment of the triple helix. The modification of the synthesized chains is arranged in the endoplasmic reticulum lumen. The modification includes elimination of the two terminals of the propeptides chain to be termed a tropocollagen. Assembly of tropocollagens happens in extracellular area to create microfibril (Minor, 1980). Another extracellular collagen modification occurs post translational; lysine residues oxidation arises by a specific enzyme, lysyl oxidase. This enzyme is important in the formation of covalent bonding among the molecules of tropocollagen, for formulation of collagen fibrils and its stabilization (Minor, 1980). The stabilization of the fibrils occurs due to cross-linking of the inter-covelant particles caused by alteration of the lysine and hydroxylisine residues. During fibril formation, the diameter of the fibrils starts small with limited length, with time and tissue maturation, the length and the size of these fibrils increase.

To identify the collagen network structure of dentine, studies have used electron microscopy (Lin et al., 1993, Perdigao et al., 1999). Atomic force microscopy (AFM) has also been used to identify and analyse collagen fibrils in dentine. Gwinnett concluded that dehydrated dentine can cause collapse of the collagen structure, and is prevented by preserving the surface of dentine under wet-state (Gwinnett, 1994). Another study showed that the collagen of dentine is affected by the etching time. It demonstrated as a damage of dentinal collagen structure after increasing the etching time by unrevealed collagen fibrils and the difficulty to detect (El Feninat et al., 1998). Habelitz et al detected

the collagen fibril structure in permanent teeth by adding a controlled deproteinisation method after demineralisation of the dentine with acid etching. D-banding periodicity was revealed in the hydrated collagen fibril, between 67 and 68 nm, whilst the distribution of the D-banding in the dehydrated samples varied between 57 nm, 62 nm and 67 nm (Habelitz et al., 2002). SEM and AFM were used to investigate collagen structure in permanent teeth, as well as examining the mechanical properties of dentinal collagen and D-banding periodicity (Marshall et al., 1993, Balooch et al., 2008, Fawzy, 2010, Bertassoni et al., 2012). Yet, to date, little is known about the ultrastructure of the dentinal collagen in primary teeth.

1.2.8 Role of dentinal collagen in clinical dentistry

Collagen is essential in increasing the durability and strength of bond in any dentine adhesive system. The competence of adhesive bonding systems relies on the micromechanical retention that is produced by infiltration of the resin into the demineralized surface of the dentine, in which a hybrid layer will form subsequently (Pashley et al., 1995) Nakabayshi et al described the hybrid layer as “a layer that allows the impregnation of the resin monomer into the intertubular collagen network and dentinal tubules” (Nakabayashi et al., 1982). The hybrid layer was produced by using acid etching that is used for collagen exposure, followed by removal of the smear layer off the surface of dentine. Numerous studies has been developed to find the ideal adhesive system protocol that can be applied to the dentine surface (Nor et al., 1996, Hosoya et al., 2000, Pioch et al., 2003). The key for exposing collagen is to obtain an optimum etching time of the dentine surface (Van Meerbeek et al., 1992). Each tooth needs to be treated with acid etch to remove the smear layer, any increase in etching time will cause excessive demineralisation and thus effect the dentinal structure in intertubular and peritubular dentine (Perdigao and Lopes, 2001). Following excessive demineralisation, dentine collagen collapses. This then increases the risk of failure due to formation of a thick hybrid layer on the dentine surface (Hashimoto et al., 2000). Therefore, it is very important to maintain the integrity of collagen structure to achieve good adhesion for restorative material.

1.2.9 Primary vs permanent teeth dentine:

The dentine microstructure of primary and permanent dentitions are not the same. In primary teeth, the thickness of the dentinal surface from the DEJ to the pulp is less than it is in permanent teeth. The S-shaped curve of the dentinal tubules can be seen in longitudinal ground cut in permanent teeth, whereas in primary teeth, the dentinal tubules follow a straight path. The S-shaped curves came from crowding of odontoblasts as they shift from margins toward the centre of pulp (Nanci, 2008). Conversely, the straight course tubules in primary teeth are due to less odontoblasts crowding and the thinner layer of dentine near the pulp (Chowdhary and Reddy, 2010).

The diameter of the dentinal tubules in primary teeth is significantly larger than in permanent teeth. The density of the dentinal tubules in primary teeth is unclear, with one study suggesting it is higher in primary teeth compared to permanent teeth (Sumikawa et al., 1999), whereas it has been reported that the dentine in primary teeth has less tubular density at 0.4 to 0.5mm from the pulp surface when compared to permanent teeth (Koutsi V et al., 1994).

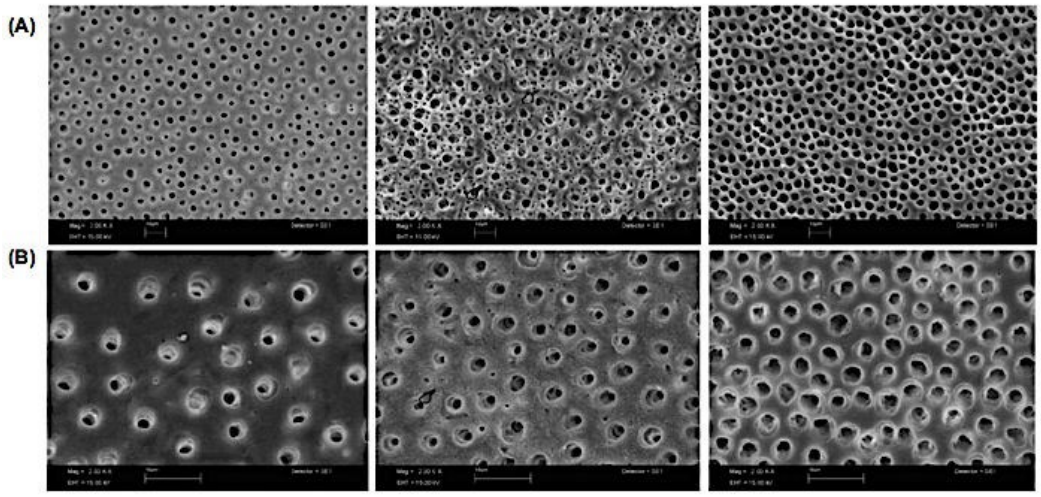

Figure 1-8 Scanning electron microscope (SEM) images of superficial, middle, and deep dentinal layers correspondingly, as seen in primary and permanent teeth. (A) Primary teeth dentinal sections, and (B) Permanent teeth. (Lenzi et al, 2013)

The hardness of dentine in both primary and permanent dentine is similar around the pulpal and peripheral dentine but differerent in coronal and apical areas. It has been found that the hardness value in primary teeth dentine is 60 KHN (Knoop Hardness

Number) and 69KHN to 82KHN in permanent teeth (Johnsen, 1988). This is because the dentine of permanent teeth is more mineralised than primary teeth (Sumikawa et al., 1999). There is less inorganic mineral concentration in peritubular and intertubular dentine in primary teeth than permanent teeth (Hirayama, 1990).

Whilst there is limited research into primary tooth dentine, more is known about bone, which is similar in structure to dentine.

1.3 Bone ultrastructure: Collagen and Matrix

1.3.1 Matrix Composition

Bone matrix is of composed of hydroxyapatite (HA) crystals in a meshwork of collagen fibrils. In addition, the extracellular matrix (ECM) contains numerous macromolecules called proteoglycans (PGs) that are important in synthesizing the collagen fibrils and preserving its structural integrity (Huber 2007; Shapiro 2013)

1.3.2 Bone collagen in relation to Osteogenesis Imperfecta

Collagen in bone can categorized by its organisation; fibrillar and non-fibrillar, or by molecular and histochemical changes (Burgeson and Nimmi, 1992). Fibrillar collagen is classified into; major fibrillar collagen (type I, II and III) that provide tissue rigidity and aligned architecture, and minor fibrillar collagen (type IX and X) that regulate fibrillogenesis (Van der Rest and Garrone, 1991; Adachi and Hayashi, 1986; Wenstrup et al., 2004). The main type of collagen found in bone is type I (Paschalis et al., 2003). Several studies have discovered different types of collagen as type VI and IX (Nerlich et al., 1998), type X (Aigner et al., 1998), types XII and XIV (Walchli et al., 1994), and type XXIV (Koch et al., 2003). The importance of type XII and XIV is to support molecular bridging between the matrix component and the fibrils (Walchli et al., 1994).

1.3.3 Fibril architecture

Since the majority of bone collagen is composed of fibrillar collagen type I, the arrangement of the fibrils is different in various tissues. Parallel arrangement of the collagen fibrils in found in trabecular and cortical bone. This is not the case in dentine, wehre the fibrils are not uniformly distributed in arrangement (Tzaphlidou et al., 2000).

Collagen fibril strength derives from intermolecular cross-links. This cross-linking is an outcome of their three-dimensional alignment (Bank et al, 2000). These cross-links occur when aldehyde side chains interact with amine groups of collagen molecules. There are two types of cross-link; enzymatic cross-link (lysine hydroxylases and lysyl oxidase) and non-enzymatic cross-link (glycation end product) (Bank et al., 2000). Any failure during the cross-linking mechanism to form the collagen fibril will affect in the bone formation. Subsequently, bone abnormalities and fragility may develop such as Osteogenesis imperfecta (Knott and Bailey, 1998)

1.4 Collagen associated disorders

1.4.1 Introduction of Collagen disorders

Various disorders are associated with collagen defects such as Ehlers-Danlos syndrome, Marfan's syndrome, Caffey's disease, scleroderma, Osteogenesis Imperfecta and Dentinogenesis Imperfecta (Myllyharju & Kivirikko, 2001)

1.5 Osteogenesis Imperfecta:

1.5.1 Definition and Classification:

Osteogenesis Imperfecta (OI) is a genetic disorder that occurs in bone characterised by bone fragility and low bone mass. Other manifestations that can be associated variably with this disorder include blue sclera, dentinogenesis Imperfecta (DI), hyperlaxity of ligaments and skin and hearing impairment. Patients with OI are likely to have a mutation in one of the two genes that encode the chains of collagen type 1 *COL1A1* and *COL1A2* (Rauch & Glorieux, 2004). Other genes have also been suggested such as CRTAP (responsible for OI type VII) and P3H1 (responsible for OI type VIII). The prevalence of OI ranges between 1:5000 to 1:20,000 among US population (Huber, 2007)

Sillence proposed four classifications of OI Imperfecta in 1979 based on the clinical and radiographic findings and inheritance mode (Sillence et al, 1984, Sillence et al, 1979). This classification was used to describe the intensity and clinical manifestation of OI with the mutation of collagen type I gene.

OI type I inheritance is predominately autosomal dominant, and presents with blue sclera, bone fragility, and presenile deafness or family history of deafness. New born babies rarely have multiple bone fractures at birth. Mild to moderate long-bone deformity and scoliosis in this OI group. This syndrome is also known as Van der Hoeve's syndrome, OI with mild long-bone disease, OI tarda levis, (Sillence et al, 1979)

Type II OI is autosomal dominant, where children were either stillborn or die in the newborn period. The newborn present with short bowed legs and the radiographs show concertina-like femora, beaded ribs and poor ossification of the cranial vault. This syndrome is also called lethal OI or OI letalis Vrolik (Sillence et al, 1979)

Progressive deformity of long bones and the spine through childhood into adult life, blue sclerae in infancy, normal to mild blue sclerae by adolescence and dentinogenesis imperfecta are the characteristics of OI type III. In patients with autosomal dominant inheritance, all patients had fractures during the first year of life or at birth. OI type III was described as osteopsathyrosis idiopathica of Lobstien, OI congenital, OI tarda gravis and OI with severe long-bone disease. (Sillence et al, 1979)

Patients with OI type IV have dominant inheritance of fragile bone without blue sclerae and DI, but no findings of presenile hearing loss.(Sillence et al, 1979)

In 2004, the Sillence classification was expanded by adding three more types of OI; type V, type VI and type VII (Rauch & Glorieux, 2004). OI type V is autosomal dominant and there is no evidence of gene type I collagen abnormality. Patients have moderate to severe bone deformity, formation of hyperplastic callus at fractured sites. Calcification in the interosseos membrane of the forearm in early life lead to limitation of hand movement and secondary dislocation of radial head. There were no findings of blue sclerae and dentinogenesis imperfecta (Rauch & Glorieux, 2004)

The autosomal recessive inheritance OI type VI relies on the histological findings of bone abnormalities that show elevated amount of osteoid lamellation (fish-scale pattern), while concentration of calcium and phosphorus in serum are normal. The clinical

conclusions illustration white sclerae and no dentinogenesis imperfecta. (Rauch & Glorieux, 2004)

Type VII OI was identified only in a community of Native Americans in North Quebec. The clinical features presented bone fragility, and absence of dentinogenesis imperfecta.(Rauch & Glorieux, 2004)

Carbal et al proposed an additional classification in 2007, the autosomal recessive inheritance Type VIII Osteogenesis imperfecta. The clinical and radiographic findings manifest a severe and lethal form of bone deformities to perinatal; thin skull, multiple fractures in long bones due to irregular callus formation.(Cabral et al., 2007)

Type	Genetics	Clinical findings	Ultrasound findings
Modified Sillence classification			
OI I	Autosomal dominant	Fractures with little or no limb deformity, blue sclerae, normal stature, hearing loss, DI	Rarely, long bone bowing or fracture
OI II	Autosomal dominant	Lethal perinatal type: undermineralized skull, micromelic bones, "beaded" ribs on x-ray, bone deformity, platyspondyly	Undermineralization, broad, crumpled and shortened limbs, thin beaded ribs, fractures, angulation or bowing of long bones, normal appearing hands, deformable calvarium
OI III	Autosomal dominant	Progressively deforming type: moderate deformity of limbs at birth, scleral hue varies, very short stature, dentinogenesis imperfecta (DI)	Thin ribs, short limbs, fractures, undermineralized skull, long bone length falls away from normal 16–18 weeks
OI IV	Autosomal dominant	Normal sclerae, mild/moderate limb deformity with fracture, variable short stature, DI, some hearing loss	Rarely, long bone bowing and/or fracture
New OI types based on bone histology			
OI V	Autosomal dominant	Similar to OI IV plus calcification of interosseous membrane of forearm, radial head dislocation, and hyperplastic callus formation	Unknown
OI VI	Unknown	More fractures than OI type IV, vertebral compression fractures, no DI	Unknown
OI VII	Autosomal recessive	Congenital fractures, white sclerae, early deformity of legs, coxa vara, osteopenia	Skeleton poorly mineralized with severe micromelia; Barnes et al. [2006]

Table 1-1: Clinical manifestation of Osteogenesis imperfecta (Marini, 2007)

In OI type IX, it is recessive autosomal form that is equivalent clinically to type II and type III that are severe. Dentinogenesis imperfecta (DI) has not been reported in patients

with OI type IX. It has been reported that chromosome 15q22.31 mutation in PPIB gene is causing OI type XI. (Van Dijk, 2009)

The autosomal recessive OI type X is one of the forms that has bone deformities and bone fractures in multiple areas, blue sclera, osteopenia and DI. (Christiansen, 2010).

It has been reported that patients with OI type XI have severe deformative progression and contracture of joints. DI was not reported in OI type XI patients. (Kelley, 2011).

OI type XII is categorised as an autosomal recessive form of OI. Clinically, patients have normal white sclera, recurrent fractures with bone deformities. The dentition is normal (no DI) but the eruption of teeth is delayed. (Lapunzina, 2010)

Many studied has reported bone deformities in OI type XIII. In 2012, Martinez-Glez et al defined OI type XIII as an autosomal recessive disorder. It has been labeled that patients have no DI, light blue sclera, osteoporosis and growth deficiency. (Martinez-Glez et al, 2012)

Patients suffer from multiple fractures and osteopenia with OI type XIV as described by Shaheen et al in 2012. The occurrence of fracture has been reported prenatally up to six years of age. DI has not been reported in this type of OI. (Shaheen et al, 2012).

Keupp et al reported patients with OI type XV have recurrent fractures, bone deformities that can cause death of infants and osteoporosis. No abnormalities were found on teeth. (Keupp et al, 2013)

1.5.2 Osteogenesis Imperfecta Gene Mutations:

OI and abnormalities of collagen type I are closely linked, collagen mutations are mostly expressed in the genes COL1A1 and COL1A2. Some patients may have abnormalities due to mutations in different genes such as Cartilage associated Protein (CRTAP) and Leucine Proline-enriched Proteoglycan (LEPRE). Partial damage of CRTAP mutation encodes prolyl-3-hydroxylase-1 (P3H1) hydroxylation of proline residue in the procollagen chain, cause OI type VII (Morello et al., 2006). While LEPRE1 mutations that

encrypt P3H1 were defined in OI type VIII (Cabral et al., 2007). Additional genes have been identified in other autosomal recessive forms of OI (Byers and Pyott, 2012). In Type VI OI, mineralisation defects were found due to serpin peptidase inhibitor, clade F, member 1 mutation (SERPINF1). Collagen P3H1 defects were observed in Type VII, VIII and IX OI (CRTAP, LEPRE1, Peptidyl- prolyl cis-trans isomerase B (PPIB). Further type of collagen defects was discovered as Collagen chaperone defects in Type X and XI OI (SERPINF1 and FKBP10). C-propeptide cleavage enzyme defect seen in Type XII OI (Bone morphogenetic protein 1 (BMP1).

1.5.3 Mutations on Type I collagen

Mutations of collagen can be categorized into two general classes (Byers & Pyott, 2012), affecting the production of type I procollagen:

1. Mutations that cause a decrease in the quantity of normal structure procollagen type I made.
2. Mutations resulting in the production of abnormal molecules, which disturb on the structure of procollagen type I.

Each molecule in collagen type 1 consists of polypeptide chains that build a triple helical structure (two α 1 and one α 2 chain). These chains interlace between each other with a glycine residue at the third position. The most common mutation of collagen type I is the single nucleotide substitution of glycine for another amino acids, affecting the triple helical structure of COlA1 or COLA2 . The variation of phenotypes of OI from very mild to lethal depends on the affected two chains, the position of the gene substitution in the triple helix, and which amino acid is substituted for glycine. (Rauch & Glorieux, 2004)

Osteogenesis imperfecta type	Inheritance	Phenotype	Gene defect
I	AD	Mild	Null COL1A1 allele
II	AD	Lethal	COL1A1 or COL1A2
III	AD	Progressive deformity	COL1A1 or COL1A2
IV	AD	Moderate	COL1A1 or COL1A2
V	AD	Distinctive histology	Unknown
VI	AR	Mineralisation defec Distinctive histology	SPRPINF1
VII	AR	Sever (Hypomorphic) Lethal	CRTAP
VIII	AR	Sever to lethal	LEPRE1
IX	AR	Moderate to lethal	PPIB
X	AR	Sever to lethal	SERPINH1
XI	AR	Progressive deformity	FKBP10
XII	AR	Moderate	SP7
XIII	AR	Sever	BMP1
XIV	AR	Variable severity	TMEM38B
XV	AR AD	Variable severity Early onset Osteoporosis	WNT1

Table 1-2: Expanded Classification of OI. AD, autosomal dominant; AR, autosomal recessive (Valaderes et al, 2014)

The mutations that affect the amount of procollagen type I synthesis usually result in one null *COL1A1* allele and, although only half of the normal amount of type I procollagen becomes synthesized, its structure is normal (Gajko-Galicka, 2002). However, type I procollagen molecules require a minimum of two pro α 1 and one pro α 2 chains to stabilize it. Any changes in the quantity of the number of chains, results in abnormal procollagen. As a consequence of incomplete merging of these pro α chains due to substitution for glycine residues within the triple helix, and occurrence of mutations in the *COL1A1* gene is formulated. In addition to this complex process, a premature

termination codons formed in COL1A1 gene coding sequence responsible in destabilizing in the mRNA due to the skipping events or a process known as nonsense-mediated decay (Rauch & Glorieux, 2004). In conclusion, the outcomes of these mutations is formation of in OI type I in bone as a mild form of Osteogenesis Imperfecta (P H Byers, 2000).

Severe forms of osteogenesis imperfecta involve mutations that cause replacement of a triple helical Glycine residue by another amino acid and mutations that alter splice sites (Marini et al., 2007). These mutations affect on the sequence of amino acid in the *COL1A1* or *COL1A2* gene and occur either in the triple helical domain or carboxyl-terminal propeptide of the encoded pro alpha chain. The common mutations in this domain are single nucleotide substitutions that alter the amino acid sequence (P H Byers, 2000). These substitutions will cause a substitution for glycine. Thus, because of the crucial role of the glycine in helix formation, substitution at two out of every nine nucleotides will result in a clinically apparent phenotype.

OI type I is described by the reduction in the amount of collagen whereas OI type II, III and IV were results from abnormal production of collagen type I (Marini et al., 2007).

1.5.4 Osteogenesis Imperfecta Associated with Dentinogenesis Imperfecta:

Gene mutations found in OI cause defects in the most major component of bone and dentine, collagen type I. as mentioned previously. DI has been reported in more than 50% of patients suffering from OI (Biria, Abbas, Mozaffar, & Ahmadi, 2012)

1.6 Dentinogenesis Imperfecta

Dentinogenesis Imperfecta (DI), or hereditary opalescent dentine, is a tooth disorder in which dentine quality is altered. Shield et al in 1973 categorized it into three main groups: DI type I (DI associated with OI, an autosomal dominant inheritance), DI type II (DI not associated with OI, an autosomal dominant inheritance), and DI type III (found in a tri-racial population from Maryland, known as Brandywine isolate). It is believed that DI occur 1 in 6000 to 8000 people (Takagi & Sasaki 1988). Figure 1-9 demonstrated the clinical features between healthy, DI type I and DI type II.

1.6.1 Dentinogenesis Imperfecta associated with Osteogenesis Imperfecta:

In 1973, Shields proposed a classification of dentine disorders into two main types: Dentinogenesis Imperfecta (DIs, types I–III) and Dentine Dysplasia (DDs, types I and II) based on clinical features and radiographic findings without the underlying molecular pathophysiology. DI was categorized to three subtypes: Dentinogenesis imperfecta type I, Dentiogenesis imperfecta type II and Dentinogenesis imperfecta type III.

The association between OI and DI is not fully understood with prevalence varying from 28 to 73% for DI patients with OI, and DI is most commonly associated with OI type III rather than types I and IV (Malmgren & Norgren 2002).

1.6.2 Dentinogenesis Imperfecta Type I:

DI type I is always associated with osteogenesis imperfecta. The clinical findings in both the primary and permanent teeth are not similar; the primary dentition is more affected than the permanent dentition. The colour of teeth varies from blue-gray to amber brown and opalescent. Because of the dentine defect, it is easy to have attrition due to enamel is easily broken off (Hart and Hart, 2007). Loss of sensation in the tooth can be seen due to obliteration of the pulp (Kim and Simmer, 2007). Radiographically, the crowns are short and bulbous, roots are narrow and constricted, and small or obliterated pulp chambers and root canals are seen. The pulp of obliteration amounts varies and occurs either after eruption or occasionally before eruption (Witkop, 1975, Barron et al., 2008).

The mantle dentine was considered normal in DI patients, possibly due to normal function of odontoblast mechanism during the dentine formation that is called “startup” matrix formation (Hall et al., 2002) whereas others suggested that there is a dysplastic manifestations in mantle dentine (Malmgren and Lindskog, 2003). Mantle dentine layer appeared like normal appearance and that is possibly due to normal function of odontoblast mechanism during the dentine formation that is called “startup” matrix formation (Hall et al., 2002).

Hypertrophy that arises from merging the dysplastic dentine with mantle dentine leads to pulp chamber and canal obliteration. Subsequently, dentine formation continues by

differentiation of mesnchymal cells to odontoblast that form the predentine. Since this differentiation is controlled by gene expression, any disruption occurs can affect dentine the mineralisation process and dysplastic manifestation is seen.

DI type I is an autosomal dominant trait. There is an association between DI type I and OI (type I, III and IV). As well as collagen type I genes mutation (COL1A1 and COL1A2), which are responsible in collagen formation that found in OI can be associated with DI. Type I collagen is the main component in the organic matrix of bone and dentine. It is observed that some patients with OI have normal teeth (Waltimo et al., 1996). In fact, There is no strong link between mutations of collagen gene and dental phenotype nonetheless in DI type I phenotype presentation can be linked to the collagen abnormalities (Ben Amor et al., 2013).

1.6.3 Dentinogenesis Imperfecta Type II

Due to mutation of DSPP, DI type II is not associated with OI. In contrast to DI type I, both the primary and permanent teeth are equally affected, normal teeth are never found in DI type II.

The dental features of DI type I and DI type II are similar in primary teeth (Hart and Hart, 2007) . As DI type I, the radiographic features are: pulp chamber obliteration that begins earlier to tooth eruption. Crown and root morphology are abnormal with bulbous crowns, with marked cervical constriction a typical feature. The roots are often narrow with small and short obliterated root canals. The severity, discolouration and attrition are more profound in DI type II (Bixler, 1976). In addition, hearing loss has also been associated to dentinogenesis imperfecta type II.

The composition of the non-collagenous part of the organic matrix is mainly composed of several proteins and the most dominant one is dentine sialophosphoprotien that is 50% of the composition. Smaller proteins that are encrypted from DSPP such as dentine sialoprotien (DSP) and dentine phosphoprotein (DPP) that are the major component in organic matrix and have and important role in tooth development, by spreading mineral crystals deposits between the collagen fibrils. Any disruption of the DSPP gene can cause DI type II (Xiao et al., 2001, Malmgren et al., 2004). Due to low expression of DSPP in bone, bone abnormalities are not associated with DI type II (Kim and Simmer, 2007).

1.6.4 Dentinogenesis Imperfecta Type III

DI type III was found in a tri-racial population known as the Brandy wine isolate from Maryland and Washington DC (Witkop et al., 1966). The clinical features were similar to those seen in DI type I and II, with severe signs of wear on occlusal and incisal surfaces, causing multiple pulp exposures of primary teeth (Shields et al., 1973). A reported case of DI type III in children showed the presence of enamel only at the gingival margins and the dentine colour was amber brown in colour without evidence of caries (Hursey et al., 1956). On radiographs, due to dentine hypertrophy, the primary teeth of DI type III appeared as hollow "shell" like appearance, (Barron, McDonnell, Mackie, & Dixon, 2008) with enlarged pulp chambers surrounded by only a thin layer of dentine. Variation in the appearance can be noticed in radiographs ranging from normal to pulpal obliteration (Shields et al., 1973). These characters were found only in young children (Witkop, 1975). In DI type III, genetically the dentin sialophosphoprotein DSPP is an important evident in stating Dentinogenesis Imperfecta type III only DPP level is distorted with normal levels of DSP. By this alteration teeth would be affected in colour as well as mineralisation of dentine matrix (Levin et al., 1983).

Figure 1-9: Clinical Intraoral images of healthy and Dentinogenesis imperfecta (DI) in primary (left column) and permanent dentition (right column). (A) Healthy teeth. (B) primary and permanent teeth with DI type I associated with COL1A1 and COL1A2 mutation in Osteogenesis Imperfecta type IV. (C) primary and permanent teeth with DI type II associated with DSPP mutation (Courtesy of EDI)

1.6.5 Histology in DI:

The three types of DI have the same pattern histologically. The matrix of dentine has irregular texture and the number of dentinal tubules is less than normal dentine (O'Connell AC, 1999). It has been found that the mantle layer of dentine, which is adjacent to the DEJ is normal (Bixler et al., 1969). Enamel in DI teeth is basically normal.

Loss of enamel does occur, but this is as a result of dentine weakening not because of enamel structure composition, nor abnormal DEJ (Majorana et al., 2010). In previous studies, it has been believed that the post-eruptive break down of the enamel surface is due to a defective in DEJ. On the other hand, a study has been done by using scanning electron microscopy showed that the loss of the enamel structure arise from either a faulty in the enamel itself or from dentine abnormality and not from a DEJ (Levin et al., 1980).

Several studies have found that the dentine in DI teeth has atubular areas (O'Connel et al., 1999; Hall et al., 2002; Ranta et al., 1993; Levin et al., 1978). An irregular kind of interglobular calcification is found on the DI dentine surface, and under electron microscopy the fibrils can't be characterized due to difficulty in identifying collagens cross striations (Gage, 1985). Majorana et al. investigated the dentine in DI teeth that is associated with OI, it has been found that the width of mantle dentine layer is normal, followed by constriction that is ended in an oversized wavy laminated area close to DEJ. In addition, the collagen fibrils direction was parallel to the long axis of odontoblast whereas the orientation of the collagen fibrils was random on the areas away from odontoblasts. Moreover, the dentine in DI teeth exhibited an inadequate mineralization (Majorana et al., 2010).

It has been suggested that odontoblasts can alter the dentinal ultrastructural variations in primary teeth affected with OI (Hall et al., 2002). The mantle dentine layer appeared normal due to an initial regular odontoblast function. The changes found in the laminated area are due to poor mineralisation that alters collagen fibrils and components of the matrix (Bateman et al., 1984; Lalic et al., 2000).

1.6.6 Dentinogenesis disorders gene mutation:

Gene mutations that encode for the organic matrix, including collagen, appear to underlie a large portion of the hereditary dentine imperfections. These imperfections or defects in OI include transformation or mutation in type I collagen and genes included in

arrangement of the collagen can be related with DI type I. Then again, the allelic change ofIn addition, the *DSPP* gene that encodes dentine sialophosphoprotein, the most abundant non-collagenous protein in dentine can be associated to DI type II and DI type III (Barron et al., 2008). This gene encodes for non-collagenous proteins (NCP) located on chromosome 4 q 21. DSPP is responsible for dentine mineralisation, therefore any defect in the mineralisation process and quality is due to a genetic mutation in DSPP (Lee et al. 2013).

1.7 The Experimental Design- Methods for assessing dentinal collagen

1.7.1 Atomic Force Microscopy (AFM)

Atomic Force Microscopy is one of the types of Scanning Probe Microscopy (SPM) that surface structures to be imaged at a subatomic resolution (Kubinek et al. 2007). Three-dimensional images can be obtained with AFM that produce high-resolution topographic images without the need to stain the samples. The mechanism of scanning is produced by the sharp tip that either contact or tap the specimen surface (Horber, 2003). In AFM, the most common tips that have been used are rocket, pyramidal and isotropic – tip. Calculating the changes in level of the probe point when moved over the surface. This tip is attached to a cantilever that is fixed on to a cylindrical piezoelectric tube. The method of scanning the sample is by the tip that scans the surface and measurement of the deflection of the tip is viewed and reflected onto photodiode. A detector then measures the difference in light intensities and converts it to voltage. The information feedback across a software control from the computer allows the tip to sustain either a constant force or constant height over the sample surface.

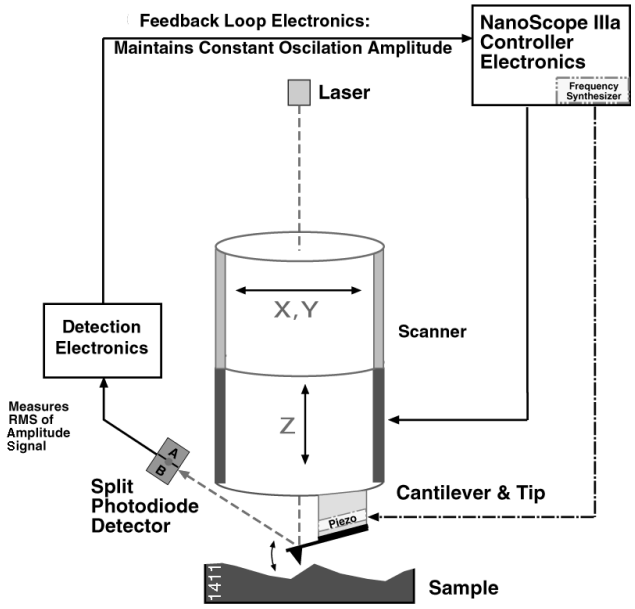

Figure 1-10: AFM mechanism of detection the sample surface and translate it to an image. (Adapted from Veeco, 2006)

There are three operating modes in AFM system; Contact mode, Non-contact mode and Tapping mode that are described as followed (Veeco, 2000);

- Contact mode: in this study, contact mode was applied on most of the samples due to the solid surface. This mode is used mostly on solid and static surfaces. During imaging, the cantilever is always in contact with the sample surface and the atomic forces produce data by the deflection that passes through the surface of the sample. This mode is simple and fast, and not requiring special tip to be mounted due the constant contact of the cantilever on the sample.

- Non –contact mode: the sample surface is not in contact with the probe. The cantilever it self move backward and forward above the sample surface with few nm amplitude. It has been believed that non-contact mode maintain the sample without any damage. However, this mode became unpopular since a soft cantilever tips have been developed for tapping mode.

- Tapping mode (Intermittent contact mode): the cantilever tip is oscillating up and down without a constant contact on the sample surface.

1.7.2 Scanning Electron Microscope (SEM)

SEM is used for imaging the samples in higher magnifications at the micron scale. The mechanism of imaging is by using a highly energetic electron beam that interacts with the surface of the sample to produce a topographic data. In such a position, the surface of the sample must be electrically conductive. For sample preparation, using a chemical fixation such as glutaraldehyde is important to prevent shrinkage. Samples are then coated with a conductive metal such as gold, palladium, tungsten or graphite for sample preparation. The electrons pass through the electron probe and travel all along the sample surface and secondary electrons produced from the sample surface and the electronic signals are identified by a mercuric cadmium telluride detector (MCT). The output signals and image will be displayed on TV-Monitor screen (Burgess et al, 1990).

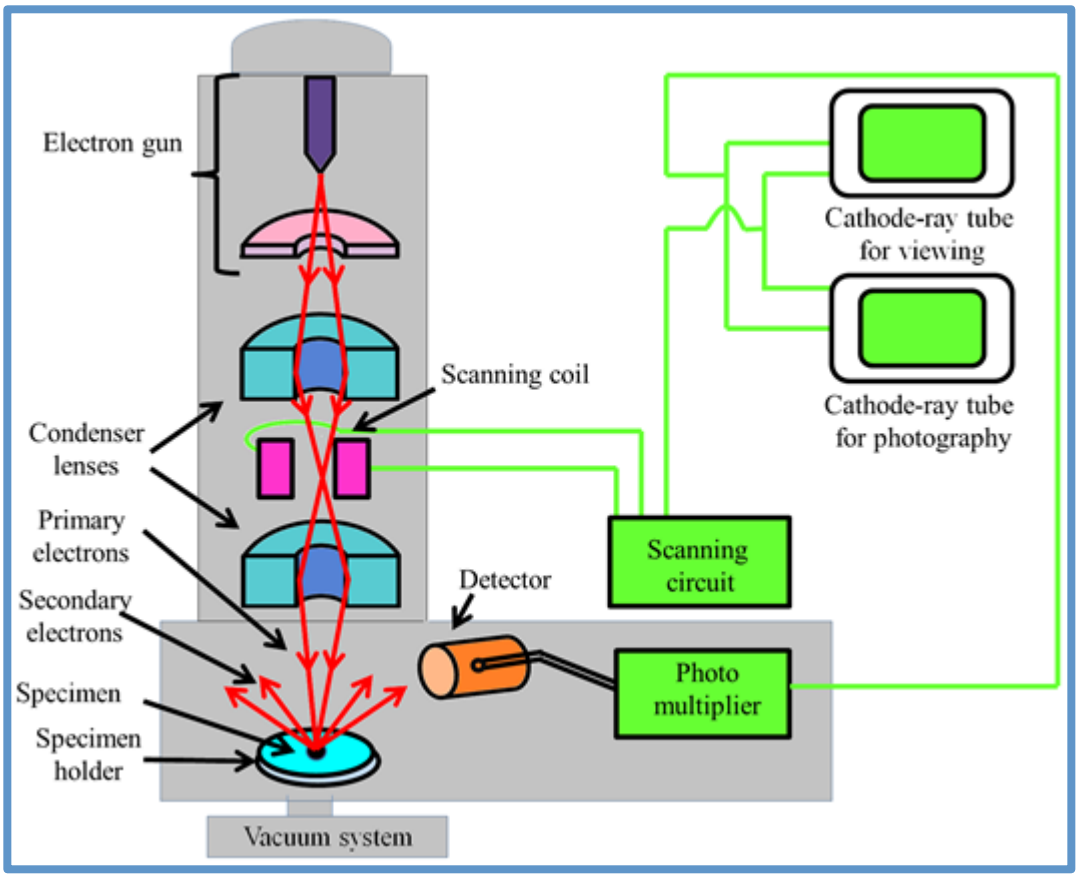

Figure 1-11: A simplified schematic diagram of a scanning electron microscope (Adapted from NPTEL 2013) http://nptel.ac.in/courses/102103044/18

1.7.3 Demineralisation protocol

For imaging the samples, all the samples should be prepared by cutting and applying demineralisation protocol to expose the collagen fibrils and remove the smear layers.

1.7.7 Background on Demineralisation protocol

In 2002, Hebtelitz et al developed a demineralisation protocol to expose collagen of dentine, by etching dentine with 10%vol citric acid for 15 seconds. Citric acid was applied to dissolve the minerals of dentine and later dentine was washed with ultra-high quality water. Then, the dentine is treated for 120 second with 6.5% sodium hypochlorite as a deproteinasing agent (Habelitz et al., 2002). This agent is used to eliminate the non-collagenous matrix protein that covers the collagen fibrils (Marshall et al., 2001). At

the end, dentine surface area was cleaned with ultrasonication in ultra high quality water for 10 seconds.

An existing protocol was created in 2013 as a part of DDent dissertation (Harith 2013), exposing the primary tooth dentine surface to 37% phosphoric acid for 3 minutes and then rinsing the sample in water steam for 1 minute. An AFM images were taken in different application timing, 1 minute, 2 minutes and 3 minutes. The results showed that the collagen exposure of dentine was not homogenous, and found areas of demineralisation and other areas were not demineralised.

1.7.4 Effect of Phosphoric acid

It is essential to understand each acid component and action on the mineralised tissues. Each acid starts by dissolving the involved minerals and causing softening of the minerals itself, while acid solution diffuses inside the structure and triggers the calcium and phosphate ions loss (Eisenburger et al., 2004). The phosphoric acid "H_3PO_4" has a buffering effect on hydroxyapatite and dentine component (Wang and Hume, 1988). The organic constituents of dentine changes as a result of the acid reaction. This change involves morphological alteration of peritubular and intertubular dentine. It is believed that the dentinal tubules unclog following demineralisation, and the collagen network is left intact (Nakabayashi and Pashley, 1998). Marshall et al reported in a study that any increase of etching time on the dentine will cause dissolution of the peritubular zone and thus widening of the dentinal tubules with collagen breakdown around the intertubular area (Marshall et al., 1993). It has been stated that phosphoric acid moderately dissolve the non-collagenous dentine proteins as phosphoproteins, glycosaminoglucans and low molecular weight peptides as well as collagen (Nakabayashi et al., 2004). It has been implied by Spencer that phosphoric acid might alter the collagen organic components (Spencer et al., 2001).

1.7.5 Effect of sodium hypochlorite

Sodium hypochlorite (NaOCl) is commonly used in endodontic dental procedures. The mode of action of hypochlorite acid that is within the sodium hypochlorite solution is to

form chloramines that is able to degrade the amino acids (Estrela et al., 2002). Since sodium hypochlorite has deproteinisation effect on dentine, it can alter the dentinal mechanical properties as modulus and dentine haedness (Marshall et al., 2001, Sim et al., 2001, Correr et al., 2004). NaOCl can affect on the quality of dental restoration by its ability to alter the resin infiltration into dentinal structure (Sim et al., 2001). Moreover, it can change the organic substrate with no alteration in the inorganic material molecular substances(O'Driscoll et al., 2002, Ramirez-Bommer et al., 2007, Morgan A et al., 2010)

1.7.6 Effect of Ethylenediaminetetraacetic acid (EDTA)

EDTA was introduced for clinical work in 1957 (Ostby, 1957). is effective in demineralisation of dentine, it opens dentinal tubules, soften the dentinal structure and increase the permeability of the surface (Calt and Serper, 2002, Hulsmann et al., 2003). The nature of EDTA solution can promote the chelating and protonation mechanism. When pH is neutral, the calcium ions bind to EDTA and increase and enhance the hydroxyapatite detachment. Then, a reduction of pH level occur due to proton exchange from EDTA with calcium ions. The reaction of protonation continues until it reaches to the balance between chelating and protonation mechanism, this method believed to reduce the amount of dentine dissolving (Carvalho et al., 1996).

1.7.8 The Main Standard Protocol:

Another modified protocol was created in 2015 also as a part of DDent dissertation (Ibrahim, 2015) to investigate and improve the previous demineralisation protocol to expose collagen in SEM. The final standardised protocol was developed and its efficacy and reproducibility was as well confirmed as shown in figure (1-12). By placing the samples for a wash in ultrapure water, then cutting and polishing them. Later, starting the demineralisation and deproteinisation process with ultrasonication. Starting with insertion the samples in 37% phosphoric acid for 15 seconds then immerse the samples in 6.5% of sodium hydrochlorite for 5 seconds. Then the samples submerged into ultrapure water ultrasonication for 5 minutes.

It has been found that ultrasonication helps in revealing the collagen meshwork that can be seen under AFM, and exposing more collagen ultrastructure characteristics.

Sonication is increasing the penetration of the phosphoric acid into the dentine structure downward and sideward that allow spreading of acid all along the sample surface area, providing a uniform etching and unblocking the dentinal tubules.

Modifying the demineralisation time of applying 37% phosphoric acid from 3 minutes to 15 seconds showed a good results of exposing collagen structure. The protocol was stand for the acid etching time that is used in vivo for restoring the caries lesion in teeth. 15 seconds of acid etching is adequate for eliminating the smear layer and demineralise the dentine surface to expose the collagen network. If the etching time took more than 15-20 seconds, will change the collagen characteristic and gelatinise it due to hydroxyapatite re-precipitation.

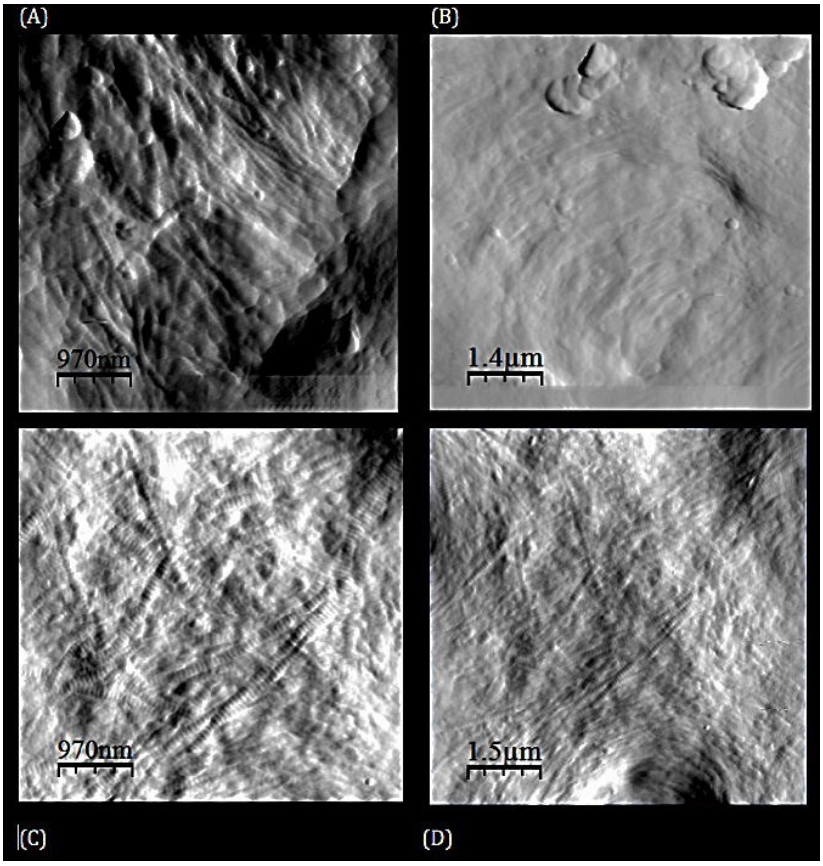

Figure 1-12: Deflection AFM images of demineralised dentine after exposing collagen, showing pre- and post modification of the demineralisation protocol of one control primary tooth sample. (A) and (B) conventional technique, (C) and (D) modified protocol.(Ibrahim S, 2015)

It has been discovered that the use of 6.5% of sodium hypochlorite may enhance removal of the covering of collagen fibrils which is made of non-collagenous proteins (Habelitz et al, 2002 and Marshall et al., 2001). 5 seconds of 6.5% of sodium hypochlorite is sufficient to remove the organic materials without distorting the collagen structure.

It was decided to follow the latest modified demineralisation and deproteinisation protocol to obtain homogeneity of the results and achieve the reproducibility of the acquired images.

1.7.9 Fourier transform infrared spectroscopy (FTIR)

Infrared spectroscopy or Fourier Transform Infrared Spectroscopy (FTIR) is used for data collection of variety of materials by measuring the frequency of the atomic bond vibration between the molecules. The calculation within the molecules occurs through photoconductivity, emission and absorption (Griffith and Haeth, 2007). The data is presented as a graph. Horizontal axis shows wavelength or frequency number and on vertical axis is IR light absorbance.

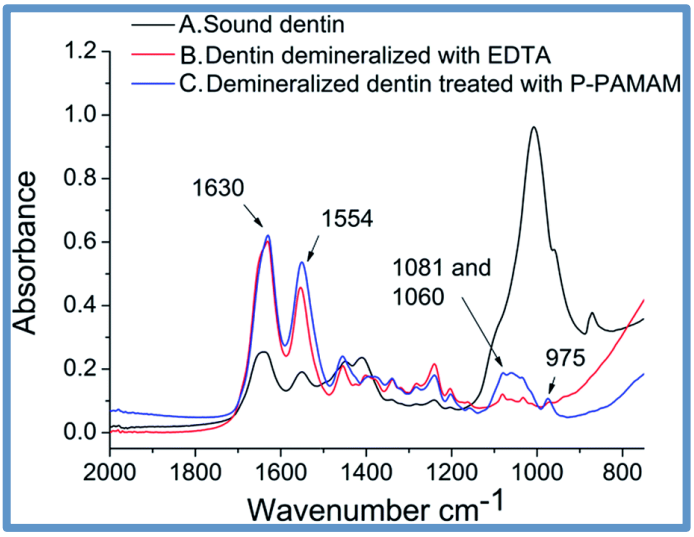

Figure 1-13: FTIR- ATR spectra on sound dentine and on demineralised dentine that has been treated with different materials (Adapted from Tianda Wand et al, 2015)

FTIR has three modes of actions that can be used:

1. Transmission mode.
2. Reflection mode
3. Attenuated Total Reflection (ATR) mode.

In the first mode, thin samples are required for developing the data. The samples for the reflection mode are highly smoothed and reflective in able to produce adequate spectra. ATR mode samples are relatively thick and opaque. The samples should be prepared to accommodate the size of the crystal surface of the instrument. For that case, samples should be wide enough to ensure the full coverage of the crystal surface opening to prevent any inaccuracy.

The data can be inaccurate if the used samples are moderately hydrated as the possibility of increase the potential absorption that interfere with the spectra. For better spectral data results, the samples must be dehydrated either completely or partially.

1.7.10 Mode of Action of (ATR)

After the sample has been prepared, it should be directly in contact with the ATR crystal, which is made with diamond. Infrared beam is directed towards the diamond prism that leads to create an internal reflection phenomenon between the sample and the prism. A transient wave is created and penetrates the sample surface about approximately 0.5 to 1.53 μm in depth. (PIKE technologies, 2011). A detector then will absorb the reflected IR beam and measure it to create an ATR absorption spectra (Perkin Elmer Life and Analytical sciences, 2005)

1.7.11 Hardness study:

The degree of tissue hardness is determined by its resistance to deformation, scratching, or abrasion. Additionally, hardness is described as the capability to resist permanent indentation (Craig, 1993) to test the hardness of the tissues, an applied force will deform the tissue surface even after the removal of the load (Meerbeck et al., 1993)

Hardness test has been based on two categorize: macro-harness and micro-hardness. Both of the tests are load dependent. The Macro-hardness test load is more than 1 kilogram-force (kgf) applied on the tissue surface. While in the micro-hardness test the load ranges between 1-1000 grams-force (gf). The load test that has been used in this

study is 300 gf in weight (2.94N), which is considered a micro-hardness test study.

Wallace indenter (H.W. Wallace, Croydon, England) has been used in this study to test the hardness of primary teeth as shown in figure (1-14). Data was obtained from control and DI teeth.

The measurement of hardness for each sample is calculated by using the formula that provides the result as the Vickers Hardness Number (VHN), which is in this Equation (1-1): VHN = F/A.

In the equation, F indicates the kilogram-force, d is the average length of the indenter diagonally in millimetres. VHN units are kilogram-force per square millimetre (kgf/mm^2). The determination of VHN is by F/A ratio; F indicated the force applied and A indicates the surface area that is obtained from the indentation. Determination of A in this formula is derived from the geometry of the indenter as shown in figure (1-14):

$A= d^2/ 2\sin(136^o/2)$

And after evaluating the sin the formula would be:

$A\approx d^2/1.8544$

D is the average length of the diagonal left by the indenter in millimeters. Therefore, the evaluated formula as follows adapted from (Fuentes et al., 2003):

$VHN= F/A \approx 1.8544F/d^2$

Where F is the load weight in grams and d is the mean diagonal of indentation in micrometers.

To convert Vickers hardness number to Mega Pascals (MPa), the force applied needs converting from kgf to newtons and the area needs converting from mm^2 to m^2 to give results in pascals. Thus, the VHN should be multiplied by 9.807 as 1 kg force = 9.807 N.

Figure 1-14: Wallace Indenter Microhardness tester.

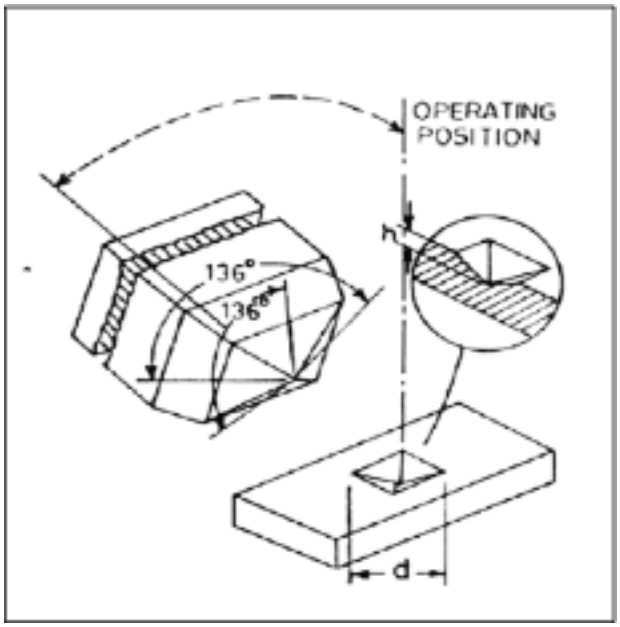

Figure (1-15): The principle of Wallace hardness indentation, where d is the average length of the diagonal measured by the surface area of indentation from the diamond indenter (adapted from Wallace indentation hardness tester instruction manual).

Chapter 2: Aim and Objectives

The evidence of the dentine properties in primary teeth is not clearly understood in both normal and DI affected primary teeth. Our research question: *Are there any differences between the collagen ultrastructure in DI and healthy primary teeth?*

The objective of this study is to understand the mechanical properties of dentine in primary dentition and the dentine ultrastructure. And compare the normal characteristics with DI type I and DI type II. In addition, to clarify the factors that lead to altering the collagen characteristics and structure. For that reason, the aim and objectives of this study are: this question will be answered in the following stages:

1. Measuring dentine hardness
2. Applying the previous demineralisation protocol for AFM to access the collagen ultrastructure.
3. Topographical assessment of collagen ultrastructure and morphology in control teeth, DI type I and DI type II by using AFM Nanotechnology and SEM.
4. Reliability and reproducibility.
5. Applying research findings to clinical setting.

Chapter 3: Material and Methods:

3.1 Study Registration and Ethical Approval

This study was conducted in the Paediatric Dentistry Department at the Eastman Dental Hospital (EDH), University College London Hospital, NHS Foundation trust. Ethical Approval for this study was obtained from the National Health Service Research Ethics Committee (NHS Rec), registration number 11/LO/0777.

3.2 Anomalies clinic and data collection

The dental anomalies clinic was set up in 2009, as a dedicated clinic for children identified as having an enamel or dental defects from the referral letter. The clinic occurs fortnightly, and sees approximately 12 new patients per session. All clinicians involved with the clinic were calibrated for data collection procedures, which included; patient's demographic details, extra oral examination findings, intra- oral examination involving detailed information regarding the enamel and dentine defects (using the DDE index), radiographic examination, diagnosis and treatment plan Appendix 3).

Patients and parents who attended the clinic, and were eligible for inclusion were informed about the study, and leaflets about the study were given to patients and parents (Appendix 1) and the voluntary nature of their participation was reinforced. Written consent was obtained from parents if they agreed to participate (Appendix 2). three copies were obtained as follows:

- One copy was given to the patient/parent.
- One copy was filed in the patient's notes.
- One copy was stored by supervisor in a filing cabinet in a locked office.

All data information taken from the patient was collected using a modified version of the DDE index (Appendix 3). All forms were stored by the secondary supervisor in a filing cabinet in a locked office. All patients attending the anomalies clinic were recorded on a password protected database on a shared drive, and any samples were anonymised, and given an ID code. Once patient's data is completed, the data is send to an electronic

database under the control of the second supervisor. Each patient's details became anonymous using a coding number. For keeping of any exfoliated teeth from patients, they were given a plastic container to store any exfoliated teeth. This was done at the end of the appointment, as well as saliva in which was collected as a part of study protocol.

3.3 Sample Selection

Patients were diagnosed in the Paediatric Dental Department at Eastman Dental hospital with dental anomalies. Patients are attending in dental anomalies clinic for examination. The inclusion criteria:

- Patients diagnosed with DI type I & II

Primary teeth were extracted as part of planned treatment or exfoliated naturally. Comparably, control primary teeth were collected for this study by extracting the teeth for orthodontic reasons or extracted as part of planned treatment.

Sample	Teeth Number	Mode of obtain & Dental Phenotype	Patient demographics (Age & Race)
Control	URE, ULE, URE, LLD &ULD	Normal, carious free, extracted for orthodontic reasons	5 patients; 2 African, 3 Caucasian, Age from 5-9, fit & healthy
DI type I	ULD, ULE, LRE, LRD, LLE	(LRE, LRD, LLE) carious extracted teeth as part of treatment plan, with diffuse yellowish/cream opacity. (ULD, ULE) carious/worn extracted teeth as part of treatment plan, with diffuse yellowish/Brown opacity.	5 patients; 2 Asian aged 6 & 8 years, 3 Caucasian aged 6-9 years. All of the OI type IV
DI type II	URE, ULD, LLD, LRD, LRE	Severely worn extracted teeth as a part of treatment plan, with diffuse yellowish/cream opacity	4 patients; 3 Asian age 5 years, 1 Caucasian aged 6 years

Table 3-1 Description of relevant patient demographics, sample size, modes of acquire, and dental phenotype of samples used in this study

3.4 Sample Size

Teeth were categorised into three groups:

- Control primary teeth.
- DI type I Primary teeth.
- DI type II primary teeth.

Samples were sectioned into two or three sections for AFM preparation and SEM preparation. Since it was difficult to collect a large sample of DI teeth, these teeth were treated with caution during the preparation and sectioning as they worn very easily.

3.5 Sample Storage

In accordance with Human Tissue Act 2009 in Eastman Dental Institute, 256 Grays Inn Road, London, protocols of teeth storage and disinfection were applied. Disinfection was made by removing tissue remnants surrounding the extracted tooth and teeth after extraction or when obtained were washed thoroughly with the use of micro-brushes and scalpel blade, and then placed in 70% concentration ethanol for 3-5 days. Next, the teeth were stored in 0.1% concentration Thymol in a locked refrigerator at 4°C until prepared. The benefit of sample storage is to prevent the microorganisms to grow within the samples as well as prevent the teeth from dehydration. However, Ethanol can cause morphological disturbances of the preserved tissue as it replaces the water molecules in biological tissues. The physical properties of the biological sample is reversed once the sample is re-hydrated as it kept in Thymol (Ritter, 2001)

3.6 Sample Preparation

3.6.1 Cutting teeth:

The tooth sample was positioned on a mounting block and set in by using thermal resistant wax. The block then was mounted onto a rotary saw with twin –mounted diamond- tipped copper blades (Testbourne, UK). All the samples were cut into one to three longitudinal sections under controlling cooling water system and each section is 1-1.5 mm in thickness. Each section has an exposed dentine of the crown and root. Cutting the teeth into longitudinal or diagonal sections (as the tooth is positioned inclined on a mounting block) will benefit in overcoming the destruction of the collagen ultrastructure since the dentinal tubules is following the direction from pulpal tissue to dentine enamel junction (DEJ) And it was showed better topographic images when the samples were cut in this method. For homogeneity of the achieved results, it is determined to cut all the samples in longitudinal sections.

The samples were polished using a polishing instrument under flowing water coolant (MD Fuga, MD Largo) according to a series of silicone-carbide grit paper (500, 1200 and 2400 grade). Polishing inhanced the smoothening of sample surface by reducing the roughness on the dentine surface after cutting phase. Thus, this method aided in producing better topographical images.

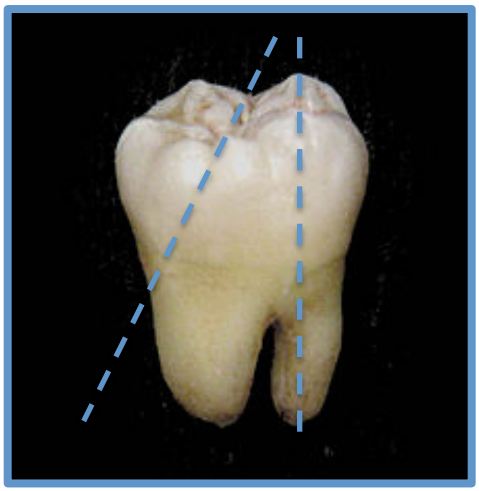

Figure 3-1: Cutting the tooth in Longitudinal and Oblique section for superior topographical images of collagen structure

3.6.2 Hardness test Measurement:

After the cut, each cleaned sample was mounted onto the plate of samples of the Wallace indenter. Wallace indenter (H.W. Wallace, Croydon, England) has been used in this study to test the hardness of primary teeth. Data was obtained from control and DI teeth. 300 grams of load was used and applied for 15 seconds on different random locations of dentine surface and data was recorded by taking the depth of the dentation (Figure 3-2). Five indentations have been taken for each sample. The sample should be flat and steady by making them as plane as possible to the Wallace indenter table to reduce any risk of obtaining incorrect reading. The data recording can be affected by sample movement or friction, pressure and instruments that are adjacent to the Wallace indenter.

The measurement of hardness for each sample is calculated by using formula that provides the result as the Vickers Hardness Number (VHN).

VHN= F/A.

Figure 3-2: Longitudinal section of tooth. Blue circles indicate the indentation points on dentine surface in random locations.

3.6.3 Demineralisation and Deproteinisation Protocol

After cutting the teeth, the demineralization and deproteinisation preparation on the samples done by exposing them to 37% Phosphoric acid (Sigma Aldrich) for 15 seconds and then to 6.5% Sodium Hypochlorite (ReAgen) for 5 seconds.

In an ultrasonic bath, sample were exposed to 37% phosphoric acid for 15 seconds, rinsed in ultrapure water, exposed to 6.5% sodium hydroxide for 5 seconds, and rinsed in ultrapure water. Samples were left to dry before further processing.

The demineralisation protocol is made for eliminating the smear layer that is packed with minerals to expose dentinal collagen by using 37% of phosphoric acid for 15 seconds and 5 seconds of deproteinisation with 6.5% sodium hypochlorite afterwards under ultrasonication.

3.6.4 Ultrasonication:

In ultrasonic bathing procedures, cavitation bubbles are encouraged by high frequency pressure waves to agitate a liquid. The agitation produces high forces on impurities adhering to substrates. This action also penetrates unsighted cavities, cracks, small fissures, and recesses (Ensminger, 2008). Because ultrasonic equipment aids high frequency sound waves to disturb an aqueous medium; this will therefore support

penetration of constricted unreachable spaces and acts on eliminating contaminated substances such as blood, dust, oil, grease, polishing compounds, and fingerprints. The prepared sample was kept in an ultrasonic bath forming of ultra-pure water for at minimum 5 minutes.

Ultrasonication of the sample in ultrapure water was done at three specific stages of sample preparation. First, sonication was done after sample cutting, next in another time during demineralisation with phosphoric acid, and finally after deproteinisation with sodium hypochlorite prior imaging analysis.

This ultrasonication procedure was confirmed in this study following a pre-existing protocol that has been developed by a former student as a part of DDent dissertation titled "Exposure and characterisation of collagen ultrastructure in primary teeth affected with Osteogenesis Imperfecta and Dentinogenesis Imperfecta" (Ibrahim, 2015)

3.6.5 Ultra-pure Water Routine:

Ultra-pure water is one that goes under purification methods to control any possible contamination and / or proliferation of particles such as bacterial agents, organic, negatively charged anionic, and metallic contaminants. It is filtered through a series of ultra filtration processes that include use of ultraviolet light, electrode ionization, and carbon filters (Nakajima & Shima 1991). All human tissue samples used in this study were handled and washed using ultra pure water to avoid any possible contamination, which could lead to false results. In addition, ultra-pure water is less conductive than normal water.

3.6.6 Fourier Transform Spectroscopy (FTIR)

As a validation method for evaluating the demineralisation protocol efficacy, FTIR was used for each tooth sample. ATR-FTIR spectra were recorded using a PE 2000 FTIR spectrometer (Perkin Elmer Spectrum 2000 FT-IR Spectrometer Perkin Elmer *I*-Series FT-IR Microscope). The IR spectra mid-range is (4000-600 cm^{-1}). The data has been recorded during to standardise the demineralisation protocol pre and post applying etching techniques on the sample surface to analyse their efficacy. The measurements were taken for control, DI type I and, DI type II samples. FTIR identify and compare the levels of Amide I band that is represents on the collagen surface, and the peak of the Phosphates, which is the mineral part on the sample surface (hydroxyapatites). First, the record was taken before etching the sample and the normal level of the phosphate peak

should be higher than the amide I band. After applying the etching agent (35% of phosphoric acid), the phosphate peak almost totally vanished and the amide I peak increased, which represents adequate demineralisation of the sample surface.

3.7 Topographic Imaging- Atomic Force Microscopy (AFM)

3.7.1 AFM Imaging:

After demineralisation and deproteination, the samples were ready to be used for topographic imaging. Samples were attached on glass slides that were held in place using tapes and mounted on the Dimension 3100 Atomic Force Microscope (Bruker, Santa Barbara, CA)

Using the contact mode in AFM, MSNL-10 (Bruker, Santa Barbara) with a spring constant of 0.03-0.1 Nm^{-1} was mounted on the cantilever holder attached to the optical head. A scanning rate average of 1 Hz was used. To optimise the contact forces on the tips, the deflection set point of 1,200 V was used for that purpose. Most of the images were scanned at 512 x 512 pixels.

Topographic images were taken in several magnification sizes and different locations. These locations were divided into three categories: a) Coronal third of dentine b) Middle third of dentine, and c) Apical third of dentine which is towards the root.

3.7.2 Image Processing:

Images were obtained and analysed by using Nanoscope Analysis Software (Version v140r1, Bruker, Santa Barbara). The software was used for editing and adjusting brightness and contrast, and flattening the images into planes to acquire an optimal outcome on images.

3.7.3 Measuring D-banding periodicity – Image Analysis:

The collagen fibril D-banding distances were determined from the shape of the fibrils in modified images. Analysis was carried out by verifying the step height of individual fibrils. The length of the sections were obtained and divided by the number of bands present.

3.7.4 Scanning Electron Microscopy (SEM) imaging

After using the samples in topographic imaging by AFM, scanning electron microscope (SEM) was used as well for imaging the samples at the micron scale. Samples were fixed for 24 hours in 3% glutaraldehyde (Agar Scientific, UK) in 0.1M sodium cacodylate solution. Samples were then dehydrated using an ethanol series, before critical point drying with HDMS (Sigma-Aldrich, UK). Samples were mounted using carbon adhesive tabs to aluminium stubs (Agar Scientific, UK), and coated in Au/Pd. Imaging was performed using a Philips XL30 FEG-SEM (FEI, Eindhoven), with an accelerating voltage of 5 kV and a spot-size of 3.

For fixation and dehydration protocol, all the samples should be fixed in 3% Gluteraldehyde (Agar Scientific, UK) in 0.1M buffer (Cacodylate) for 10 minutes at temperature of 4 degrees Celsius. Then dehydration is done by using graded ethyl alcohls at room temperature in series. 70% ethanol for 10 minutes followe by 90% ethanol for 10 minutes. Then 100% absolute ethanol for 5 minutes.

3.8 Statistical analysis:

For dentine hardness analysis, the VHN values for all groups were analyzed statistically using Origin Pro Software (OriginLab, Northampton, MA). The analysis was done by using One Way Analysis of Variance (**ANOVA**) that is called Kruskal Wallis Test Analysis, which is a statistical **method** used to test differences between the groups.

Kruskal – Wallis test was performed to analyse the results. It is the generally used form of statistical analysis in tests where one measurement and one nominal variable is being analysed. It is used as a non parametric method of determining dissemination origin of groups of samples studied, and testing whether their mean ranks are similar, (McDonald, 2008). Kruskal Wallis test was used to analyse topographic data obtained from SEM and AFM images of dentinal tubules and collagen fibrils. Variables analysed were dentinal tubules number and diameter, and collagen fibril diameter.

Mann-Whitney U test was implemented to analyse the dentinal tubules data between the groups. This test is usually used to compare differences between two independent

groups when the dependent variable is either ordinal or continuous, but not normally distributed

Special acknowledges to my colleague (Adam Strange), as he carried out some parts of the Statistical Analysis.

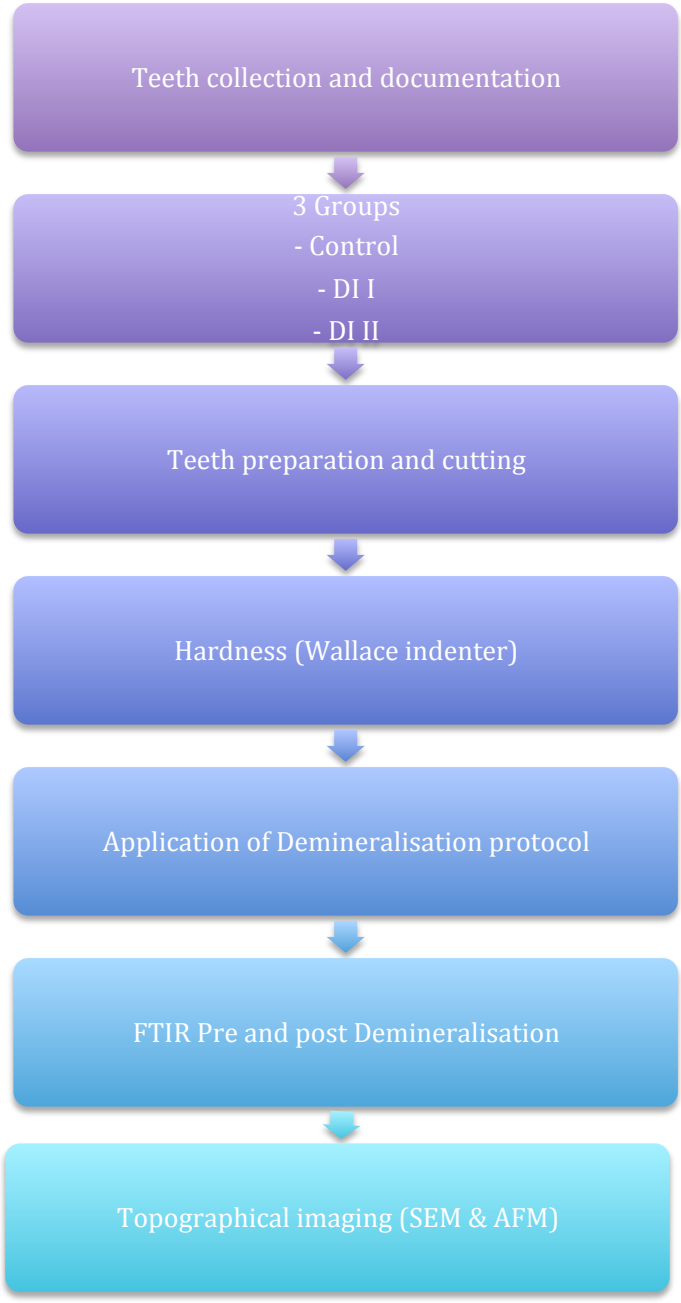

Figure 3-2: Experiment method Flow chart.

Chapter 4 Evaluation of Physical Properties Of Dentine (Hardness of Dentine)

Hardness of dentine was measured to evaluate its physical property to resist any deformities that can be done after application of loads. The hardness of dentine been measured after application of 300 grams of load for 15 seconds on 5 different indentation area on each tooth of control, DI type I, and DI type II surfaces. The decision of characterising the mechanical properties of dentine is made to compare the obtained results in this study with the results from other investigators . Hardness of dentine was measured before application of any demineralisation protocol on the teeth as the purpose of demineralisation was to remove the mineral of dentine. In addition, demineralised samples can impact on the results by differentiating the mineral phase and the collagen phase and not measuring the dentine surface as a whole sound surface.

Tables 4-1 to 4-3 show the results of the hardness test in MPa, using Wallace Hardness instrument on control teeth. Teeth from 1-5 were control teeth, 6 -10 were DI type I, and 11-15 were DI type II. These teeth were collected from 14 patients aged between 5 and 9 years. The VHN was calculated with the use of the previously mentioned formula (Equation 1-1). In addition, VHN was converted to MPa by multiplying the VHN by 9.807 as 1 kg force = 9.807 N.

Sample Number	d (Diagonal)	VHN	Standard Deviation	Mega Pascal MPa
Control 1	98.2	57.7	±1.0	565.9
Control 2	102.6	52.9	±3.2	518.8
Control 3	94.5	62.4	±3.4	612
Control 4	100.8	54.8	±2.1	537.4
Control 5	101.3	54.3	±2.4	532.5

Table 4-1: Dentine hardness in Control teeth (n=25 of indentation). VHN Values and MPa values at 300 gram of load.

Sample Number	d (Diagonal)	VHN	Standard Deviation	Mega MPa	Pascal
DI type I 1	149.8	25.4	±4.8	249.1	
DI type I 2	160.1	21.8	±1.6	213.8	
DI type I 3	164.7	20.8	±3.4	204	
DI type I 4	161.2	21.4	±2.2	209.9	
DI type I 5	165.9	20.3	±1.3	199.2	

Table 4-2: Dentine hardness in DI type I teeth (n=25 of indentation). VHN Values and MPa values at 300 gram of load.

Sample Number	d (Diagonal)	VHN	Standard Deviation	Mega MPa	Pascal
DI type II 1	132.1	32.2	±4.4	317.7	
DI type II 2	129.2	33.5	±3.6	328.5	
DI type II 3	124.5	36.2	±4.4	355	
DI type II 4	129.1	33.5	±2.1	328.5	
DI type II 5	134.2	31.0	±2.0	304	

Table 4-3: Dentine hardness in DI type II teeth (n=25 of indentation). VHN Values and MPa values at 300 gram of load.

The obtained VHNs of dentine ranged from 52.9 ± minimum to 62.4 ± maximum for the control primary teeth. The mean VHN for dentine of control primary teeth was ± 56.42.

The VHN in DI type I teeth was recorded from 20.3 ± minimum to 25.4±, and for DI type II teeth from 31 ± minimum to 36.2 ±. In comparison with the control teeth, the VHN value was reduced in DI teeth compared to the control. Micro-hardness of the teeth recorded in this study is showed on Figure 4-1 indicating the the hardness in MPa values for control teeth in comparison to DI teeth.

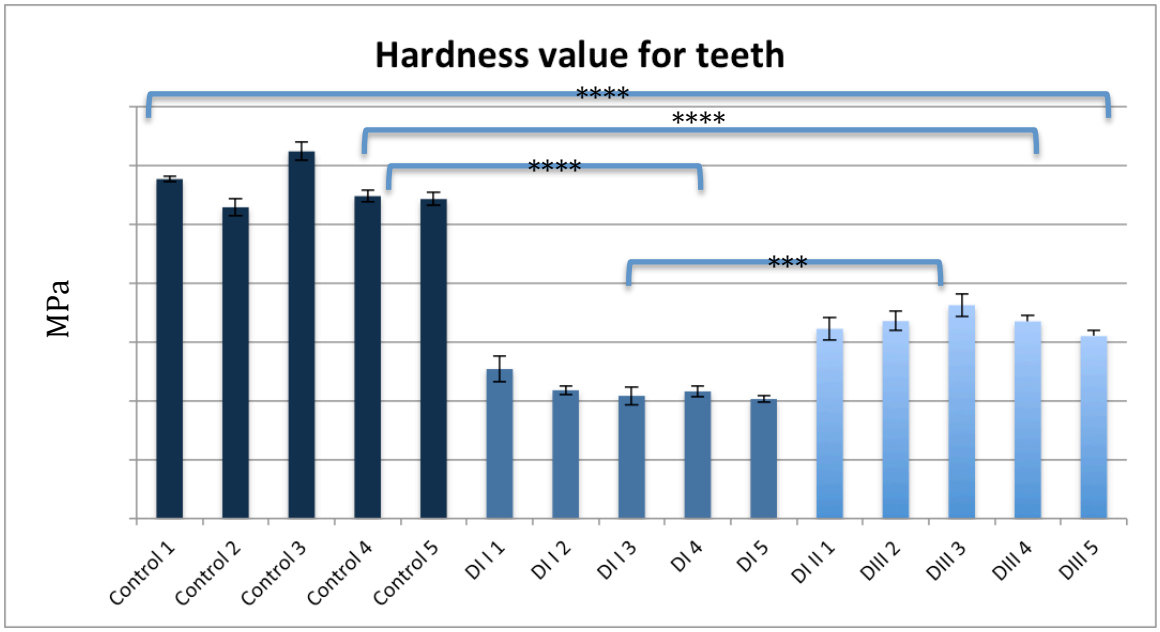

Figure 4-1: Dentine hardness (MPa) of teeth (5 control teeth in comparison to the hardness value of 5 DI type I teeth and 5 DI type II in each group).

4.1 Statistical analysis of dentine hardness

The VHN values for all groups were analysed statistically using Origin Pro Software (OriginLab, Northampton, MA). The analysis was done by using Kruskal Wallis test “one way Analysis of Variance (**ANOVA**)”. Figure 4-2 represents box plot graph comparing between the MPa of the three groups; control, DI type I, and DI type II. Medians of VHN

values were represented very differently. There were a significant different between control and DI type I, control and DI type II, and between both DI groups (P < 0.05).

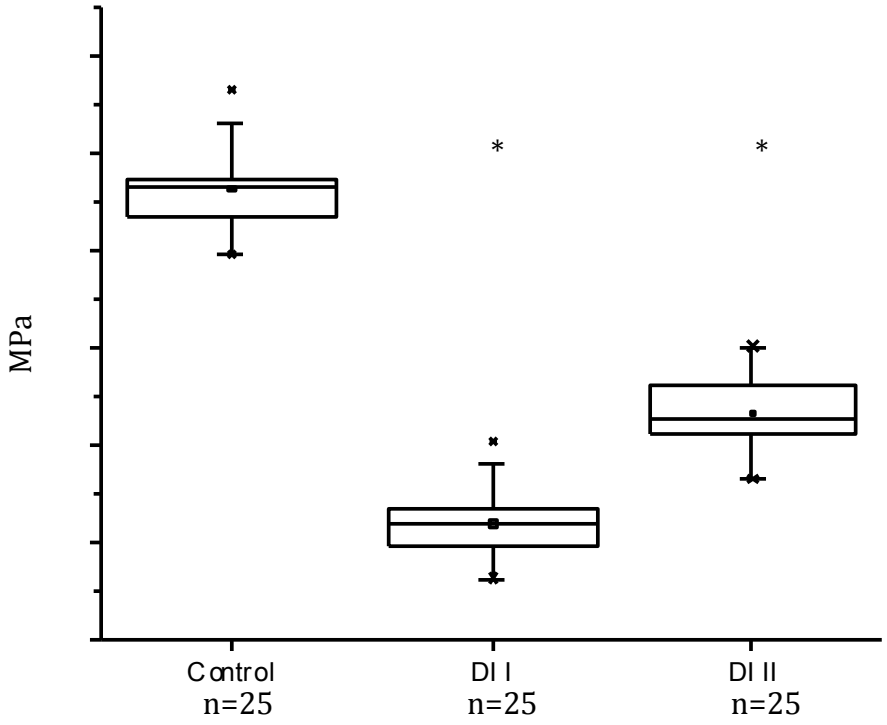

Figure 4-2: Kruskal Wallis Test analysis of Hardness test values (MPa) in control, DI type I, and DI type II samples. There is a significant difference between the 3 groups as the medians are very different.

4.2 Summary of Result (Hardness test) and Discussion:

The obtained VHN that has been recorded in this study significant varies in the 3 groups. The sample size number is small (5 control teeth, 5 DI type I, and 5 DI type II). Dentine hardness test and VHN for both DI type I and II were significantly decreased from VHN values of dentine of normal control primary teeth (P ≤ 0.0001). and the dentine hardness were significantly different between control and DI type I, and between control and DI type II groups (P ≤ 0.0001). In addition, a significant difference between DI type I and DI

type II groups were noted (P ≤ 0.001). The teeth that have been measured for the hardness test were also used for topographical imaging.

The N number equal for each group was 25, which indicated 25 indentations for each group. The different dentine locations for indentation was treated as an individual dentine sample. The compared results of dentine hardness of five DI type I and five DI type II with five control healthy dentine were significantly different in this study. The mean hardness value for control teeth was VHN 56.42± 6.1 and the mean VHN value for DI type I teeth was VHN 21.98±4.31, and for DI type II teeth the mean value was VHN 33.3±2.94. The mean VHN values reported in this study for sound dentin (from 52.9 to 62) is in accordance with previously reported values (57, 60 and 62) with the same measurement procedure (Fross et al, 1991, Willems G, 1992, and Fuentes, 2003). The resemblance of reported values is positively due to the reproducible micro-indentation techniques occupied. The small difference in VHN reading between previous studies and this study might be due to some teeth variation and the sensitivity of the use of the Wallace hardness test instrument. Alternatively the measurements reading could well be affected by the sample flatness and its surface condition (Lysaght et al., 1969; Lasheras, 1981). In addition, there were no previous studies comparing between the sound and diseased dentinal hardness.

The reduction of hardness of dentine was statically significant between the DI teeth in both groups and control group. In addition, there was a significant difference between DI type I and DI type II. Which means a reduction in dentine hardness were found more in DI type I more than DI type II teeth. This finding states that there is a structure difference between DI type I teeth that is associated with osteogenesis imperfecta thus affected by mutation in COL1A1 and COL1A2, and DI type II teeth that is affected by DSPP mutations. Collagen structure in dentine gives the strength and support to the dentinal tissues and any mutation in COL1A1 and COL1A2 will affect on dentinal stability and strength. As well as dentinal phosphoprotiene which plays an important role in hydroxyapatite crystal formation during mineralisation process of dentine (Weinstock et al., 1973,Nanci, 2008). Therefore, any abnormality of DSPP will affect on the hardness of DI type II teeth and dentine structure.

It is well recognised that dentine hardness is affected by the stability of the intertubular dentine (Kinney et al., 1996) and the highly mineralised peritubular dentine (Pashley et al., 1989). This study showed that DI type II teeth were relatively higher in dentine hardness when compared to DI type I teeth, which means that the mineral content would be different in DI type II than in DI type I or either in control teeth. However, since the causative factor of DI type I teeth is COL1A1 and COL1A2 mutation that affects the collagen stability and elasticity of dentine, It can be assumed that the collagen in dentine contributes in dentine hardness of primary teeth. The hardness of all DI teeth in both types showed decreased hardness from those of normal dentine. The probable justification of reduced hardness of DI type I teeth is the distorted function of odontoblast due to the unusual collagen secretion which later affects the dentine matrix secreted by the odontoblast. A previous study on hardness has been performed on sound and carious primary dentine with the use of Nano-indentation techniques. It has been suggested that the hardness of dentine affected by the mineral content and there were a reduction in hardness is the carious due to loss of the minerals (Angker et al, 2005)

The overall number of collected primary teeth was five and it was collected from five children aged between 5 and 9 years old. This was essentially a convenience sample limited by the availability of teeth with DI. There is one previous study compared the hardness of dentine in permanent teeth with mature root and open apex in upper incisors. It showed that the dentine hardness result was approximately it was insignificance statistically between the young patient group that aged between 8 to 10 years old and from the old patient group that aged between 56 to 60 years old (Dalitz, 1962). In this study, the aim was to compare among the groups and focused on the patient's age range to reduce the errors in the outcome of the measurements of the dentine hardness.

Wallace Hardness Tester Indenter was the equipment of choice to measure the dentine of primary dentine in each group of control and both DI types. The measurements were taken randomly targeting five indentation locations around the surface area to be able to determine the different dentine locations as; peritubular dentine, intertubular dentine, DEJ area, outermost area of dentine and innermost zone of dentine close to the pulp. A weight of 300 grams was employed in this study. There were numerous previous researches of dentine hardness using both 300 grams or 500 grams load (Marshall et

al., 1982; Hegdahl et al., 1972). However, the hardness measurements difference due to weight dependence will probably be minute in comparison with the differences caused by experimental errors (Marshall et al., 1982; Hegdahl et al., 1972).

One of the aspects that can disturb the hardness measurement is the difficulty to stabilize the sample (sectioned dentine) during recording of the measurements. The difficulty arose particularly when using small models of sectioned and polished dentine. The width of each sample which was not more than 4mm, making the handling of each sample extremely difficult. In this study, the DI teeth used were upper and lower primary molars in almost all the mouth quadrants. It has been a challenge to prepare the sample dentine discs of the DI teeth due to the small teeth size and because some of the samples and lost various parts of dentine due to occlusal wear. As it is recognized that it is essential to obtain a flat surface in the cutting sections for the hardness measurement process, the small amount of the DI teeth samples has probably compromised the sample preparation thus would have altered the indentation moves throughout hardness measurement.

The performed microindentation technique in this study was the Vicker Hardness test indentor. It has been used in this study a square shaped diamond with a pyramid base that is forced into several polished surfaces of materials under a precise load that is chose by the researcher. The Vickers test is appropriate for verifying the hardness of extremely delicate materials such as tooth structure (Lysaght et al., 1969). It has been stated that the evident increase in hardness with reduction in load is mostly caused by two factors: 1) the determination of the size of the indentation, or failure to record the final micron of the indentations, specifically when indentations are less than 100μm (Lysaght et al., 1969; Colleys et al., 1992), and 2) the elastic recovery of the indentation (Lysaght et al., 1969). For Knoop hardness, elastic recovery occurs after unloading the force mainly occurs along the shortest diagonal and depth, but the longest diagonal stays moderately unaltered (Shannon et al., 1976; Marshall et al., 1982). Thus, the hardness measurements taken by this approach are practically insensitive to the elastic recovery of the material. Based on this, Vickers hardness test was indicated in this research to gauge the dentine hardness of teeth samples.

The number of previous studies of dentine hardness is few, and most of the studies were comparing between the hardness of sound permanent, sound primary, carious dentine, on the dehydrated and hydrated dentine surfaces hardness, as well the hydration of dentine in carious lesion (Fusayama et al., 1966; Marshall et al., 2001; Ogawa et al., 1983; Shimizu et al., 1986; Fuentes et al, 2003). In fact, researches on the dentine hardness of sound and teeth affected with DI teeth are very limited.

The previous published studies have concentrated on measuring the mechanical properties of permanent teeth dentine (Fusayama et al., 1966; Marshall et al., 2001; Ogawa et al., 1983; Shimizu et al., 1986; Fuentes et al, 2003). Very few studies have been established to evaluate primary dentine (Angker et al., 2003; Mahoney et al., 2000), and even less have focused in diseased teeth such as DI teeth in primary dentine.

Chapter 5 Collagen Ultrastructure Exposure (Demineralisation of Dentine)

5.1 Adaptation of pre-existing demineralisation protocols:

Demineralisation of dentine was performed by removing the minerals and smear layer in order to expose the collagen ultrastructure. Different demineralisation techniques have been established previously on healthy dentine. These techniques have been performed by using different acids with different application times. In this study, the protocol developed was been adapted from previous studies as mentioned in the introduction and applied to all the sample groups. This protocol focussed on the use of 37% phosphoric acid applied directly on dentine. To obtain a systematic standard demineralisation protocol applicable to all tooth sample, a validation of the method was carried out using a spectroscopic approach. The merit of the demineralisation protocol was evaluated with an FTIR spectrometer by monitoring the intensity of the phosphate band in relation with the amide I band. The success of the demineralisation approach was evaluated by recording the decrease of the intensity of the phosphate peak and increase of that of the amide I peak. The FTIR results were found to be reproducible on control samples but not on the diseased group. To remedy to this issue, another demineralisation technique was applied on the DI type I and DI type II groups by using 17% of EDTA. This was then subsequently evaluated with FTIR.

5.1.1 Evaluation of Main Demineralisation Protocol:

After cutting the samples, a smear layer formed on the surface of the samples. The demineralisation protocol was applied in order to expose the collagen structure. This was done by applying phosphoric acid onto the entire sample in an ultrasonic bath for 15 seconds. FTIR was used prior to this step to compare pre and post collagen exposure which was indicated by an increase in the amide I peak intensity. The amide I peak is characteristic of the collagen content in the dentine, whilst the phosphate peak is characteristic of its mineral contents (hydroxyapatite). Satisfactory AFM and SEM topographical images were obtained after demineralisation.

Obtaining a clear exposure of the collagen meshwork is needed for topographical imaging to reveal the collagen ultrastructure. This can be obtained by doing a sufficient demineralisation protocol on the sample surface as in Figure 5-1.

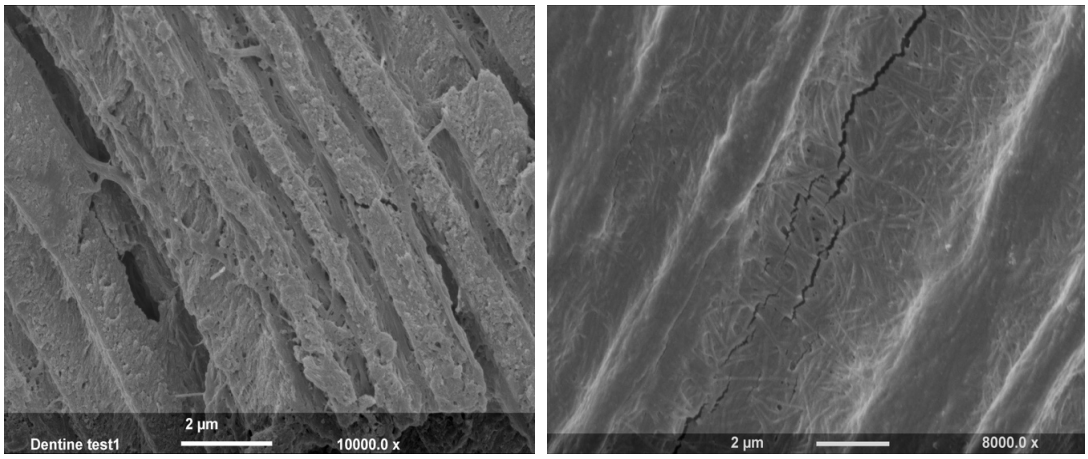

Figure 5-1: SEM images at two different magnifications of demineralised dentinal surface and exposed collagen, showing (A) pre demineralisation and (B) post demineralisation protocol of one control primary tooth sample.

A previous study Figure 5-2 shows pre and post demineralisation infrared spectra of a control sample. After acid etching for 15 seconds, (spectrum shown in black in Figure 4-4), the phosphate peak was greatly reduced and almost completely disappeared suggesting sufficient and/or complete removal of inorganic surface minerals. Amide I and II bands representing collagen type I was then clearly amplified, suggesting collagen exposure.

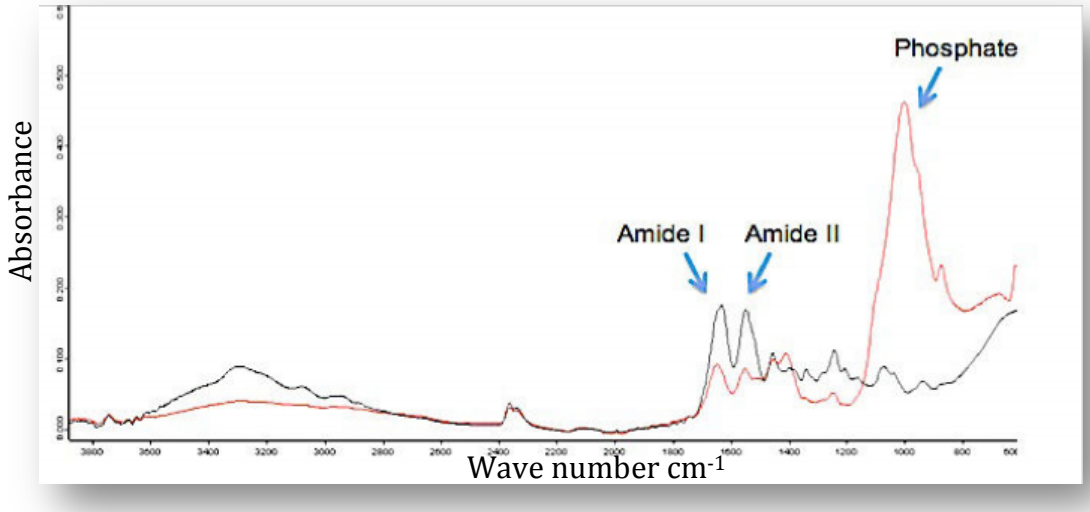

Figure 5-2 : Fourier transform infrared (FTIR) spectrum of control primary tooth at pre (red spectra) and post (black spectra) demineralisation.

Unfortunately, an increase in the demineralisation time can lead to denaturation of the collagen fibrils and damage the collagen structure. (Ibrahim, 2015). In order to avoid this scenario, a gradual decrease in the intensity of the Phosphate peak was obtained by modulating the exposure time of the acid . In Figure 5-3, the phosphate peak has been monitored in different times from 0 point to 15 seconds. The gradual reduction of phosphate peak has been recorded in relation with amide peaks. This reduction indicates the partial or complete removal of the minerals on the dentine surface.

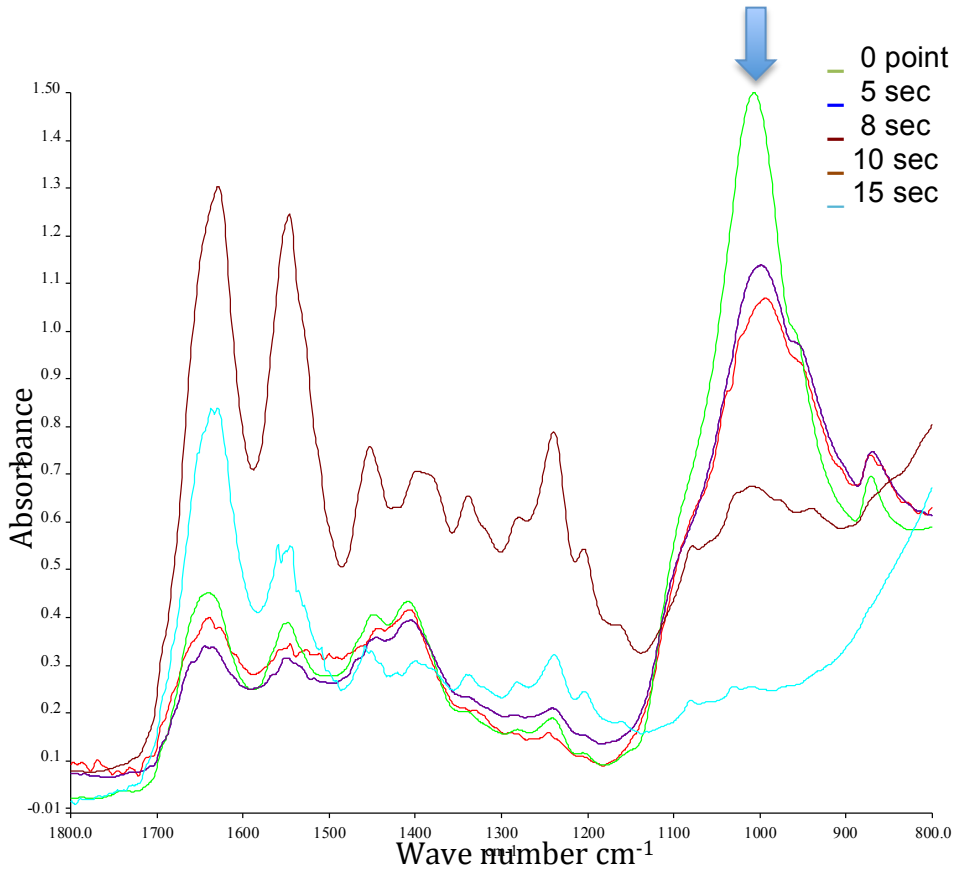

Figure 5-3 Fourier transform infrared (FTIR) spectra of control primary tooth. Spectra shown in green is at 0 min, prior to acid etching, and light blue spectra is post demineralisation spectra after 15 s. the gradual reduction of phosphate peak (Blue arrow) is recorded in 5,8,10 toward 15 sec.

In this study, it has been decided to apply demineralisation on samples for 15 seconds for most favourable results as it has been shown on topographic images in the next chapter. On the other hand, 15 seconds of etching is the approximate time that is being used on carious lesion restoration with adhesives composites. 15 seconds of acid etching that is made of 37% phosphoric acid, was found to be appropriate for acceptable demineralisation of dentine surface, smear layer removal, dentinal tubule unblocking, and collagen exposure.

This acid exposure of 15 seconds on healthy dentine produced superior topographic images for AFM and SEM since the collagen ultrastructure is clearly revealed as presented later on.

5.1.2 Ultrasonication Technique during Demineralisation:

It was also beneficial to introduce a sonication step in the demineralisation protocol of samples. The sonication enabled a deeper penetration of the acid inside the surface area and allowed it to spread in multiple directions along the dentinal tubules. The ultra sonication of the phosphoric acid created a homogenous etching on the entire surface, better penetration and removal of dentinal tubules obturation.

5.1.3 Deproteinisation Method on Dentine:

A futher step was added, consisting in the deproteinisation of the smear layer that may reside at the surface of the demineralised dentine surface. To do so, 6.5% vol of Sodium Hypochlorite (NaOCl) was used to eliminate the non-collagenous substances such as proteins that cover the surface of collagen fibrils (Habelitz et al, 2002 and Marshall et al., 2001). NaOCl is a bleaching agent and acts like a solvent, this has been used for root canal irrigation throughout clinical endodontic treatment for many years. The benefit of using NaOCl as an irrigation solvent was to dissolve and remove the organic substances and eliminate any bacterial infection (Yazd, 2008). The prolonged application of NaOCl with high concentration may lead to collagen surface dissolution and can modify the mechanical properties such as reducing the hardness and modulus of elasticity (Marshall et al, 2001). It has been stated that using 6.5% vol of sodium hypochlorite for 5

seconds will maintain the structure integrity of collagen without damaging it. This allows us to obtain an improved quality of topographical images in both AFM and SEM with a clear presence of collagen meshwork. Figure 5-4 showed dentinal surface of control tooth post demineralisation application. (A) without deproteinisation, and (B) after application of 6.5% NaOcl for 5 seconds.

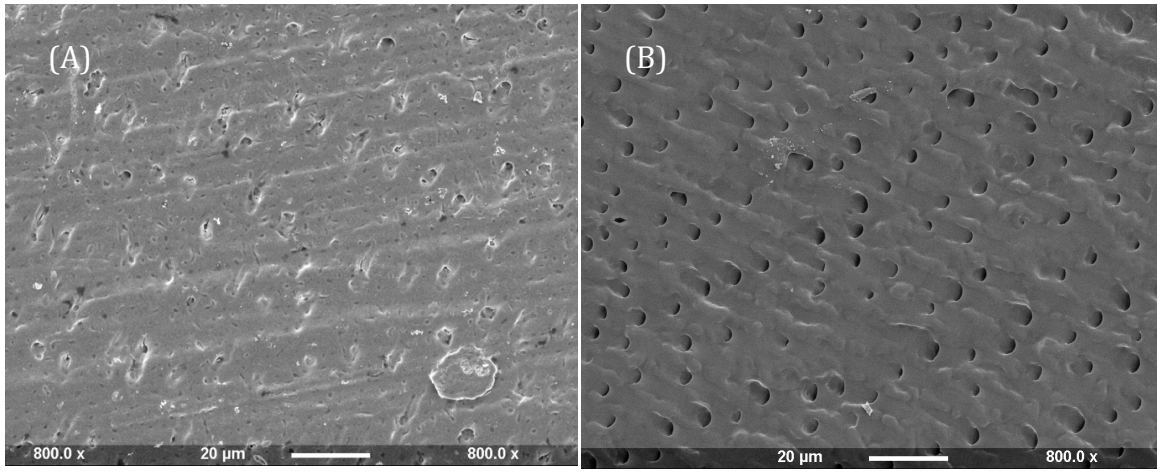

Figure 5-4: SEM images of dentinal surface of control tooth after demineralisation with phosphoric acid. (A) without deproteinisation. (B) with deproteinisation by using 6.5% NaOCl for 5 seconds.

5.2 Application of the Demineralisation Protocol on Control and OI / DI Affected Teeth Samples

In order to evaluate the value of the demineralisation technique and protocol for each sample, FTIR has been used pre and post demineralisation at 15 seconds of time with phosphoric acids. All the samples of each group (Control, DI type I and DI type II) has been assessed.

5.2.1 FTIR results on Control:

Examination of the data focussed on the intensities of the amide I band/peak relative to the phosphate peak. As such, the intensities of the Amide I vs Phosphate bands were measured pre and post demineralisation on the control samples. A net reduction in the intensity in the phosphate peak was observed after 15sec etching as anticipated. This implies the complete removal of minerals and exposure of collagen as shown in Figure 5-5. It is worth noting that these measurements were performed with an FTIR Attenuated

Total Reflectance which has a sampling depth of 2um. This means that we can safely assume that the surface of the dentine has been completely demineralised down to a depth of 2um.

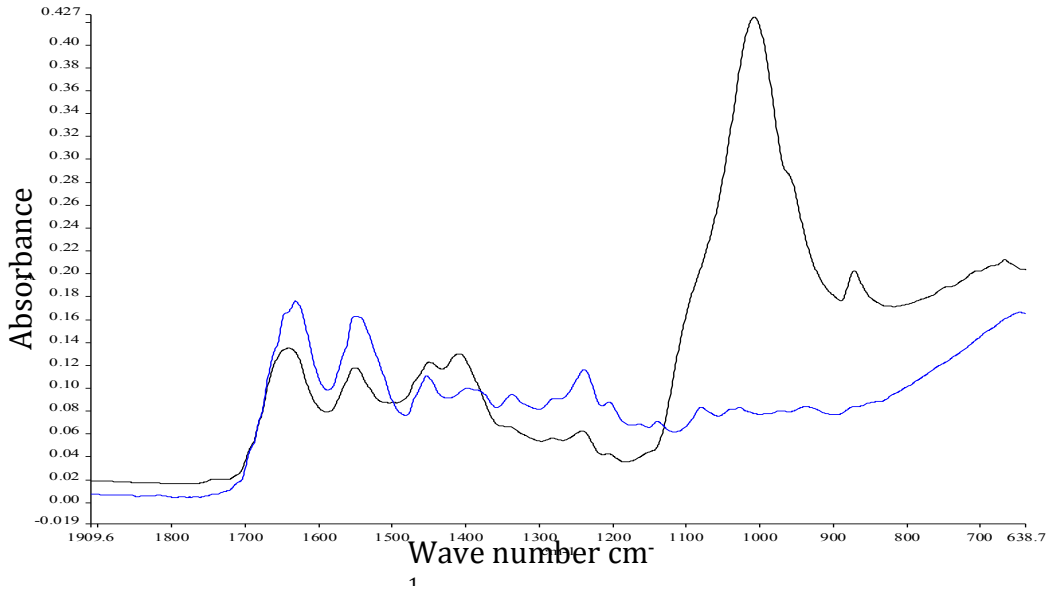

Figure 5-5 Fourier transform infrared (FTIR) spectra of control primary tooth. Spectra shown in black is at 0 min, prior to acid etching, and blue spectra is post demineralisation. Spectra after 15 s.

In order to have a good surface penetration for the infrared beam and complete coverage of the ATR diamond/crystal, the sample surface should be high- quality smooth, uniformly flat, and polished. If the sample is not in contact with the ATR diamond, air and humidity may disturb on the data and provides an inaccurate reading. Additional reports of the demineralisation mechanism are mandatory to observe whether etching power (acid concentration), sample nature, and /or collagen rate of denaturation are causative factors on exposing the collagen.

5.2.2 FTIR on DI teeth:

Similarly to the control samples, the intensities of the Amide I vs Phosphate bands were measured pre and post demineralisation on the DI samples. The results were compared with the results obtained on the control teeth. Unlike the control sample, each of the DI sample required a different demineralisation time to achieve the complete removal of the phosphate band. Thus, the demineralisation of DI teeth was performed by applying the acid etch over different times exposure: 5, 10, 15 seconds. Figure (5-6) presents the spectra of the same DI type I tooth sample comparing two different demineralisation times (5 and 15 seconds). The phosphate peak has been greatly reduced when the etching time was applied for 5 seconds, which suggested removal of the mineral and exposing collagen. However, the phosphate peak intensified and became more prominent than amide band peaks after application of dentine acid etch for additional 10 seconds and the total demineralisation time was 15 seconds. It implies that there was incomplete demineralisation on the dentine surface of the DI type II sample and the collagen was covered up by HA. Figure (5-7) shows SEM images of samples after application of 5 seconds and 15 seconds of phosphoric acid. The dentine surface presented with over demineralised surface and no collagen ultrastructure was detected.

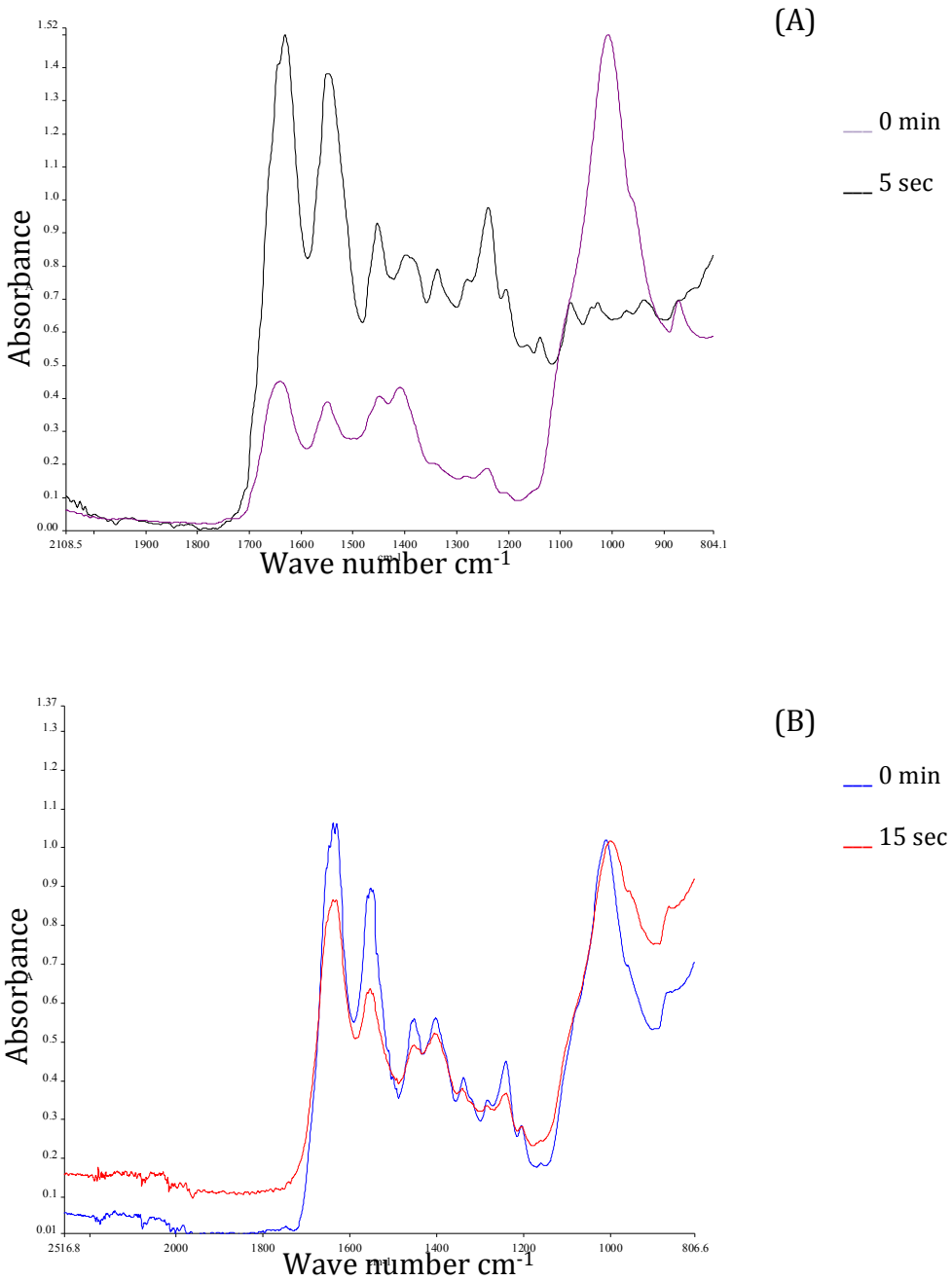

Figure 5-6 Fourier transform infrared (FTIR) spectra of DI type I primary tooth. (A)Spectra shown in purple is at 0 min, prior to acid etching, and black spectra is 5 seconds post demineralisation. (B) Spectra shown in blue is at 0 min, prior to acid etching, and red spectra after 15 seconds.

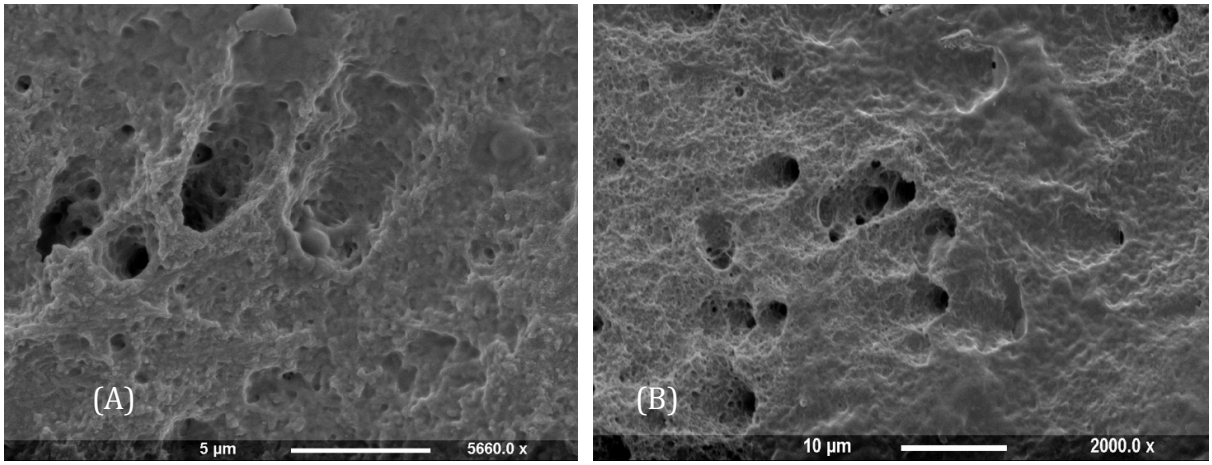

Figure 5-7 Scanning electron microscope (SEM) micro photographs of DI type I primary tooth dentine samples at different acid etching times by 37 % Phosphoric acid. (A) 15 secondes etching, (B) 5 seconds etching time.

5.3 Evaluation of Demineralisation with 17% EDTA:

In order to minimise the acid exposure in the case of the DI teeth, one sample from each group been analysed with FTIR after application of 17% EDTA. The reason of using this chelation agent is to perform the demineralisation on DI whilst maintaining an undamaged collagen network. Thus, each sample was demineralised with 17% in EDTA for 10, 15, and 30 minutes in an ultrasonication bath. Then, the demineralisation efficiency was monitored by FTIR as done previously. Figure (5-8) shows pre and post demineralisation infrared spectra obtained for the 3 groups. The complete demineralisation was observed in DI type I and DI type II in 30 minutes after the EDTA had been applied. In contrast, the 30 minutes demineralisation in control group had not been accomplished, as the intensity of the phosphate peak was still relatively high. Following the demineralisation, all the samples were imaged using SEM. The findings of DI groups demonstrated collagen scaffold presence on the dentinal surfaces.

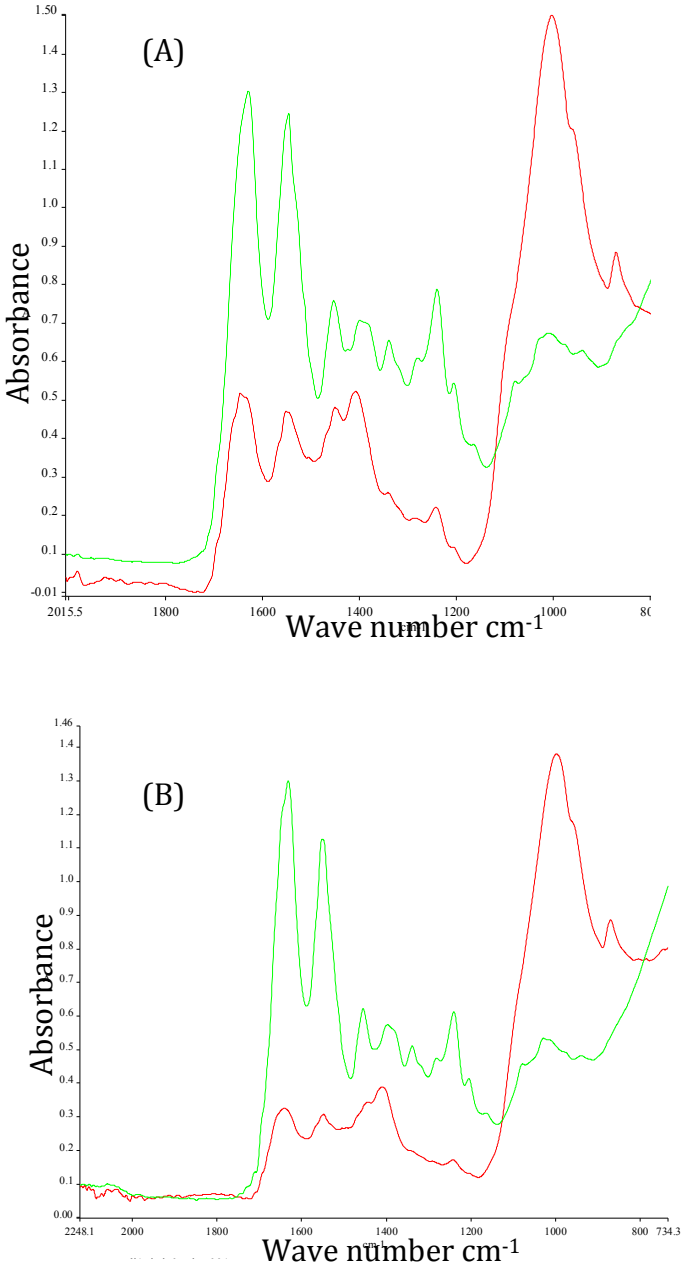

Figure 5-8 Fourier transform infrared (FTIR) spectra of DI primary tooth after applying 17% of EDTA. Spectra shown in red is at 0 min, prior to demineralisation, and Green spectra is post demineralisation. (A) Spectra after 30 minutes on DI type I, (B) Spectra after 30 minutes on DI type II.

5.4 Merits of the demineralisation protocols:

The aim of this project is to elucidate differences in collagen structure between healthy and DI primary teeth. The adapted protocol for demineralisation was to use 37% phosphoric acid under sonication to eliminate off debris and the smear layer after cutting the teeth, and assist the penetration of the etching acid on the sample surface. Phosphoric acid was preferred as it is the conventional etching material used before placing an adhesive restoration in the clinical success. The characteristic of the acid is really important in when to apply it on this study, it is stated that phosphoric acid is potent with pH of 0.9 – 1 (Ferracane et al, 2013). The phosphoric acid used in this study was in liquid form. Numerous studies have stated than the strength of the liquid acid is higher and more potent when used of the gel form of the acid (Okamoto et al, 1991 and Oyarzuan et al, 2000 and Perdigao et al, 1996). In this study, 15 seconds of application of 37% phosphoric acid was sufficient to expose the collagen and remove the mineral surface on dentine.

The deproteinisation agent of choice in this study was Sodium Hypochlorite (NaOCL) which is used in routinely in endodontic treatment. 6.6% NaOCl for 5 seconds aided in optimizing superior images due to capability of removing some minerals such as; calcium, carbonate, and magnesium (Heredia et al, 2008 and Sakae et al, 1988).

The ultrasonication method was included in this study to increase the penetration of the acid and unblock the dentinal tubules. In addition, the sonication aided in spreading the acid for the demineralisation process in several directions rather than downward direction that comes from the gravity.

However, the demineralisation time which is 15 seconds in the protocol has aided in exposing dentine of the healthy samples and it can be modulated by increasing or decreasing the demineralisation time for DI I or DI II since we are believing that the collagen structure is weakened in DI. In figure 5-9, the AFM images shows the collagen fibrils structure on DI I teeth with an evident of that the D-banding periodicity was not clear in the image (A) when it is compared to the control tooth (B), and the demineralisation protocol was implemented on both of the samples. The demineralisation protocol might be affecting on the structure of collagen in DI samples in which can produce particular damage on the sample surface and making it very soft prior topographical imaging. Otherwise, a smear layer can be created after the demineralisation protocol by etching the sample for a longer time on DI teeth or under

demineralisation of the DI samples.

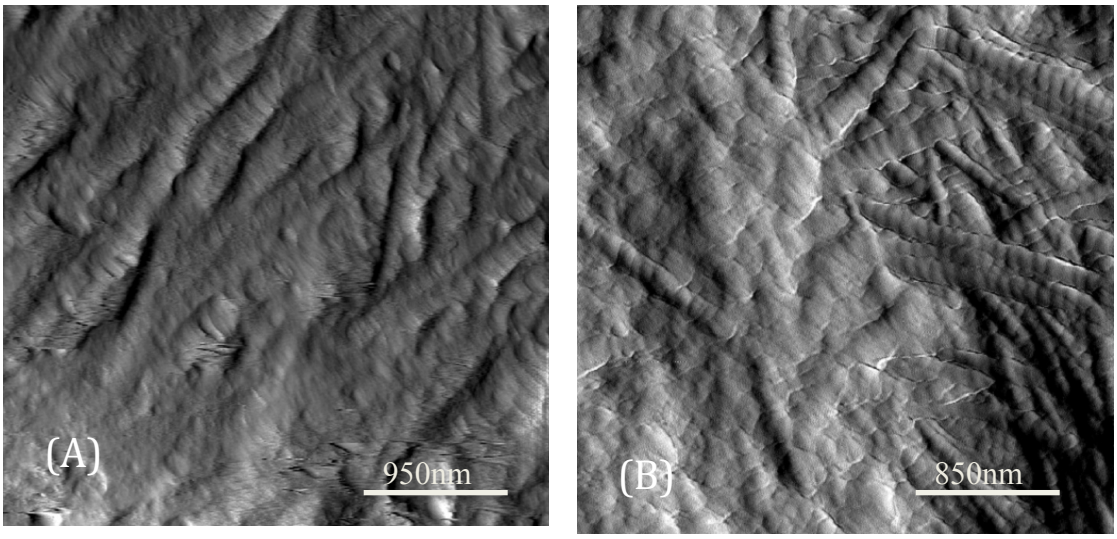

Figure 5-9: AFM images post demineralisation protocol in DI and Control healthy samples (2.6 um). (A) D-banding periodicity is distorted in DI when it is compared to the control sample (B).

5.4.1 Mineral Content

Spheroid like structures were found in DI type II when sample has imaged with AFM (Figure 5-10). It can be due to re- formation of the smear layer of HA that is created with the etching acid post demineralisation due to the delicate dentine structure or the alteration of the quality of the mineral in DI type II. In fact, these spheroid like structure might be a residual of the minerals that were resistance to demineralisation. Additional factors can influence in formation of these structures is the surface roughness, concentration of the acid etch, and time of demineralisation application. A study was done in 2005, suggested that the spheroid structures are Amorphous HA or remnant of crystals of calcium phosphate that has been created following demineralisation (Bozec et al. 2005). This can be referred as the quality of the mineral is affected by the DSPP that plays an important role in mineralisation of dentine and collagen during dentinogenesis. In addition, mutation of DSPP is responsible in DI type II

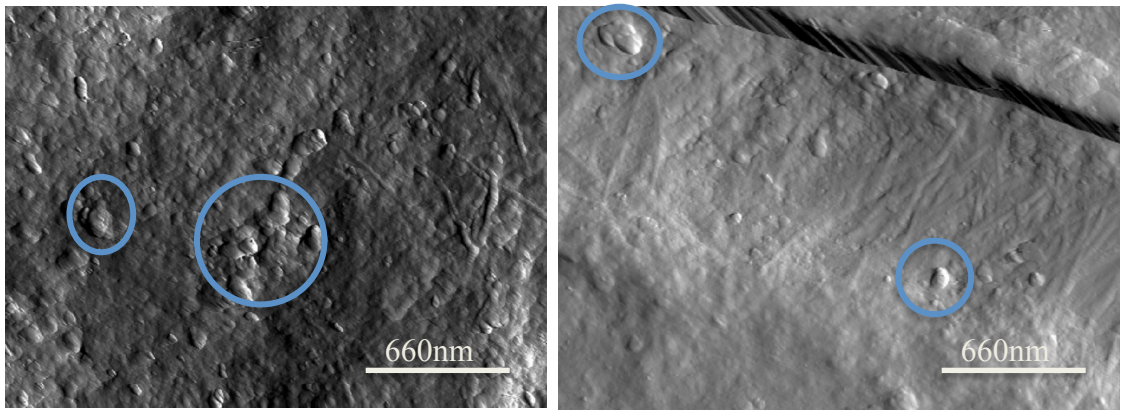

Figure 5-10: AFM images post demineralisation with phosphoric acid on DI type II. The blues circles indicates the spheroid like structures (variation of sizes) on the dentine surface.

This study studied as well the demineralisation time on the DI samples and considered that the 37% of phosphoric acid could be strong on the diseased teeth. Thus, different application times of the phosphoric acid has been employed on DI samples. It has been showed that 5 seconds is sufficient to demineralise the teeth as teeth were monitored with the use of FTIR. A study been suggested that phosphoric acid can dentaurate or distress the collagen of dentine (Okamoto et al., 1991). Therefore, application of 17% of EDTA was been performed only on DI teeth to reveal the ultrastructure of dentinal collagen network. Previous studies has been performed application of EDTA for 8 weeks on sound dentine then observe the dentinal structure under TEM (Waltimo, 1994). Another study has been done in 2013 used 17% of EDTA and stored is with control teeth for 12 months was less erosive and there was an evident of mineral removal and dentinal collagen exposure. The chelating action of EDTA will bound the non collagneous proteins together as these proteins intimately integrated with the hydroxyapatite (Harith, 2013). The findings of this study showed that the application of EDTA 17% for 30 minutes on DI teeth is sufficient to demineralise dentine and expose collagen with distorting it as it showed in the SEM images.

Chapter 6 Investigation of Collagen Ultrastructure (Topographical assessment)

After demineralisation of the samples, part of them were mounted for AFM imaging. Then the images were viewed and analysed by using Nanoscope analysis software. In addition, the number of dentinal tubules was counted, dentinal tubules and the periodicity of collagen D-banding were measured randomly from the imaged samples. However, some of the data was difficult to obtain from AFM imaging particularly the diseased teeth. Then, several modifications in the demineralisation process performed on the control and both DI teeth. Since the method of obtaining the AFM images was decelerated, the investigation and analysis was performed through SEM images mainly and few on AFM images. The reason was that SEM facilitates a greater surface area exploration and method of obtaining images is more rapid than in AFM. Images of each proposed group contain images of AFM. 5 teeth sample of each group were involved in evaluation of collagen ultrastructure.

6.1 Topographic Micro-scale Assessment (SEM imaging):

6.1.1 Collagen Structure following demineralisation with 37% Phosphoric acid:

6.1.1.a Control samples.

Scanning Electron Microscopy (SEM) imaging of samples was performed on demineralised control sample. As displayed in Figure (6-1), images showed smooth debris free surface with clearly adjusted, unclogged, and well-designed dentinal tubules in lower magnification is 650x. Relatively great amounts of dentinal tubules were distinguished with an average 6 tubules per 20 μm square area of surface. The mean values of diameter of a dentinal tubule ranged between 2 to 4 μm, and few of large tubule size up to 6 μm. Table 6-1 displayed the mean value of dentinal tubules per 20 μm square area of surface in control, DI type I and DI type II.

Sample Group	Control	DI type I	DI type II
Dentinal Tubules	6	2	2

Table 6-1: The dentinal tubules count per 20 µm square area of surface in control, DI type I and DI type II (Data extracted from 5 images in each group).

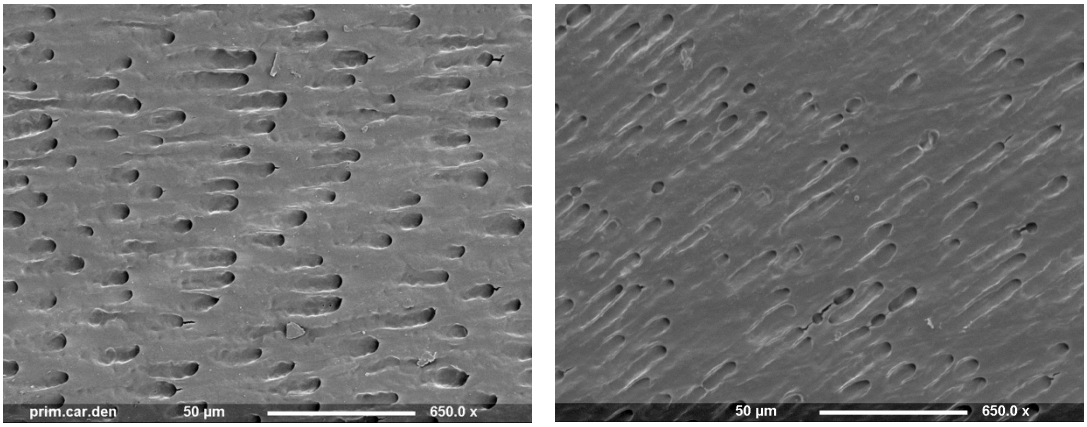

Figure 6-1: Scanning Electron Microscope (SEM) photo micrograph showing dentinal tubules distribution at different areas of demineralised control sample

In higher magnification images as 8000x and above, as shown in figure (6-3) and figure (6-2), the collagen fibrils were evidently identifies in both intertubular and intratubular zones. The collagen fibril thickness was repeatedly persistent and the mean value of diameter ranged between 20 to 80 nm

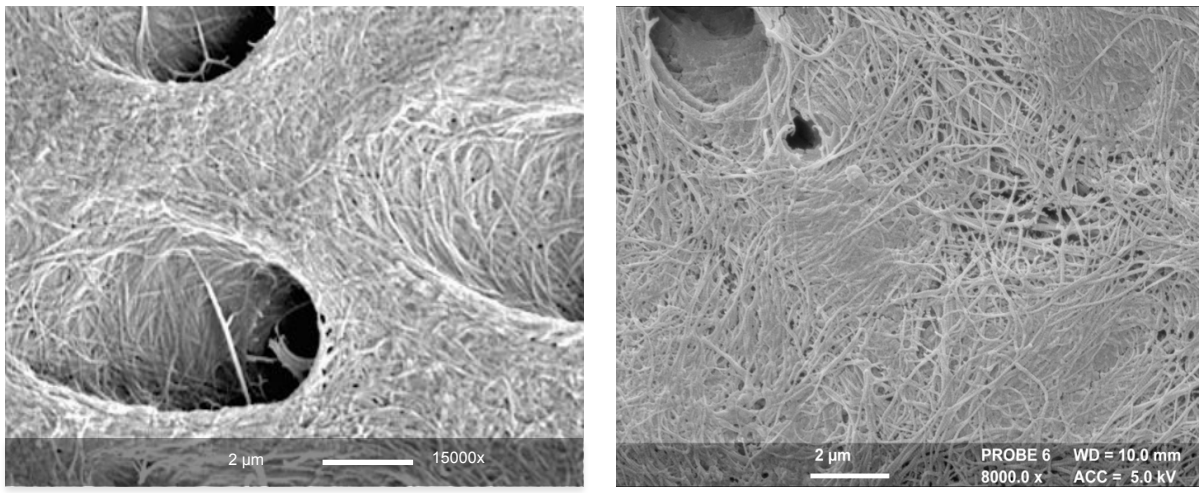

Figure 6-2: Scanning electron microscope (SEM) photo micrograph showing dentinal tubules distribution at different areas of demineralised control sample surface at higher magnifications of 15000x and 8000x

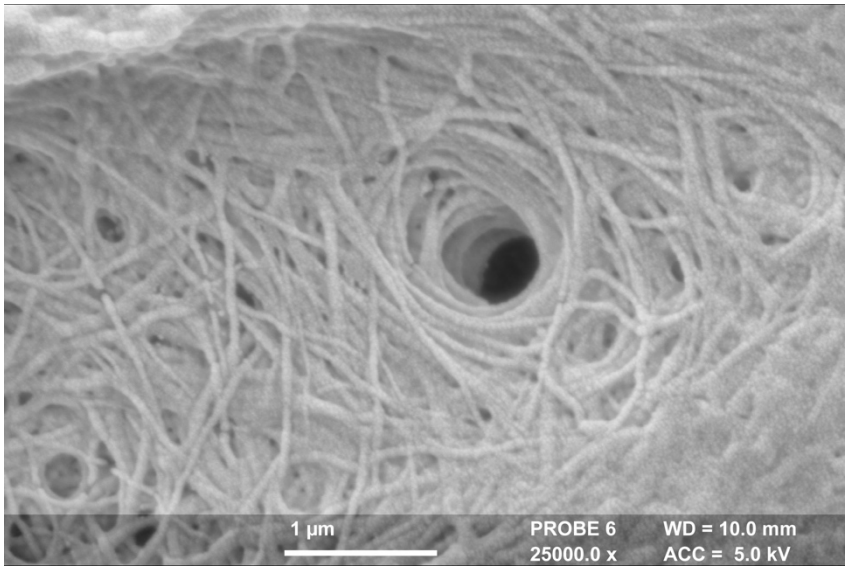

Figure 6-3: Scanning Electron Microscopy (SEM) photo micrographs showing collagen ultrastructure of demineralised control sample at high magnification of 25000x

Additional notable finding were the present on the SEM images. Numerous crack like areas on the surface of the dentine were seen as shown in figure (6-4) is called desiccation cracks. These cracks may be produced at any stage of the sample preparation such as; cutting and polishing the teeth, intense dehydration of the sample before coating the sample with metal. In addition, etching the samples will reduce the dentine integrity and with eliminating the mineral the “crack” appears on the dentine surface

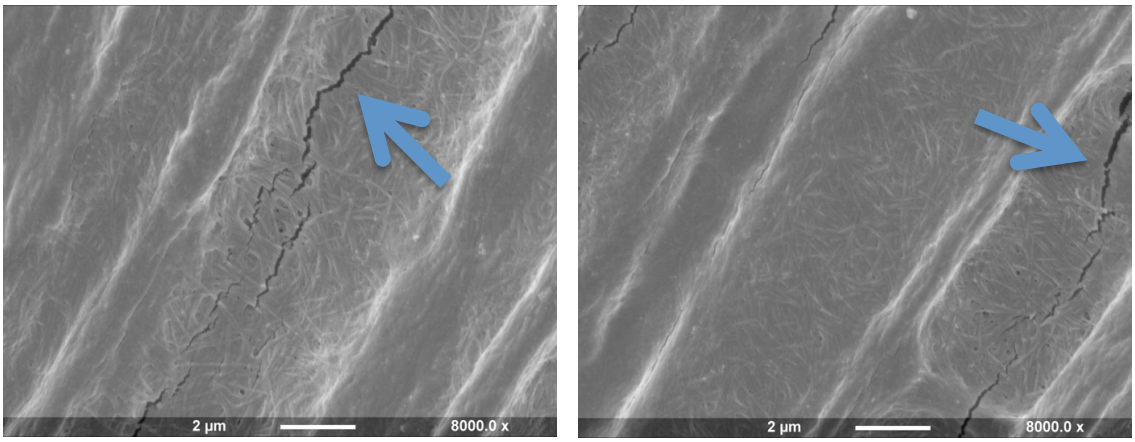

Figure 6-4: Desiccation crack like area on the dentine surface pointed with blue arrows.

6.1.1.b Samples of DI type I

The obtained images for SEM in DI type I sample were taken with high magnification to understand the dentine surface and collagen structure. In Figure (6-5), the dentine surface observed over-etch with difference in contrasts. It is suggested that there is differences in the mineral content and quality of the DI type I sample. The dentinal tubules were unclogged and visibly clear with no debris on the surface. The number of dentinal tubules was less than the control teeth with mean average of 2 tubules per 20 µm square surface.

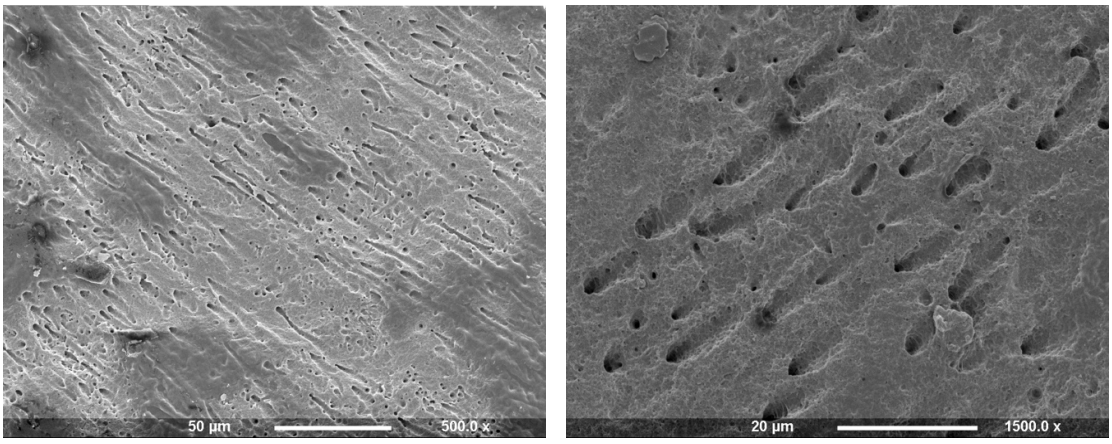

Figure 6-5: Scanning electron microscopy (SEM) photo micrographs of DI type I – associated with OI demineralised sample, showing dentinal tubules at different magnifications of 500x, and 5500x

In higher magnification images as 8000x and above, the collagen fibrils are detected in the intertubular area of dentine. In figure (6-6), and the collagen fibril is radiating within the dentinal tubules as indicated by blue arrows with no evident of intratubular collagen network. It was difficult to detect the D- banding periodicity onthe collagen fibrils. The mean value of the collagen fibril diameter ranged from 20 to 90 nm.

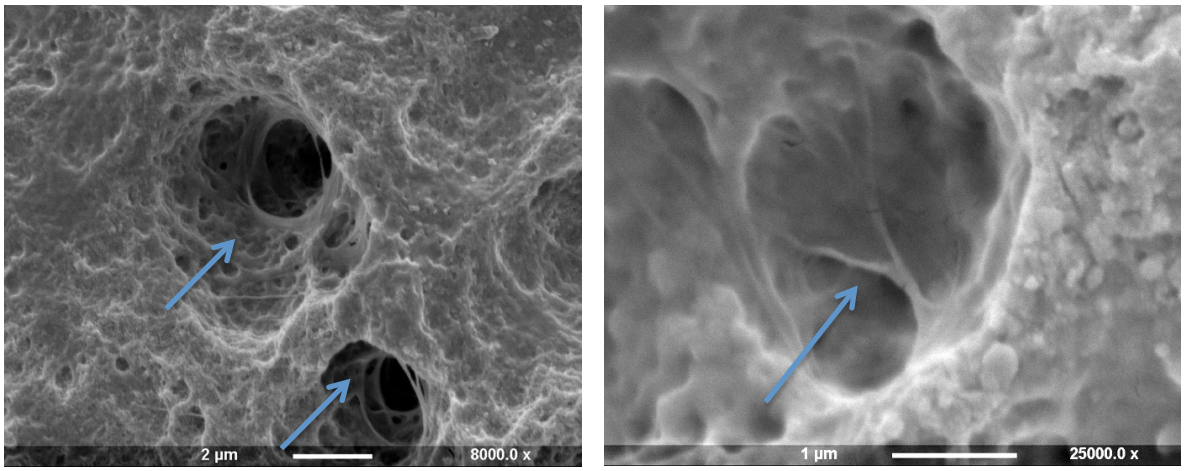

Figure 6-6: Scanning Electron Microscopy (SEM) photo micrographs showing collagen ultrastructure of demineralised DI type I sample at different high magnifications of 8000x, 25000x. Blue arrows indicated the collagen fibrils radiating in intertubular dentine area.

6.1.1.c Samples of DI type II

After demineralisation of DI type II sample, dentine showed in figure (6-7) with over-etched surface similar to DI type I findings. Unlike in DI type I, there were detected areas of clogged dentinal tubules and other areas where they were clearly unblocked. The dentinal tubules were observed with smaller number less than DI type I with an average 2 tubules per 20 μm square surface area.

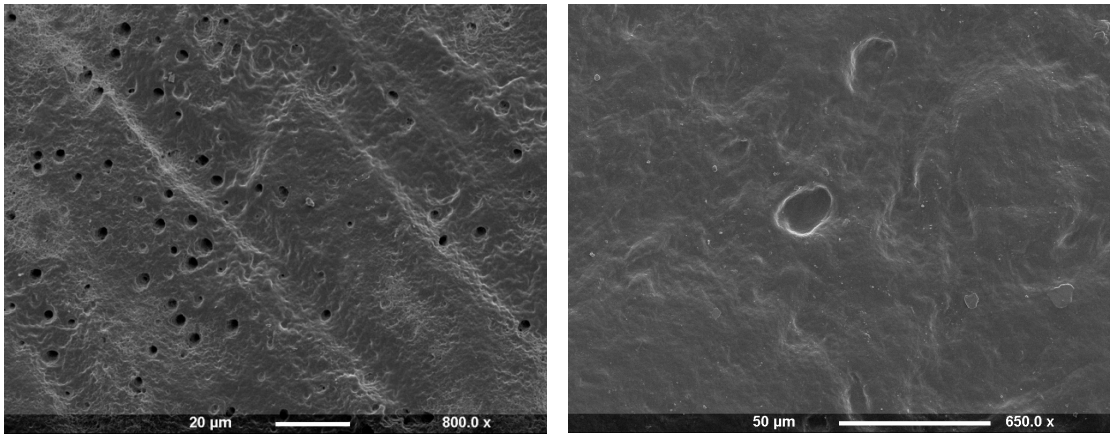

Figure 6-7: Scanning electron microscope (SEM) photo micrographs of DI type II demineralised sample showing dentinal tubules distribution at different magnifications of 800x and 650x.

In figure (6-8), a higher magnification been used on demineralised samples as 8000x and above. It was noted that the dentine surface was not uniform as showed in areas of severe over-etched (red arrow) and areas of smear layer formation on the surface (blue arrow). Similar to DI type I findings, it is suggested that the quality of the mineral HA is different than healthy teeth and phosphoric acid damaged the dentinal surface thus the collagen network. In addition, the collagen fibrils were found inside the dentinal tubules and were denaturated and conceivably gelatinised after demineralisation as indicated in figure (6-8) in red circle. Another finding was noted that dentinal tubules exhibited poorly formed and developed tubule within tubule phenomenon, or internal splitting, was also seen as indicated in the blue square.

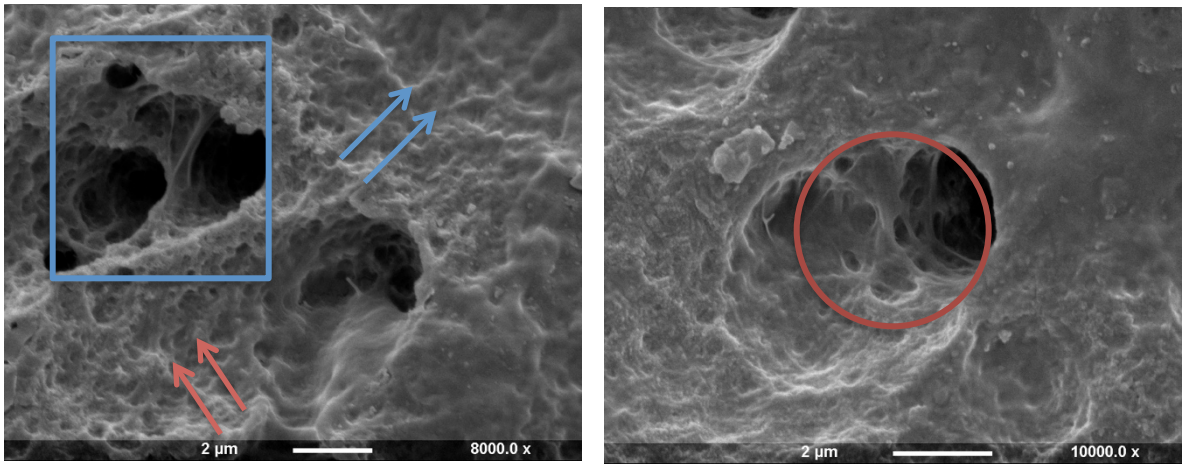

Figure 6-8 Scanning electron microscope (SEM) photo micrograph of DI type II demineralised sample showing '' tubule within tubule'' branching phenomenon and malformed dentinal tubules ultrastructure at different magnification of 8000x, 10000x.

6.1.2 Collagen structure of DI teeth post Demineralisation with EDTA 17%:

It has been noted that each tooth has reacted differently after application of demineralisation protocol with 37% of Phosphoric acid. Since the dentine structure is compromised in both types of DI teeth, the mineral quality and content could be affected following the demineralisation. In addition, the dentine etchant could be strong and can damage the collagen ultrastructure network. For that, the concept of using 17% of EDTA has been applied on the DI samples. EDTA 17% was applied on the polished samples for 30 minutes and monitored by FTIR. The Phosphate and Amide I peak been evaluated to test on the effective of demineralisation. The samples only imaged with the use of SEM to obtain a faster rate topographic images. In figure (6-9). The dentine surface of DI type I sample showed smooth unclogged dentinal tubule (A) and DI type II dentine surface showed similar to DI type I findings.

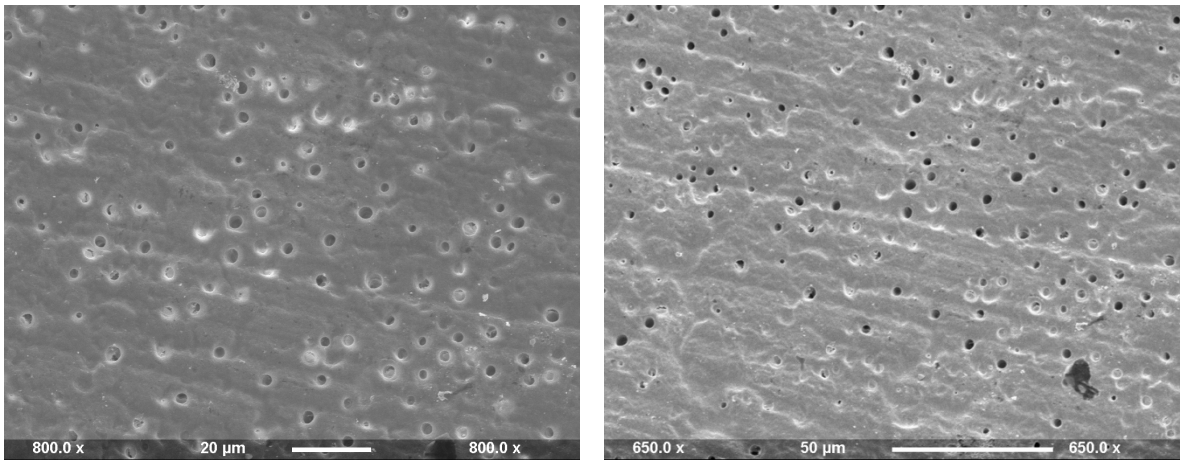

Figure 6-9 Scanning electron microscope (SEM) photo micrographs of (A) DI type I demineralised sample showing dentinal tubules distribution at magnifications of 800x and (B) of DI type II at magnification of 650x

In figure (6-10), the image DI type I sample showed collagen network and D- banding periodicity was visible. The collagen was closely packed located in both intertubular and intratubular areas on dentine surface, and the behaviour of the collagen organisation was similar to the observed collagen fibrils of control samples. In DI type II samples, the results is extremely similar to DI type I. However, local swellings of collagen fibrils observed in both DI samples as indicated in red circles.

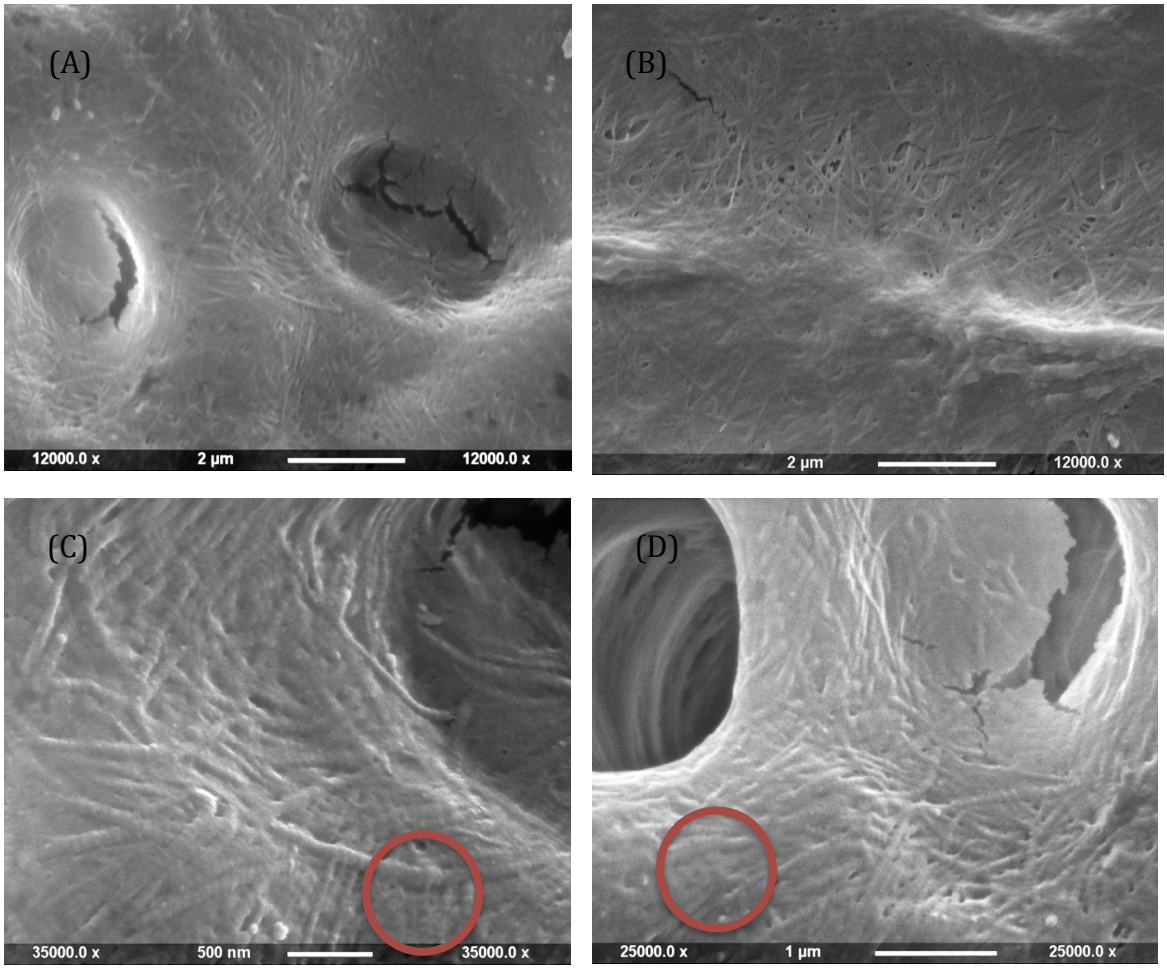

Figure 6-10 Scanning Electron Microscopy (SEM) photo micrographs of demineralised DI sample showing collagen ultrastructure (A and C) DI type I at high magnifications of 12000x and 35000x, and (B and D) DI type II at magnification of 12000x and 25000x. The red circles indicates local swellings of collagen fibrils.

6.2 Topographic Nano-scale assessment (AFM imaging):

6.2.1 Control samples:

The advantage of the AFM images that is gives a superior imaging quality and the ease of investigating the sample in high resolution..

AFM images for control teeth were taken prior and post demineralisation. In Pre-demineralisation as in figure (6-11), images showed the dentinal tubules that were concealed with a mineral layer. The images were acquired in different magnifications in figure 4-. The images interpret that the smear layer is blocking the dentinal tubules and the collagen structure not recognized in these images.

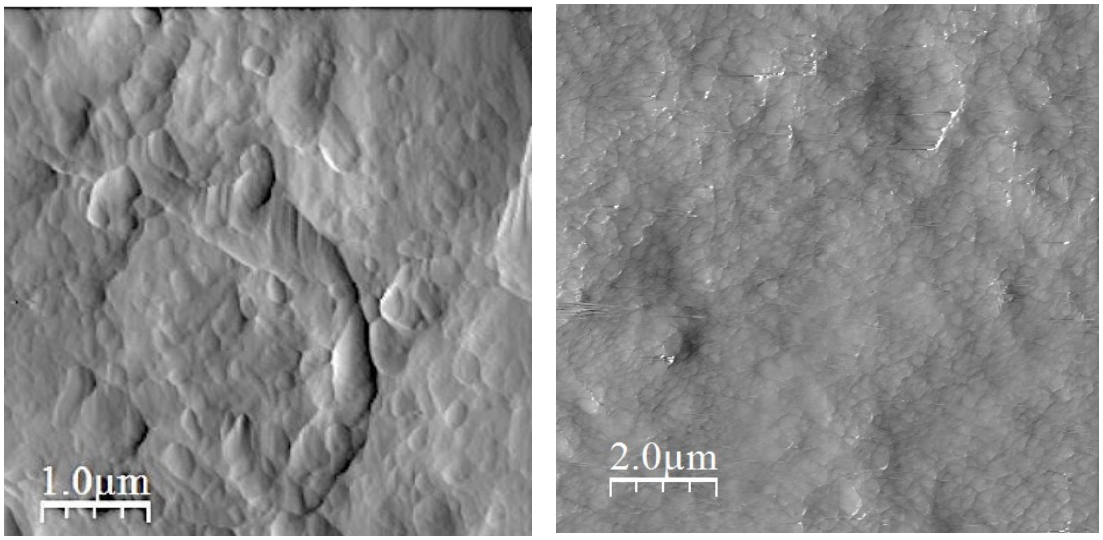

Figure 6-11: images at different magnifications of a control sample before demineralisation protocol is implemented.

The demineralisation technique was applied on the sample, 37% of Phosphoric Acid for 15 seconds in a sonicated bath followed by 6.5% Sodium hypochlorite for 5 seconds. Images were taken topographically and the dentine surface is clear from debris. The collagen fibril structure is recognised in various images and the D-band periodicity is uniform and visibly aligned as in figure (6-12).

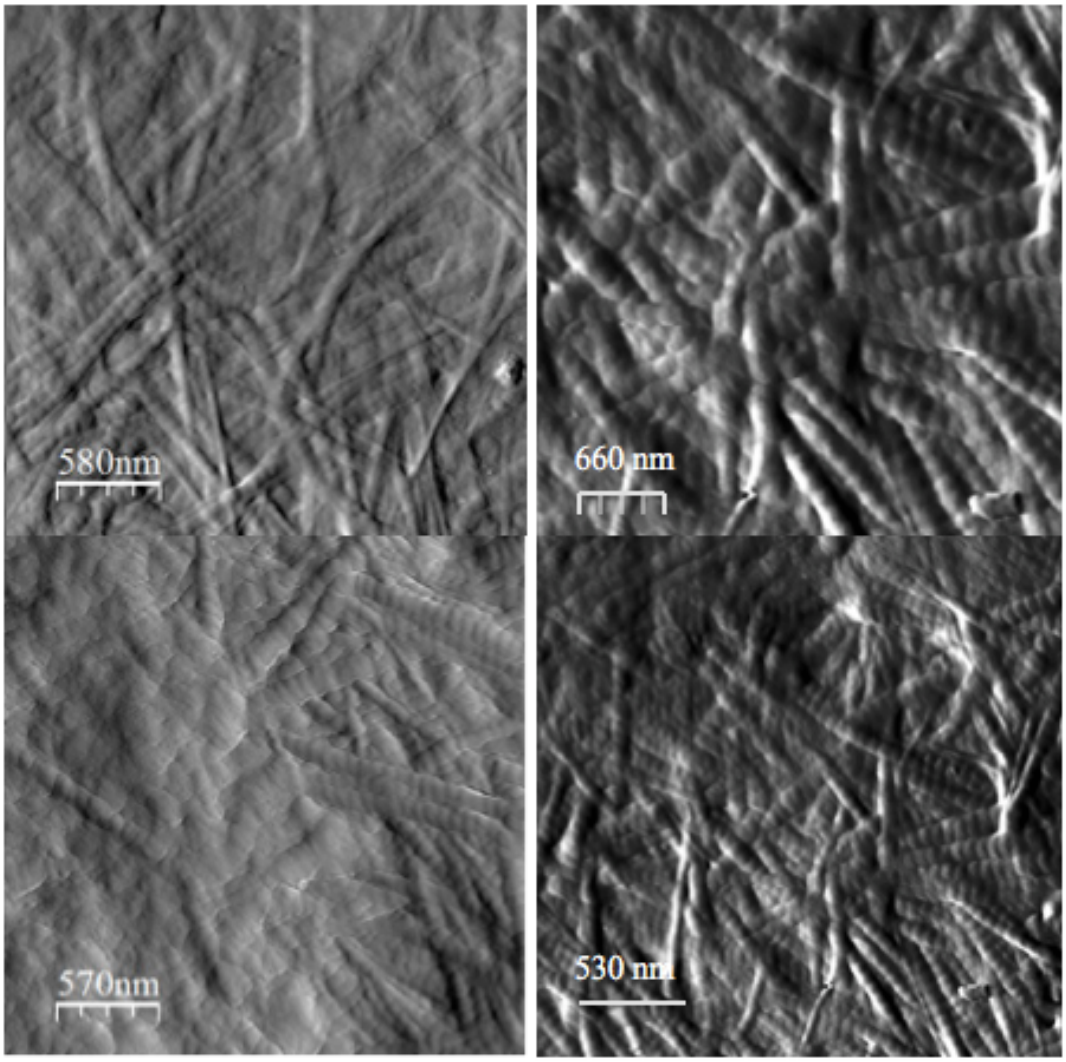

Figure 6-12: Atomic Force Microscopy (AFM) images at various magnifications of a control samples after demineralisation, and verifying effectiveness of standardized protocol on healthy teeth.

6.2.2 DI type I samples:

After applying the demineralizing protocol on DI I teeth, images were taken in different length scales under AFM. The D-banding periodicity of the collagen fibrils is not very visibly revealed in different areas in the images as indicated by arrows. The collagen structure may be different in DI teeth when it is compared to the control teeth. In figure (6-13), collagen fibrils were and difficult to identify them. The D-bandings periodicity was not clear as shown in control image.

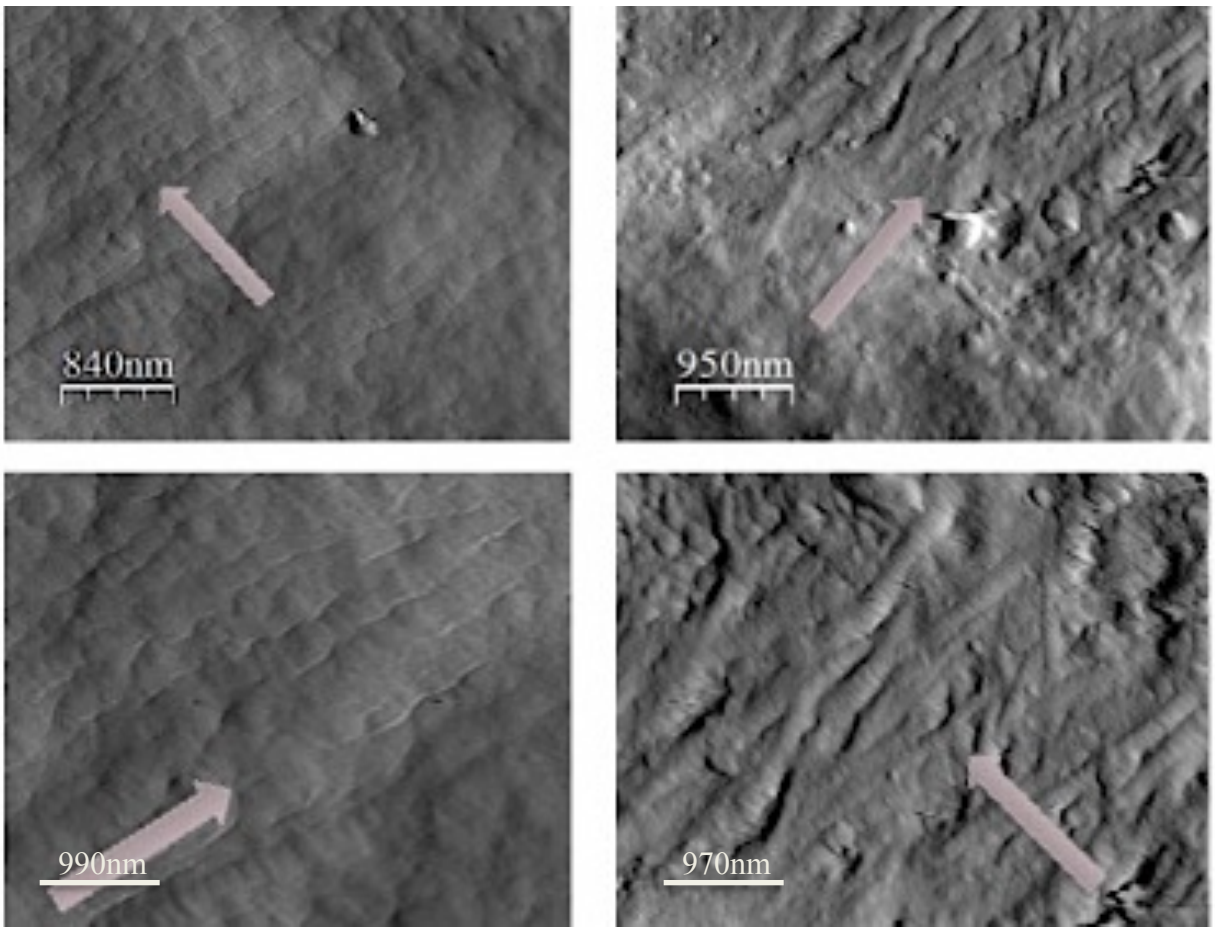

Figure 6-13: AFM images showing collagen fibrils in different magnification DI I. (collagen fibrils discontinuity and unusual morphology as indicated by arrows)

6.2.3 DI type II samples:

It was challenging to recognise the collagen fibrils including their periodicity of the D-bands in the images of Figure (6-14). The presence of spherical substances with a different variation of sizes as implied in circles that are found some areas of the sample surface might indicates that the dentine structure and quality is different than in healthy and DI I teeth.

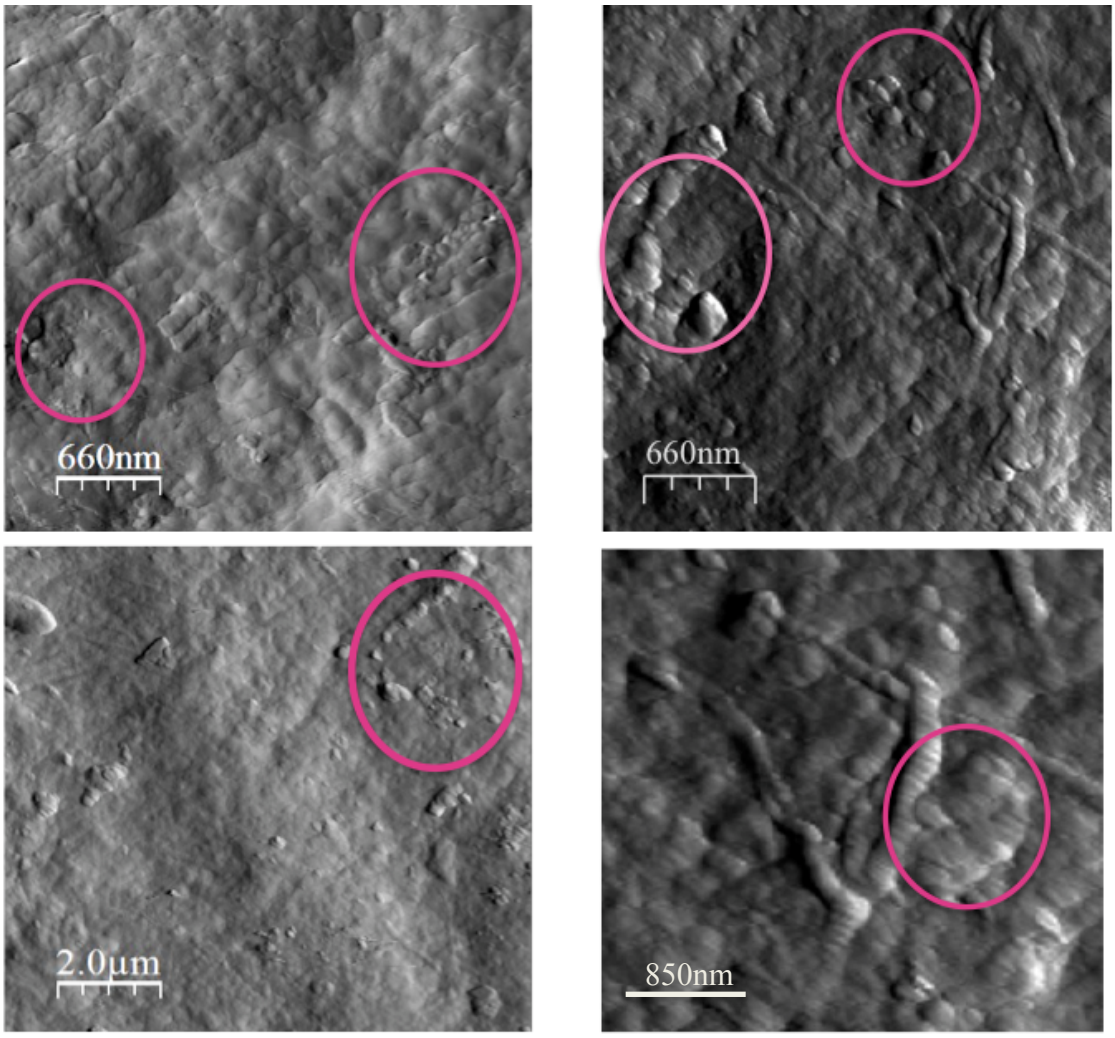

Figure 6-14: AFM images showing collagen fibrils in different magnification DI II. Collagen fibrils and the D-banding periodicity was not clear and spherical substances was on the sample surface as indicated by the circles.

6.3 Ultrastructural findings in Control, DI type I, and DI type II samples:

The obtained results of the dentinal tubules numbers, diameter and the collagen fibrils diameter from each group were investigated by measuring them at numerous random locations on the sample surface. The data was assessed through SEM and AFM imaging and a statistical analysis been performed and graphs has been created as presented for control, DI type I and DI type II groups.

6.3.1 The Number Dentinal tubules:

The dentinal tubules numbers were varied among the three groups, this is due the alteration of the dentinal structure in DI teeth when compared to control. The dentinal tubules count been performed by using lower magnification of 5 images in each group and the amount of dentinal tubules in per 20 µm square area were counted form the SEM images. The increased number of dentinal tubules found in control teeth N= 972, followed by DI type I N= 276 and the least dentinal tubules count found in DI type II N= 221.

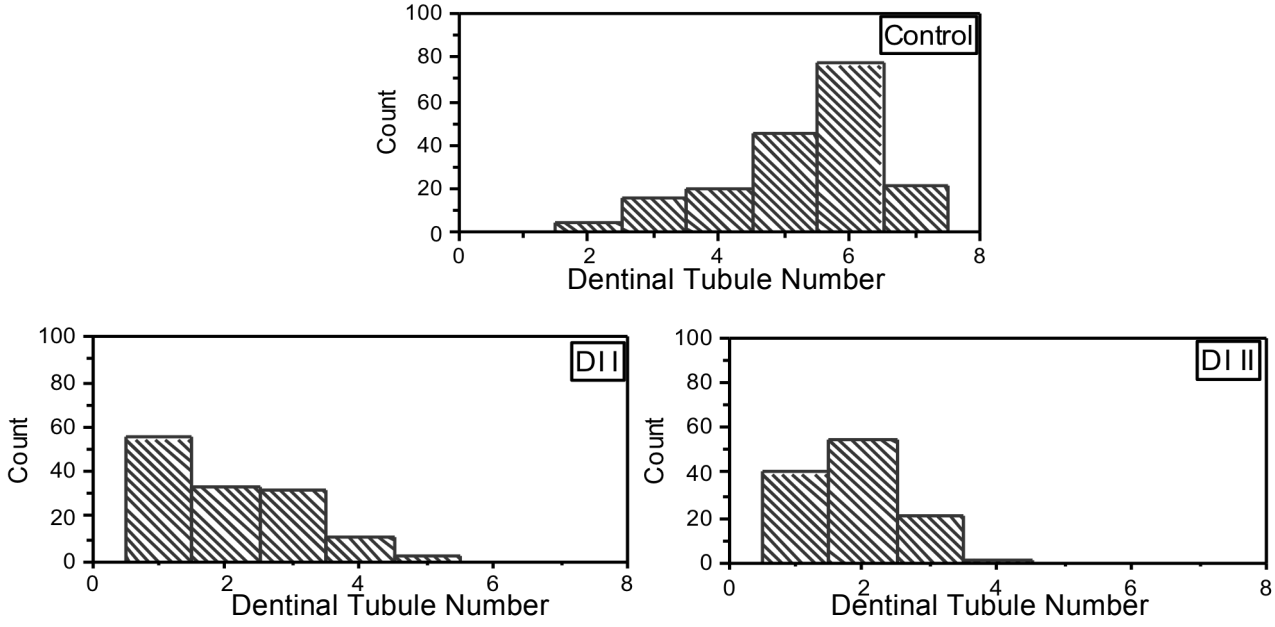

Figure 6-15: Three graphs displaying the count of dentinal tubules number per 20 µm square area in control, DI type I and DI type II.

In Figure 6-15, statistical analysis of the samples was carried out and dentinal tubules number represented. In control teeth: 972 of dentinal tubules were found in different location with a median of 6 tubules per 20 μm square area. However, dentinal tubules count of DI type I 276 with a median of 2 tubules per 20 μm square area. Finally, similar finding with DI type II dentinal tubule (n= 221), with a median of 2 tubules per 20 μm square area of surface.

Maan Whitney U test analysis was carried out to compare the data findings between the groups and Kruskal Wallis test. This test has been chosen because the samples where not equally distributed and to compare the values. There was a significant difference in the dentinal tubules count per 20 μm square area between control and DI type I, control and DI type II and between both DI groups as plotted as a boxplot graph in figure 6-16. It has been noted that both DI groups represented with equal median results.

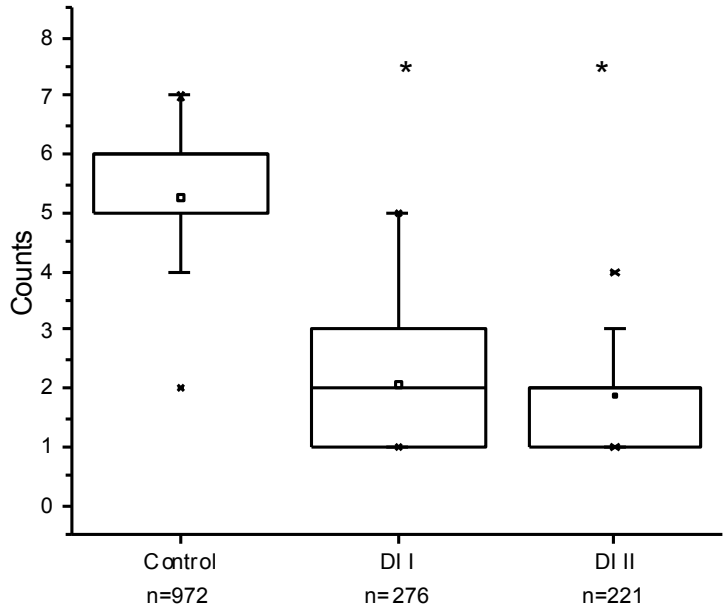

Figure 6-16: Kruskal Wallis Test Analysis of dentinal tubule number in control, DI type I, and DI type II samples

6.3.2 The Dentinal Tubule Diameter:

There were evident variations of dentinal tubules diameter between the three groups. the calculation of dentinal tubules diameter assessed by measuring a multiple random SEM imaging.

In figure 6-17, the statistical analysis showed that in control teeth; 1020 dentinal tubule diameter were assessed and measured, and the diameter ranged between 1 µm to 5.5 µm with the highest percentage at 3 µm. The number of measured dentinal tubules of DI type I was 217 and their diameter ranged between 0.1 to 6.6 µm, with a the greater percentage between 0.1 µm to 1.5 µm. Lastly, 107 of dentinal tubules of DI type II were measured and their diameter ranged between 0.1 µm to 5.5 µm with a larger percentage between 1 µm to 4.5 µm.

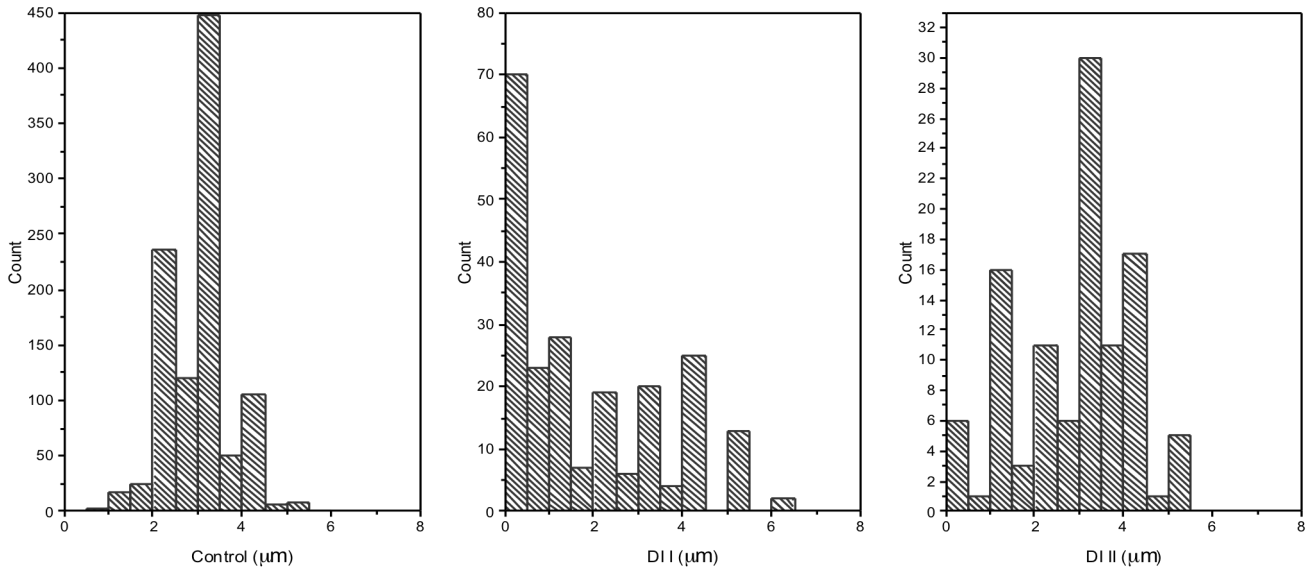

Figure 6-17 Three graphs presenting dentinal tubules diameter of control (n=1020), DI type I (n=217), and DI type II (n=107).

Then, Kruskal Wallis test and Maan Whitney tests were carried out and plotted as in figure 6-18. The control, DI type I and DI type II values were compared and the Median of the dentinal tubules represented differently. There was a significant difference between control and DI type I group, as well as a significant difference between DI type I and DI type II. However, there the dentinal tubules diameter difference between the control and DI type II was insignificant.

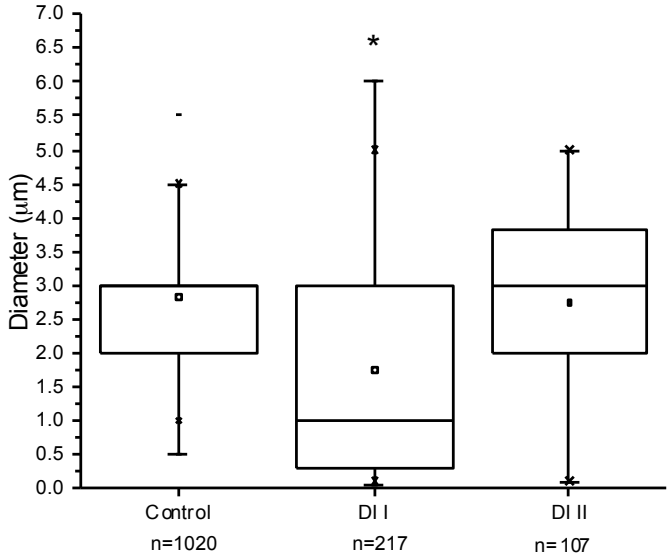

Figure 6-18: Kruskal Wallis Test Analysis of dentinal tubule diameter in control (Median = 3), DI type I (Median = 1), and DI type II (Median = 3) samples. Noting the similarity of the Medians of control and DI type II samples.

6.3.3 The Diameter of Collagen Fibrils

Collagen fibrils diameter were assessed and measured randomly at various non-specific location of the dentinal surface. The data was obtained through SEM and AFM imaging from the three groups. 150 collagen fibrils were measured from control, DI type I and DI type II samples and a statistical analysis was performed as showed in figure 6-19.

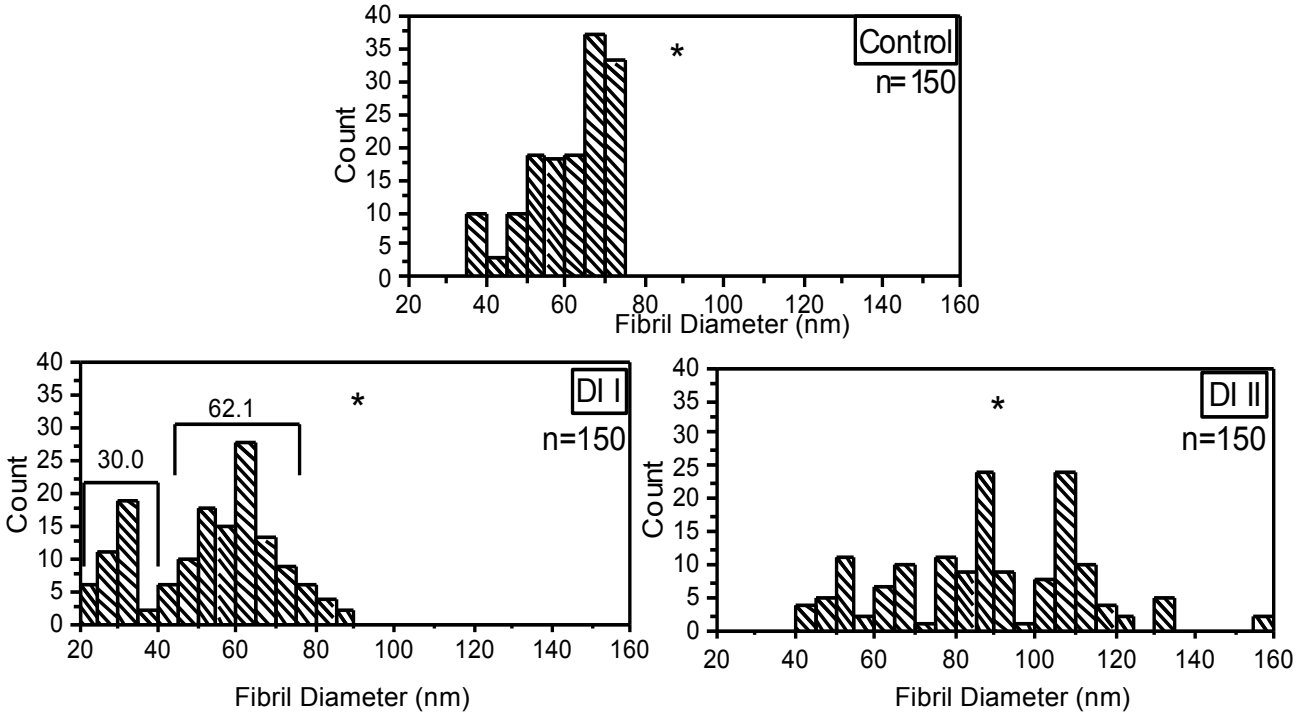

Figure 6-19: Three count graphs presenting collagen fibril diameter of control, DI type I, and DI type II.

In figure 6-20, the collagen fibril diameter was measured and ranged between 35 nm to 75 nm. The greatest percentage in diameter width was counted between 60 nm and 75 nm. DI type I collagen fibrils count varied between 20 nm to 90 nm with the highest percentage found between an average of 30 nm and 62.1 nm. Finally, DI type II collagen fibril diameter ranged between 40 nm to 160 nm with the greatest percentage found at 85 nm and 110 nm.

Kruskal Wallis test analysis was performed, the Median in control group was 88.8, DI type I was 55.5, and DI type II was 64.8 nm. The results displayed a significant different in collagen fibril diameter between control and DI type I samples, control and DI type II samples, and between DI type I and DI type II samples.

6.3.4 Measuring the D- Banding width:

The D-banding periodicity is a feature of collagen type I and it is a result from alternated self-assembly of individual collagen molecules into a greater fibril. The D-banding distances data has been measured by taking a line profile that measures grey value in a distance (500 nm) to calculate the width of the D-band. Ten randomised collagen fibrils been measured in every image and five images been assessed in each group. In this study there was a substantial difference in the D-band width that varied from 65 nm to 74 nm. Obtaining a baseline data of a control healthy tooth is crucial for future comparison between normal and DI collagen fibril D- banding width. Thus, indicates collagen malformation.

In figure (6-20), the collagen type I fibril in control teeth and dentine. The D-banding distance in collagen fibril is approximately 71.4 nm. control (average is 74.0 ± 6.1 nm)

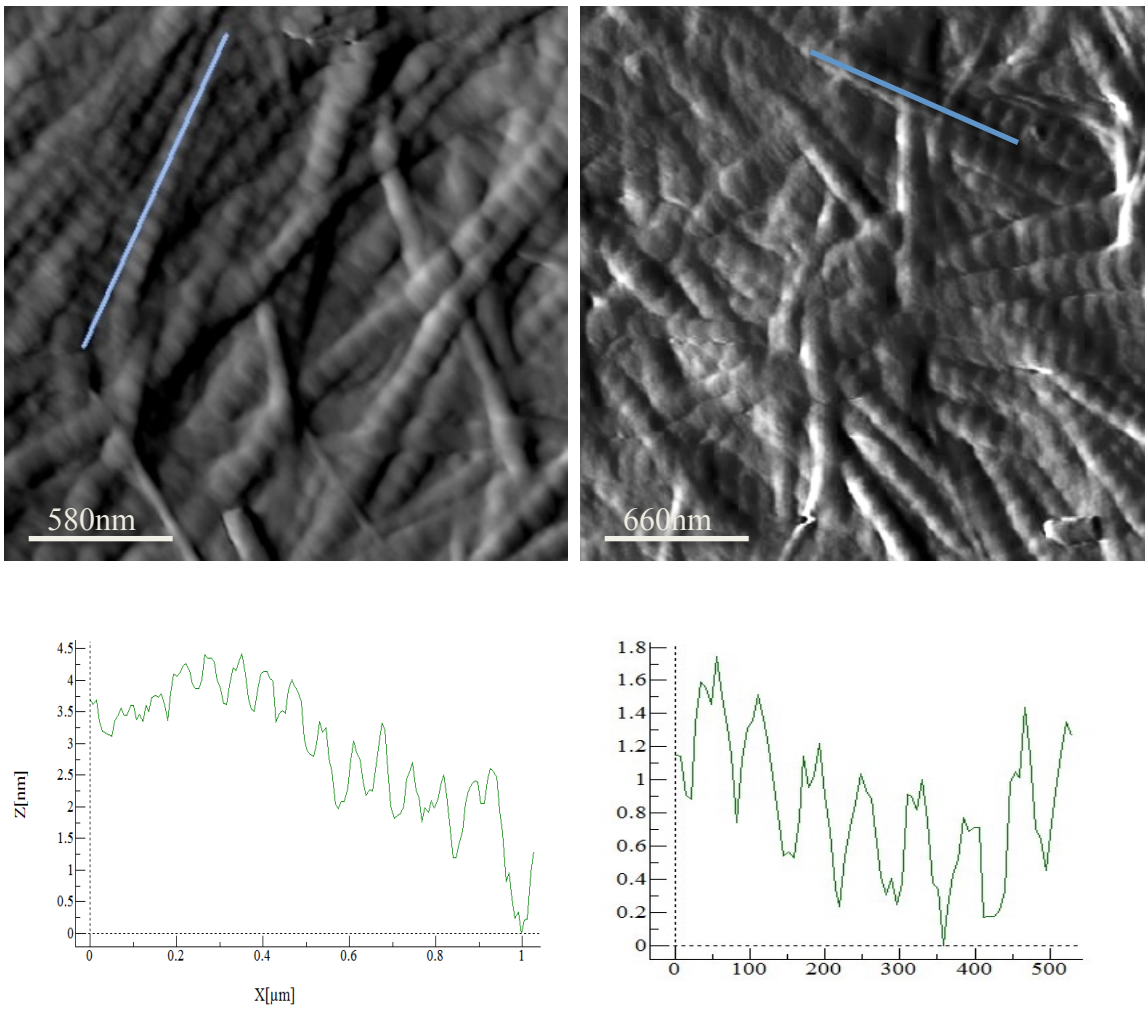

Figure 6-20: measuring the D- band width by taking line profile for each collagen fibril.

6.5 Ultra structure findings and comparisons:

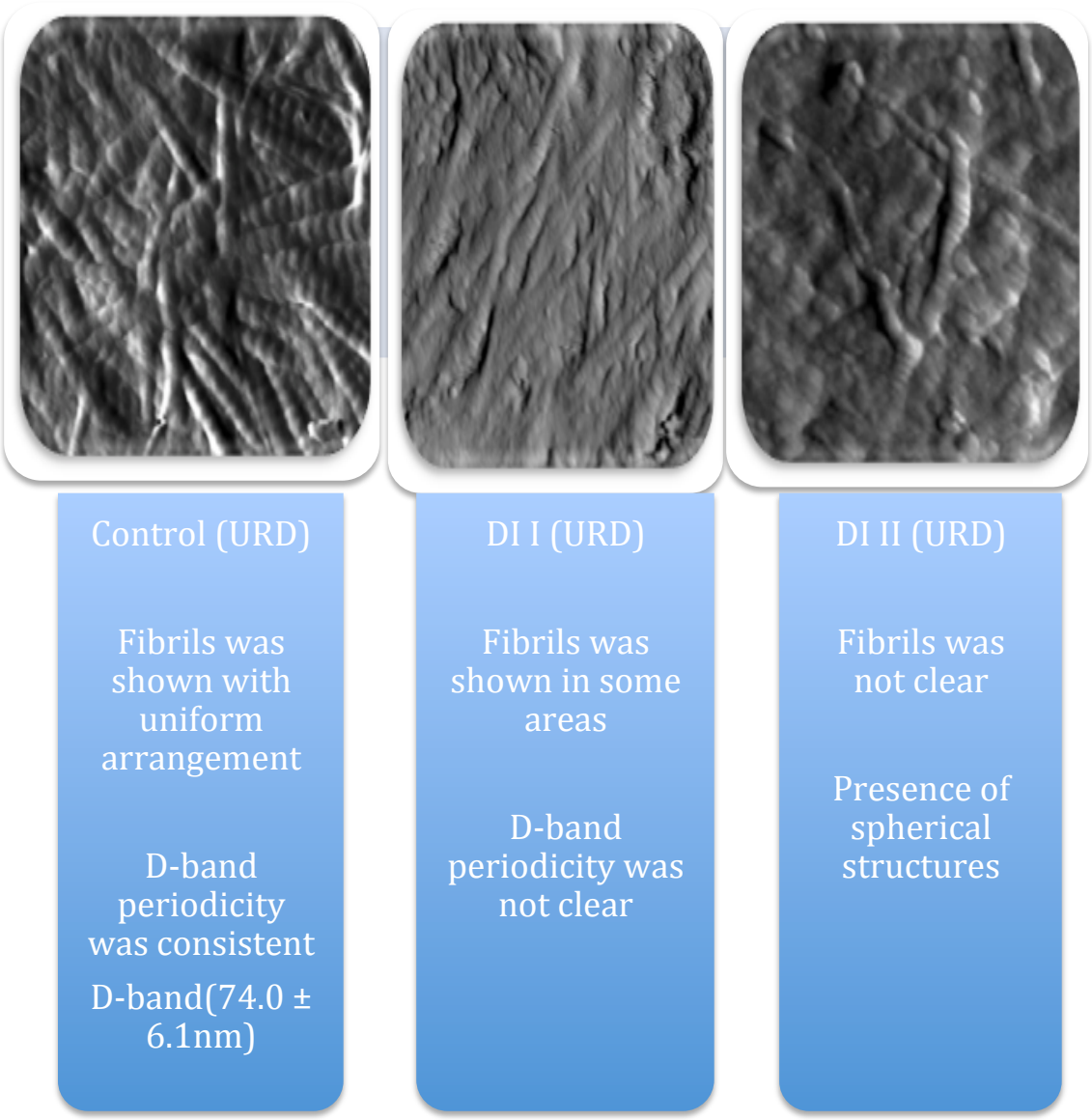

Figure 6-21: Comparison between collagen fibrils in control and both DI types in primary teeth.

6.6 Discussion on Topographical assessment results:

6.6.1 Dentinal Tubules Ultrastructure

Researches of the dentinal structure were established several years ago with various techniques and equipment such as; light microscopes, immune-fluorescence microscopy, microradiograph, and recently with SEM, AFM, Transmission Electron Microscopy (TEM). Most of the studies were employed to observe the dentine surface structures such as dentinal tubules distribution, diameter size, dentinal tubules branching, and observe dentine in different locations as in coronal, middle and root dentine. In addition they also studied the differences of dentine structure in primary, permanent teeth. Previous studies have indicated that the numbers of dentinal tubules increase relatively when they approach to pulp (Schilke et al, 2000). This study showed that the number of dentinal tubules is few in DI teeth when compared to healthy teeth when it's close to the pulp. This is might be due to over-mineralisation and resultant pulp obliteration.

The branching of the dentinal tubules in this study was also seen in every group. The tubule within tubule and inter- tubular branching was recorded clearly in control and in DI type II. As well as comparing the sizes of the dentinal tubules diameter were significantly larger in sound primary dentine than in both DI types. These tubules were found larger in the middle dentine area in centre part of the tooth. Previous study was done with X- ray microtomography (XMT) found similar results regarding dentine diameter size in sound healthy teeth (Davis et al, 2015).

6.6.2 Collagen Ultrastructure:

The process of imaging the samples is by using the contact mode. The cantilever is in contact with the sample surface in which translate it to an image by the feedback loop to a topographic image. Choosing the contact mode is preferred while the samples are solid and static. After applying the demineralisation protocol on DI teeth, it is suggested that surface of the sample and the collagen is soft and contact mode may harm and damage the collagen. In future, Intermittent contract (tapping) AFM mode might be used.

The D-banding distances data has been measured by taking a line profile that measures grey value in a distance (500 nm) to calculate the width of the D- band. Previous studies on bone found the D- band distance in collagen fibril is approximately 67 nm. In this study there was a significant difference in the d-band width that varied from 65 nm to 74 nm. Obtaining a baseline data of a control healthy tooth is crucial for future comparison between normal and DI collagen fibril D- banding width. Thus, indicates collagen malformation.

From previous literature, we know that the D banding periodicity average of the normal collagen fibril is always consistent. The D-banding periodicity of the dentinal collagen in DI has not studied before. Shapiro studied the D- banding periodicity on collagen of bone in OI patient. It has been observed that there is broadening and space variability between the D-bands (Shapiro, 2013). A similar result has been noticed in this study regarding the broadening of D- banding in DI type I teeth. As well as the morphology of the collagen fibril is different than the control group. Presence of wide parts or swelling on some areas on the fibril or and areas of constricted fibril diameter or incoherence. In 1995, a study has been established on collagen fibrils on bone and atypical fibril morphology has been found with sudden breakage (Cassella et al, 1995). The morphology of bone collagen fibrils in OI type III showed to have a unusual organization, described as fused, composite fibrils. The collagen fibre bundles were also distorted and swirled (Sarathchandra and Pope, 2005).

In figure 6-17, the collagen type I fibril in both rat tail and dentine. The classic banded fibril structures can be observed clearly in rat tail collagen, which demonstrates the high degree of structure and regularity possible in collagen fibres. The D-banding distance in collagen fibril of rat tail is approximately 66.6 nm. While in dentine, the D- band width was measured approximately 71.4 nm in a control healthy tooth.

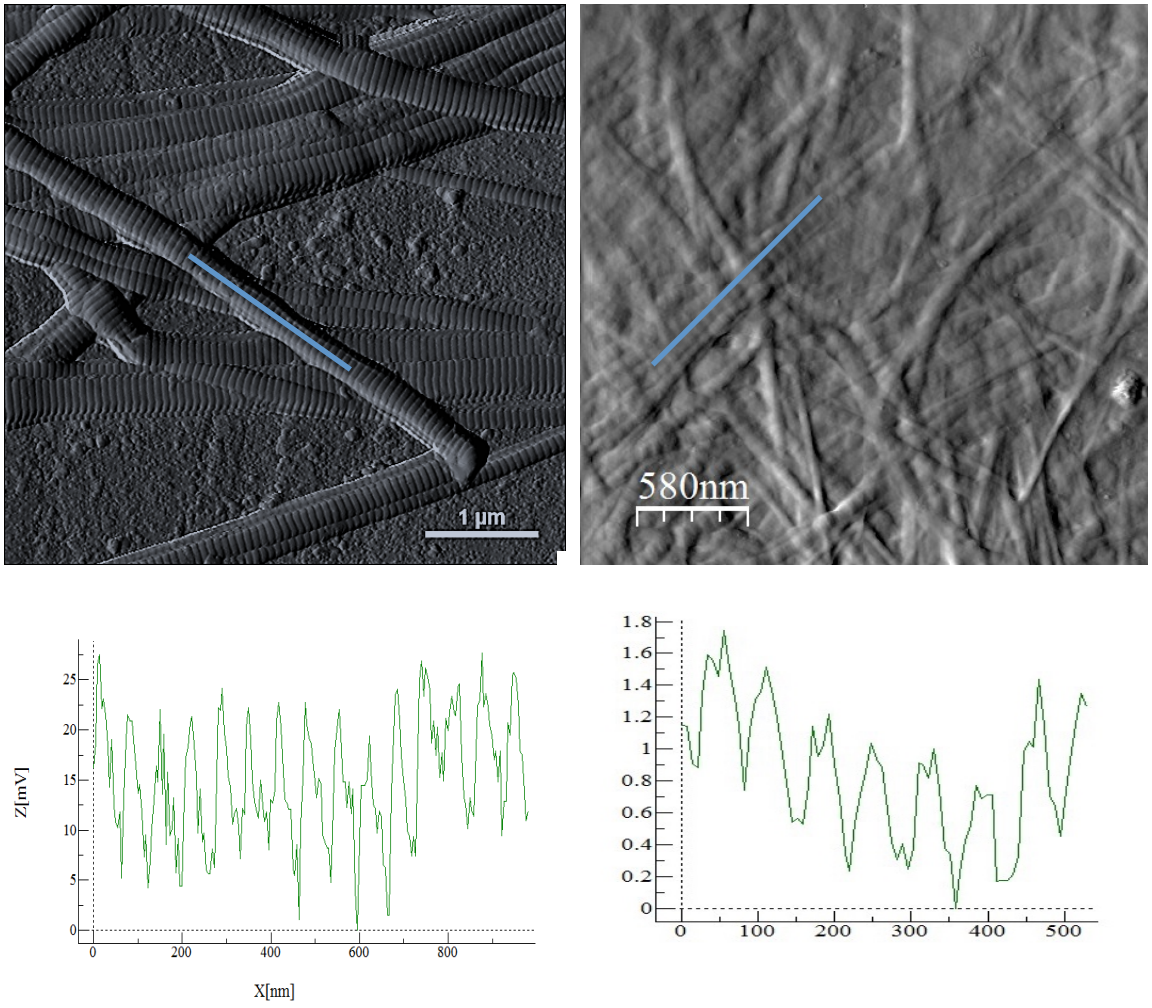

Figure 6-17: Line profile for Collagen fibrils in rat tail and dentine (line profile in rat tail was 66.6 (A), and in dentine is 71.4 (B) (the image of Rat tail adapted from A. Strange)

A previous study was established in 2012, the results in OI affected mice that presented significantly greater variability of D banding distances of bone collagen fibril (ranging from 56 to 75nm) (Wallace, 2012). There was a significant difference in collagen fibril morphology and distribution due to mutation of COL1A1 in gene (G349C) (Wallace, 2012).

Further investigations are currently on going to find the topographies in the ultrastructure morphology to the modification in the nano-scale mechanical behaviour of type I collagen.

Chapter 7 Challenges:

1) Limited Number of samples

The major limitation of this study that should to be emphasized was the small sample number. Great effort was carried out to obtain DI teeth from patients. However, obtaining DI teeth was only possible if teeth required extraction as part of their dental treatment plan, or donated their exfoliated primary teeth. Second, several of the patients that has the teeth criteria declined to take part in this study. It must be remembered that DI is a rare dental anomaly with very few patients available to recruit during the course of this study.

2) Mirco-indentation for Hardness test

The stability of the sample during measuring dentine hardness is one of the challenges that have been taken in consideration, in which it can affect on the hardness measurements. The difficulty developed when preparing small teeth samples especially the primary teeth. In addition, the DI teeth surfaces width is smaller due to the wearied surface of the tooth. The samples were placed on the indenter and the surface of the sample must be flat to reduce the measured reading errors.

2) Demineralisation technique

Demineralisation of the sample is very technique sensitive. It depends on the acid concentration and the applied duration. Any increase in the duration time will have an effect on the sample outcome. It is believed that each tooth has its own unique physical properties and mechanical properties. Control teeth and DI teeth differs in the quality of the structure thus the quality of dentine. The only valid technique that has been used to evaluate the accuracy of the demineralisation protocol was FTIR Spectrum. Particular number of teeth needs prolonger time to expose collagen and remove the minerals form it. In addition, DI teeth need less time for demineralisation process to reduce the damage of collagen structure. The study was strictly performed in all group sample with 15 seconds application of phosphoric acid.

3) Topographic imaging:

Teeth required to be dehydrated prior fixation for SEM imaging. This is done by fixing the samples first for 24 hours in 3% glutaraldehyde in 0.1M sodium cacodylate solution.

Then the samples undergo dehydration procedure by using an ethanol series. In this study, crack like areas were found on numerous areas on dentinal surface of the sample. Which is believed that excessive dehydration can lead to create this desiccation cracks. Thus damaging the collagen fibrils and weakening of the sample.

AFM generates a high-resolution image of a nanometer-scale surface. Images were more superior in resolution when compared to SEM as provides a three-dimensional surface profile. Details and information regarding collagen ultrastructure can be gained in a single image. A disadvantage of AFM compared with SEM is the scan image size. In one pass, the SEM can image an area on the order of square millimeters with a depth of field on the order of millimeters. Whereas the AFM can only image a maximum height on the order of 10-20 micrometers and a maximum scanning area of about 150×150 micrometers.The scanning speed of an AFM is also a limitation. AFM requires several minutes for a typical scan, while a SEM is capable of scanning at near real-time, although at relatively low quality.

As with any other imaging technique, there is the possibility of image artefacts, which could be induced by an unsuitable tip, a poor operating environment, or even by the sample itself. These image artefacts are unavoidable however, their occurrence and effect on results can be reduced through various methods.

Due to the nature of AFM probes, they cannot normally measure steep walls or overhangs. Specially made cantilevers and AFMs can be used to modulate the probe sideways as well as up and down (as with dynamic contact and non-contact modes) to measure sidewalls, at the cost of more expensive cantilevers, lower lateral resolution and additional artefact's.

Chapter 8 Clinical relevance of the study

It is well known that the bond strength of restorative materials to dentine depends on the mechanical properties of the dentine. These involve the dentine depth, dentine hardness and mineral components of dentine (Yoshikawa et al., 1999). Therefore, any knowledge of dentine hardness of DI teeth from this study will certainly contribute in restorative administration on the patients with DI type II or DI type I. This outcome with other previous discoveries, would deliver information on how DI teeth would respond during clinical treatment and the possibility of structuring various superior materials than another, which is suitable for DI dentine. The clinical effectiveness and longevity of the materials in lifetime might also possibly be predicted.

It has been examined that several DI type II patients have suffered from tooth wear specifically on the anterior teeth. As well as these groups of patients are more prone to have early tooth surface loss due to abnormal structure of dentine. Any preventive measures and intervention will absolutely advantage these patients. Early plan of restorative management is necessary for DI type II patients once their teeth are erupted. This would prevent the patients from having progressive wear of their dentition and unnecessary extraction.

One of the fundamental difficulties confronted in the clinical dental treatment while treating OI/DI patients is the difficulty to restore concerned dentitions. Approach for treating DI patients will vary subjecting upon the significance of the clinical expression. Actions must be taken while treating patients determined to have DI type I, associated with OI, if surgical methodology or forceful extractions that could transmit strengths to jaw bone and increment the danger of fracture (American Academy of Pediatric Dentistry, 2013). Preventive care through early recognition of dental disease throughout regular dental check ups and screening is basic. Stressing on maintaining of oral hygiene and directions that involves every day brushing utilizing fluoride toothpastes as a part of expansion to a low sugar and low acid diet routine, must be performed. DI patients would not typically encounter any kind of dental pain due to pulpal obliteration and the moderately normal caries/periodontal disease. Nonetheless, patient's conceivable increased anxiety towards any restorative or dental treatment, experience concerns, and develop of continuous incident of numerous abscesses that may prompt

to early teeth extraction and possible future malocclusion. High occurrence of class III malocclusion and posterior cross- bites and open- bites was accounted for in cases of DI type I (O'Connell and Marini, 1999). In severe cases of tooth wear, excessive tooth wear and notable discoloration of teeth that is aesthetically unpleasing is seen. The composite restorations tend to fail in DI patients due to unsuccessfully in bonding capability of the adhesive restorations. Glass ionomer materials is frequently used as means of restoring DI teeth as it does not require any mechanical interlocking with collagen, (Perdigao, 2009). On the other hand, the life span of these restorations is questionable. Full coverage restorations, for example, stainless steel crowns (SSC) and overlay dentures, is not a perfect treatment decision for youthful patients; might become necessary to preserve aesthetics, function, and prevent loss of vertical dimension, (Sapir and Shapira, 2001).

It is uncertain the mode of restoration application and improper etching of teeth prior to performing of dental composites, or possible dentinal matrix or collagen alterations; that might be ultra structurally damaged with a reduced quality and mechanically weaker thus creating an ineffective hybrid layer during bonding; is the contributing factor. (Yang et al, 2005) demonstrated that changes in the helical structure of dentinal collagen and mechanical properties will have a significant effect on determination of bond strength. It is believed that collagen ultrastructure alterations decreases its mechanical properties and result in impaired durability of the dentine – resin interface, and effect the quality of bonding (Nakabayashi and Pashley, 1998). Selecting the proper etching agent will effect on dentine-resin bond and increase the longevity of the resin restoration. This study demonstrated that DI teeth could be demineralised with EDTA to remove the smear layer rather than using 37% of phosphoric acid that could be damaging to DI teeth thus distorting the collagen network.

In summery, this study showed that demineralisation of dentine can be obtained with several agents depending on the tooth condition. In sound dentine, etching with 15 seconds of phosphoric acid followed by sodium hypochlorite is sufficient to expose collagen network, while EDTA could me the material of choice in future dentistry for demineralizing DI teeth prior tooth restoration. Further studies are necessary to determine the effect of bond strength of restorative materials for agents that were used in this study.

Chapter 9 Conclusion

Any variations in dental tissues whether it is due to a genetic mutation that leads to alteration in development of the tissues (Amelogenesis Imperfecta, Dentinogenesis Imperfecta) may produce teeth with different morphological features and mechanical properties. This means, extra support is necessary in the rehabilitation process of the teeth with possible alteration in clinical and preventive management of these teeth.

Evaluating hardness has been shown to be a reasonable method of examining the mineral content of calcified tissues including teeth in healthy and affected teeth with DI. Also, it would help to improve restorative treatment industry and allows prediction of the behaviour of dentine-restoration interfaces. It has been found that there is a strong relationship exists between microhardness of dentine and the respective bond strength (Panighi et al., 1993).

The dentine hardness in DI teeth is reduced when compared to the healthy primary teeth. There was a significant reduction in dentine hardness between DI and control group ($P \leq 0.0001$), and between DI type I and DI type II ($P \leq 0.001$). There is a correlation between the hardness of dentine and the mineral content of its structure. The responsible factor that led to this alteration is genetic mutation. Decreased in mineral content of the tooth structure is strongly associated with developing tooth wear. Subsequently, the DI teeth would develop pulpal recession and obliteration and formation of Dentine Bridge. Several DI patients are representing the similar features in the clinical and radiographical picture of the disease.

There were numerous earlier reports describing the collagen fibrils in dentine, by using SEM (Takahashi, 1981; Kobayashi, 1984; Sogaard-Pedersen et al., 1989). A few additional stages and various preparations of the samples, including fixation, dehydration and demineralization, needed to be done in order to enable images of collagen fibrils to be recorded with the SEM instrument. Since DI type I is a disease featuring an abnormality in the collagen, efforts will be made to observe the structures of collagen fibrils in the DI teeth, as well as collagen in the control teeth in this study. This would provide extra information on the difference of structure of DI teeth in comparison to normal teeth, which would aid in the future preventive plan and restorative management for patients with this disease. Adding different approaches and possible

extra software program is to be used in combination with SEM, to compare the results of collagen structure and to record the data. In that case, introduction of AFM for topographical imaging was included in this study to obtain superior images with high resolution. Unlike SEM, The tested sample does not require addition preparation for AFM. This study proves that the sample can be easily damaged during preparation and handling of the sample prior imaging. Carful sample selection, handling and implementing new different technique in future could be beneficial in future studies.

Phosphoric acid 37% was used in this study to remove the smear layer of the tooth surface segment, as it is the material used routinely in the dental clinic for all restorative procedures, therefore is practically significant in this study. Previous studies performed the demineralisation protocol by application of EDTA 17%. The choice of the acid was determined in order to obtain similar outcomes in the clinical settings.

FTIR procedure was performed to evaluate the significance of the demineralization protocol and to evaluate the mineral content removal from the sample surface. Developing the same outcomes on the patient's teeth is challenging, because demineralisation procedure is a technique sensitive depends on the operator and duration. Any increase of demineralisation duration can affect in minerals removal, thus exposure of collagen structure.

Furthermore, application of the ultrasonication theory through the use of an ultrasonic probe during etching, thus aiding in better demineralisation and exposure of collagen network.

In this study there was a substantial difference in the D-band width that varied from 65 nm to 74 nm. Obtaining a baseline data of a control healthy tooth is crucial for future comparison between normal and DI collagen fibril D- banding width. Thus, indicates collagen malformation. Further studies of DI/OI collagen mechanical properties will hopefully guide us into better understanding of their possible effects on restoration bonding and adhesion properties.

Chapter 10 Future Work

- Increase imaging the sample that has been collected in our library.
- Possible further experimentation with preparation techniques used in demineralisation protocols.
- Experimenting with etching techniques within a clinical setting, and determining the applicability of ultrasonication in regards to teeth restoration.
- Modulate the demineralisation protocol for DI teeth.
- Quantification of AFM images and compare the results in all groups (D-band width and periodicity - collagen fibril morphology)
- Using different mode for AFM (Tapping mode)
- Perform AFM mechanics (indentation on teeth - tensile modulus of individual fibrils)
- Examine the spherites structure
- Possible teeth staining to investigate scaffold ultrastructure.

Chapter 11 References:

Adachi E, Hayashi T. In Vitro Formation Of Hybrid Fibrils Of Type V Collagen And Type I Collagen. Limited Growth Of Type I Collagen Into Thick Fibrils By Type V Collagen. Connect Tissue Res. 1986;14(4):257-66.

Aiello, L., & Dean, C. (2002). Chapter Seven - The Microanatomy And Development Of Teeth Bt - An Introduction To Human Evolutionary Anatomy, 106–132.

Aigner T, Gluckert K, Mark K. Activation Of Fibrillar Collagen Synthesis And Phenotypic Modulation Of Chondrocytes In Early Human Osteoarthritic Cartilage Lesions. Osteoarthr Cartil. 1997;5:183–189. Doi: 10.1016/S1063-4584(97)80013-1.

Alanay Y, Avaygan H, Camacho N, Utine Ge, Boduroglu K, Aktas D, Et Al. Mutations In The Gene Encoding The Rer Protein Fkbp65 Cause Autosomal-Recessive Osteogenesis Imperfecta. Am J Hum Genet. 2010;86:551-9.

Angker Linny, Swain Michael, & Kilpatrick Nicky. (2005). Characterising the micro-mechanical behaviour of the carious dentine of primary teeth using nano-indentation. *Journal of Biomechanics*, *38*(7), 1535–1542.

Atkinson,H.F.,Andsaunsbury,P.: An Investigation Into The Hardness Of Human Enamel, Brit. D.J.94:249,1953.

Avery, J. K. (Ed.) 2002. Oral Development And Histology: Thieme.
Bailey Aj, Paul Rg, Knott L. Mechanisms Of Maturation And Ageing Of Collagen. Mech Ageing Dev. 1998 Dec 1;106(1-2):1-56.

Balooch, M., Habelitz, S., Kinney, J. H., Marshall, S. J. & Marshall, G. W. 2008. Mechanical Properties Of Mineralized Collagen Fibrils As Influenced By Demineralization. J Struct Biol, 162, 404-10.

Bank, R. A., Tekoppele, J. M., Janus, G. J., Wassen, M. H., Pruijs, H. E., Van Der Sluijs, H. A. & Sakkers, R. J. 2000. Pyridinium Cross-Links In Bone Of Patients With Osteogenesis Imperfecta: Evidence Of A Normal Intrafibrillar Collagen Packing. J Bone Miner Res, 15, 1330-6.

Barron, M. J., Mcdonnell, S. T., Mackie, I. & Dixon, M. J. 2008. Hereditary Dentine Disorders: Dentinogenesis Imperfecta And Dentine Dysplasia. Orphanet J Rare Dis, 3, 31.

Bateman J, Chan Danny, Mascara Thomas. Collagen Defects In Lethal Perinatal Osteogenesis Imperfecta. Biochem J, 1986.

Ben Amor, M., Rauch, F., Monti, E. & Antoniazzi, F. 2013. Osteogenesis Imperfecta. Pediatr Endocrinol Rev, 10 Suppl 2, 397-405.

Biria, M., Abbas, F. M., Mozaffar, S., & Ahmadi, R. (2012). Dentinogenesis Imperfecta Associated With Osteogenesis Imperfecta. Dental Research Journal, 9(4), 489–94.

Bertassoni, L. E., Marshall, G. W. & Swain, M. V. 2012. Mechanical Heterogeneity Of Dentin At Different Length Scales As Determined By Afm Phase Contrast. Micron, 43, 1364-71.

Bixler, D. (Ed.) 1976. Heritable Disorders Affecting Dentin: Mosby. Bordin-Aykroyd, S., Sefron, J. & Davies, E. 1992. In Vitro Bond Strengths Of Three Current Dentin Adhesives To Primary And Permanent Teeth. J Dent Mater 8, 74-78.

Boskey, L. Spevak, M. Tan, S.B. Doty & Butler, W. T. 2000. Dentin Sialoprotein (Dsp) Has Limited Effects On In Vitro Apatite Formation And Growth. Calcif. Tissue Int., 67, 472-478.

Bozec L., De Groot, Odlyha, Nicholls, Horton Ma. Mineralised Tissues As Nanomaterials: Analysis By Atomic Force Microscopy. Iee Proceedings - Nanobiotechnology 2005; 152.

Burg,F.:Neue Spezielle Hdrtebestimmungen Des Hartsubstan Zen Des Zahnes,Disserta- Tion, Jena, 1921.

Burgeson R, Nimmi E, 1992 Collagen Types. Molecular Structure And Tissue Distribution. Clin Orthop Relat Res 1992;282 25072 .

Byers, P. H. 2000. Osteogenesis Imperfecta: Perspectives And Opportunities. Curr Opin Pediatr, 12, 603-9.

Byers, P. H. & Pyott, S. M. 2012. Recessively Inherited Forms Of Osteogenesis Imperfecta. Annu Rev Genet, 46, 475-97.

Cabral, W. A., Chang, W., Barnes, A. M., Weis, M., Scott, M. A., Leikin, S., Makareeva, E., Kuznetsova, N. V., Rosenbaum, K. N., Tifft, C. J., Bulas, D. I., Kozma, C., Smith, P. A., Eyre, D. R. &

Cabral, W. A., Chang, W., Barnes, A. M., Weis, M., Scott, M. A., Leikin, S., Makareeva, E., Kuznetsova, N. V., Rosenbaum, K. N., Tifft, C. J., Bulas, D. I., Kozma, C., Smith, P. A., Eyre, D. R. & Marini, J. C. 2007b. Prolyl 3-Hydroxylase 1 Deficiency Causes A Recessive Metabolic Bone Disorder Resembling Lethal/Severe Osteogenesis Imperfecta. Nat Genet, 39, 359-65.

Caldwell,R.C.,Muntz,M.L.,Gilmore,R.W.,Andpigman,W.:Microhardness Of Intact Surface Enamel, J. D. Res. 36: 732, 1957.

Cassella Jp, Stamp Tcb, Ali Sy. A Morphological And Ultrastructural Study Of Bone In Osteogenesis Imperfecta. *Calcified Tissue International* 1996; 58: 155– 165.
Chapman J, Tzaphlidou M, Meek K, Kadler K. The Collagen Fibril—A Model System For Studying The Staining And Fixation Of A Protein. Electron Microscopy Reviews 1990; 3: 143–182.

Chen, Z., Zhao, G. & Kong, X. 2001. Dentinogenesis Imperfecta 1 With Or Without Progressive Hearing Loss Is Associated With Distinct Mutations In Dspp. Nat Genet, 27, 201-4.

Chernoff, E.A.G & Chernoff., D. A. 1992. Atomic Force Microscope Images Of

Collagen Fibers. J. Vac. Sci. Technol. A, 10, 596–599.

Chowdhary, N. & Reddy, V. S. 2010 Dentin Comparison In Primary And Permanent Molars Under Transmitted And Polarised Light Microscopy: An In Vitro Study. J Indian Soc Pedod Prev Dent., 28, 167-172.

Christiansen He, Schwarze U, Pyott Sm, Alswaid A, Al Balwi M, Alrasheed S, Et Al. Homozygosity For A Missense Mutation In Ser- Pinh1, Which Encodes The Collagen Chaperone Protein Hsp47 Results In Severe Recessive Osteogenesis Imperfecta. Am J Hum Genet. 2010;86:389-98.

Dalitz, G.P. 1962. Hardness Of Dentin Related To Age. Australian Dental Journal 7:463– 464.

Di Lullo G. Mapping The Ligand-Binding Sites And Disease-Associated Mutations On The Most Abundant Protein In The Human, Type I Collagen. Journal Of Biological Chemistry 2001; 277: 4223–4231.

Dummett Co Jr. Anomalies Of The Developing Dentition. In: Pinkham Jr, Casamassimo Ps, Fields Hw Jr, Mctigue Dj, Nowak Aj, Eds. Pediatric Dentistry: Infancy Through Adolescence. 4th Ed. St. Louis, Mo: Elsevier Saunders; 2005:61-73.

El Feninat, F., Ellis, T. H., Sacher, E. & Stangel, I. 1998. Moisture-Dependent Renaturation Of Collagen In Phosphoric Acid Etched Human Dentin. J Biomed Mater Res, 42, 549-53.

Ensanya A. Abou Neel, Laurent Bozec, Jonathan C. Knowles, Omaer Syed, Vivek Mudera, Richard Day, Jung Keun Hyun. Collagen — Emerging Collagen Based Therapies Hit The Patient. Advanced Drug Delivery Reviews 2013; 65: 429–456

Ensminger D, Stulen Fb (Eds.). *Ultrasonics: Data, Equations, Applications*. Taylor & Francis: Boca Raton, 2008.

Fawzy, A. S. 2010. Variations In Collagen Fibrils Network Structure And Surface Dehydration Of Acid Demineralized Intertubular Dentin: Effect Of Dentin Depth And Air-Exposure Time. J Dent Mater, 26, 35-43.

Ferracane, Jack L., Paul R. Cooper, And Anthony J. Smith. "Dentin Matrix Component Solubilization By Solutions Of Ph Relevant To Self-Etching Dental Adhesives." *The Journal Of Adhesive Dentistry* 15, No. 5 (2013): 407-412.

Forlino, A., Cabral, W. A, Barnes, A. M., & Marini, J. C. (2011). New Perspectives On Osteogenesis Imperfecta. Nature Reviews. Endocrinology, 7(9), 540–557.

Fuentes V, Toledano M, Osorio R, Carvalho R.M. 2003. Microhardness Of Superficial And Deep Sound Human Dentin. Wiley Periodicals, Inc. Journal Of Biomedical Material 66:850–853.

Gage, J. P. (1985), Dentinogenesis Imperfecta. A New Perspective. Australian Dental Journal, 30: 285–290. Doi:10.1111/J.1834-7819.1985.Tb02510.X

Gajiko-Galicka, A. 2002. Mutation In Type I Collagen Genes Resulting In Osteogenesis Imperfecta In Human. Acta Biochem, 49, 433-441.

Gelse. Collagens—Structure, Function, And Biosynthesis. Advanced Drug Delivery Reviews 2003; 55: 1531–1546.

Gotliv, Robach Js & A, V. 2006. The Composition And Structure Of Bovine Peritubular Dentin: Mapping By Time Of Flight Secondary Ion Mass Spectroscopy. J Struct Biol. , 156, 320-333.

Griffiths P, De Haseth J. Fourier Transform Infrared Spectrometry. 2007.

Gustafson, G., And Kling, 6.: Micro-Hardness Measurements In The Human Dental Enamel, Odontol. Tidskr. 56: 23, 1948.

Gw Marshall, Jr, M. S., Kinney Jh & M., B. 1997. The Dentin Substrate: Structure

And Properties Related To Bonding. J Dent. Res, 25, 441-458.

Gwinnett Aj: Altered Tissue Contribution To Interfacial Bond Strength With Acid Conditioned Dentin. Am J Dent. 1994 Oct;7(5):243-6.

Habelitz, S., B.J. Rodriguez, S.J. Marshall, G.W. Marshall, S.V. Kalinin & Gruverman3, A. 2007. Peritubular Dentin Lacks Piezoelectricity. J Dent Res, 86, 908-911.

Habelitz, S., Balooch, M., Marshall, S. J., Balooch, G. & Marshall, G. W., Jr. 2002. In Situ Atomic Force Microscopy Of Partially Demineralized Human Dentin Collagen Fibrils. J Struct Biol, 138, 227-36.

Habelitz, S., Marshall, S. J., Marshall, G. W., Jr. & Balooch, M. 2001. Mechanical Properties Of Human Dental Enamel On The Nanometre Scale. Arch Oral Biol, 46, 173- 83.

Habelitz, S., Balooch, M., Marshall, S. J., Balooch, G. & Marshall, G. W., Jr. 2002. In Situ Atomic Force Microscopy Of Partially Demineralized Human Dentin Collagen Fibrils. J Struct Biol, 138, 227-36.

Hall, R. K., Maniere, M. C., Palamara, J. & Hemmerle, J. 2002. Odontoblast Dysfunction In Osteogenesis Imperfecta: An Lm, Sem, And Ultrastructural Study. Connect Tissue Res, 43, 401-5.

Harith, Nsb; (2013) Dentinal Ultrastructure In Osteogenesis Imperfecta And Dentinogenesis Imperfecta. Doctoral Thesis, Ucl (University College London).

Hart Sp, Hart Tc. Disorders Of Human Dentin. *Cells Tissues Organs* 2007; 186: 70–77.

Hart, P. S. & Hart, T. C. 2007. Disorders Of Human Dentin. Cells Tissues Organs, 186, 70-7.

Hashimoto, M., Ohno, H., Endo, K., Kaga, M., Sano, H. & Oguchi, H. 2000. The Effect Of Hybrid Layer Thickness On Bond Strength: Demineralized Dentin Zone Of The Hybrid Layer.J Dent Mater, 16, 406-11.

Hirayama, A. 1990. Experimental Analytical Electroni Microscopic Studies On The Quantitative Analysis Of Elemiental Concenitrationis In Biological Thini Specimens And Its Application To Dental Science. Shlikzan Gahuko, 90, 1019-1036.

Hodge, A. J. & Petruska, J. A. (Eds.) 1963. Recent Studies With The Electron Microscope On Ordered Aggregates Of The Tropocollagen Molecule: Academic Press.

Hodge,H.C.,Andmckay,H.: The Microhardness Of Teeth, J.A.D.A.20:227,1933.

Horber J. Scanning Probe Evolution In Biology. Science 2003; 302: 1002–1005.

Hosoya Y, Marshall Gw Jr. 2004. The Nano-Hardness And Elastic Modulus Of Carious And Sound Primary Canine Dentin. Oper Dent 29:142–149.

Hosoya Y, Marshall Sj, Watanabe Lg, Marshall Gw. 2000. Microhardness Of Carious Deciduous Dentin. Oper Dent 25:81–89.

Hosoya Y, Ono T, Marshall Gw Jr. 2002. Microhardness Of Carious Primary Canine Dentin. Pediatr Dent J 12:91–98.

Hosoya Y. 2006. Hardness And Elasticity Of Bonded Carious And Sound Primary Tooth Dentin. J Dent Res 34:164–171.

Hosoya Y, Marshall G.W. 2005. The Nano-Hardness And Elastic Modulus Of Sound Deciduous Canine Dentin And Young Premolar Dentin - Preliminary Study. Journal Of Materials Science: Materials In Medicine 16:1–8.

Howlin Rp, Fabbri S, Offin Dg, Symonds N, Kiang Ks, Knee Rj *Et Al.* Removal Of Dental Biofilms With An Ultrasonically Activated Water Stream. *Journal Of Dental Research* 2015.

Huber M. Osteogenesis Imperfecta. *Oral Surgery, Oral Medicine, Oral Pathology, Oral Radiology, And Endodontology* 2007; 103: 314–320.

Hursey, R. J., Jr., Witkop, C. J., Jr., Miklashek, D. & Sackett, L. M. 1956. Dentinogenesis Imperfecta In A Racial Isolate With Multiple Hereditary Defects. Oral Surg Oral Med Oral Pathol, 9, 641-58.

Ibrahim, S. Doctorate, C., & Dentistry, P. (N.D.). 2015. Exposure And Characterisation Of Collagen Ultrastructure In Primary Teeth Affected With Osteogenesis Imperfecta And Dentinogenesis Imperfecta.

Johnsen, D. (Ed.) 1994. Comparisoni Of Primary And Permanent Teeth. In: Oral Developmeint And Histology: Philadelphia: B.C. Decker.

K. Van Der Mark, Components Of The Organic Extracellular Matrix Of Bone And Cartilage, In: S.P.R.M.J. Seibel, J.P. Bilezikian (Eds.), Dynamics Of Bone And Carti-Lage Metabolism, Academic Press, San Diego, Ca, 1999, Pp. 3–40.

Kadler, K. 2007. Collagen Pretzels Revealed By Electron Microscopy. Biochem J, 404, E7-8. Kadler, K. E., Holmes, D. F., Trotter, J. A. & Chapman, J. A. 1996. Collagen Fibril

Keller, D. & Cung, C. C. 1991. Reconstruction Of Stm And Afm Images Distorted By Finite- Size Tip. Surface Science, 253, 353-364.

Kelley Bp, Malfait F, Bonafe L, Baldridge D, Homan E, Symoens S, Et Al. Mutations In Fkbp10 Cause Recessive Osteogenesis Imper- Fecta And Bruck Syndrome. J Bone Miner Res. 2011;26:666-72.

Keupp K, Beleggia F, Kayserili H, Barnes Am, Steiner M, Semler O, Et Al. Mutations In Wnt1 Cause Different Forms Of Bone Fragility. Am J Hum Genet. 2013;92:565-74.

Kim, J. W. & Simmer, J. P. 2007. Hereditary Dentin Defects. J Dent Res, 86, 392-9.

Kinney Jh, Balooch M, Marshall Gw, Marshall Sj. 1999. A Micromechanics Model Of The Elastic Properties Of Human Dentine. Arch Oral Biol 44:813–822.

Kinney Jh, Balooch M, Marshall Sj, Marshall Gw Jr, Weihs Tp. 1996. Hardness And Young's Modulus Of Human Peritubular And Intertubular Dentine. Arch Oral Biol 41:9– 13.

Kinney, J. H., Balooch, M., Marshall, S. J. And Marshall, G. W., Weihs, T. P. 1996. Atomic Force Microscope Measurements Of The Hardness And Elasticity Of Peritubular And Intertubular Dentin. Journal Of Biomechanical Engineering 118:133–135.

Klinger,A.: Studies On Enamel Hardness,D.Record60:291,1940.

Koch, M. Et Al. (2003) Collagen Xxiv, A Vertebrate Fibrillar Collagen With Structural Features Of Invertebrate Collagens: Selective Expression In Developing Cornea And Bone. J. Biol. Chem. 278, 43236–43244

Koutsi V, Noonan Rg, Horner Ja, Simpson Md, Matthews Wg & Dh, P. 1994. The Effect Of Dentin Depth On The Permeability And Ultrastructure Of Primary Molars. Pediatric Dent Material, 16, 29-35.

Koutsi, V., Noonan, R. G., Horner, J. A., Simpson, M. D., Matthews, W. G. & Pashley, D. H. 1994. The Effect Of Dentin Depth On The Permeability And Ultrastructure Of Primary Molars. Pediatric Dent, 16, 29-35.

Kramer, I. R. H. 1951. The Distribution Of Collagen Fistrils In The Dentin Matrix. Brit. Dent. J, 91, 1-7.

Kubínek R, Zapletalová Z, VůJtek M, Novotný R, KolářOvá H, ChmelíčKová H Et Al. Sealing Of Open Dentinal Tubules By Laser Irradiation: Afm And Sem Observations Of Dentine Surfaces. Journal Of Molecular Recognition 2007; 20: 476–482.

Lapunzina P, Aglan M, Temtamy S, Caparros-Martin Ja, Valencia M, Leton R, Et Al. Identification Of A Frameshift Mutation In Osterix In A Patient With Recessive Osteogenesis Imperfecta. Am J Hum Genet. 2010;87:110-4.

Leblond, C. P. 1989. Synthesis And Secretion Of Collagen By Cells Of Connective Tissue, Bone, And Dentin. The Anatomical Record, 224, 123-38.

Lee S-K, Lee K-E, Song Sj, Hyun H-K, Lee S-H, Kim J-W. A Dspp Mutation Causing Dentinogenesis Imperfecta And Characterization Of The Mutational Effect. Biomed Research International 2013; 2013: 1–7.

Levin, L. S., Leaf, S. H., Jelmini, R. J., Rose, J. J. & Rosenbaum, K. N. 1983. Dentinogenesis Imperfecta In The Brandywine Isolate (Di Type Iii): Clinical, Radiologic, And Scanning Electron Microscopic Studies Of The Dentition. Oral Surg Oral Med Oral Pathol, 56, 267-74.

Lin Cp, Douglas Wh, Erlandsen Sl. 1993. Scanning Electron Microscopy Of Type I Collagen At The Dentin Enamel Junction Of Human Teeth. J Histochem Cytochem 41:381–388.

Linde, A. 1989. Dentin Matrix Proteins: Composition And Possible Functions In Calcification. . Anat Rec, 224, 154-166.

Linde, A. & Goldberg, M. 1993. Dentinogenesis. Critical Reviews In Oral Biology And Medicine,, 4, 679-728.

M. Macdougall, D. Simmons, X. Luan, J. Nydegger, J. Feng & Gu, T. T. 1997. Dentin Phosphoprotein And Dentin Sialoprotein Are Cleavage Products Expressed From A Single Transcript Coded By A Gene On Human Chromosome 4. Dentin Phosphoprotein Dna Sequence Determination). J. Biol. Chem, 272, 835-842.

Mahoney E.K, Kilpatrick N.M, Swain M.V. 2006. Behaviour Of Primary Incisor Caries: A Micromechanical Study. International Journal Of Peadiatric Dentistry 16:270–277.

Malmgren, B., Lindskog, S., Elgadi, A. & Norgren, S. 2004. Clinical, Histopathologic, And Genetic Investigation In Two Large Families With Dentinogenesis Imperfecta Type Ii. Hum Genet, 114, 491-8.

Marini, J. (Ed.) 2004. Osteogenesis Imperfecta: Philadelphia:Sauders.

Marshall, G.W. 1993. Dentin Microstructure And Characterization. Quintessence International 24:606–611.

Marini, J. C., Forlino, A., Cabral, W. A., Barnes, A. M., San Antonio, J. D., Milgrom, S., Hyland, J. C., Korkko, J., Prockop, D. J., De Paepe, A., Coucke, P., Symoens, S., Glorieux, F. H., Roughley, P. J., Lund, A. M., Kuurila-Svahn, K., Hartikka, H., Cohn, D. H., Krakow, D., Mottes, M., Schwarze, U., Chen, D., Yang, K., Kuslich, C., Troendle, J., Dalgleish, R. & Byers, P. H. 2007. Consortium For Osteogenesis Imperfecta Mutations In The Helical Domain Of Type I Collagen: Regions Rich In Lethal Mutations Align With Collagen Binding Sites For Integrins And Proteoglycans. Hum Mutation, 28, 209-21.

Marini, J. C. 2007a. Prolyl 3-Hydroxylase 1 Deficiency Causes A Recessive Metabolic Bone Disorder Resembling Lethal/Severe Osteogenesis Imperfecta. Nat Genet, 39, 359-65.

Marshall, G. W., Jr., Inai, N., Wu-Magidi, I. C., Balooch, M., Kinney, J. H., Tagami, J. & Marshall, S. J. 1997c. Dentin Demineralization: Effects Of Dentin Depth, Ph And Different Acids. J Dent Mater, 13, 338-43.

Marshall, G. W., Yucel, N., Balooch, M., Kinney, J. H., Habelitz, S. & Marshall, A. 2001. Sodium Hypochlorite Alterations Of Dentine And Dentine Collagen. Surf Science, 491, 444-455.

Martinez-Glez V, Valencia M, Caparros-Martin Ja, Aglan M, Tem- Tamy S, Tenorio J, Et Al. Identification Of A Mutation Causing Deficient Bmp1/Mtld Proteolytic Activity In Autosomal Reces- Sive Osteogenesis Imperfecta. Hum Mutat. 2012;33:343-50.

Milan A.M, Sugars R.V, Embery G & R.J, W. 2006. Adsorption And Interactions Of Dentine Phosphoprotein With Hydroxyapatite And Collagen. Eur. J. Oral. Sci, 114, 223-231.

Minor, R. 1980. Collagen Metabolism:A Comparison Of Disease Of Collagen And Disease Affecting Collagen. Am J Patho, 98, 227-280.

Mjör, I. A. 2009. Dentin Permeability: The Basis For Understanding Pulp Reactions And Adhesive Technology. Braz Dent J, 20, 3-16.

Mohamed Ibrahim, Nb. A Study Of The Genetics And Physical Properties Of Dentine Defects, Ucl (University College London). Ucl (University College London) 2013-10-28.

Myllyharju, J., & Kivirikko, K. I. (2001). Collagens And Collagen-Related Diseases. Annals Of Medicine, 33(1), 7–21.

Nakabayashi, N., Kojima, K. & Masuhara, E. 1982. The Promotion Of Adhesion By The Infiltration Of Monomers Into Tooth Substrates. J Biomed Mater Res, 16, 265-73.

Nakabayashi, N., Nakamura, M. & Yasuda, N. 1991. Hybrid Layer As A Dentin-Bonding Mechanism. J Esth Dent, 3, 133-8.

Nakabayashi, N. & Pashley, A. (Eds.) 1998. A Hybridization Of Dental Hard Tissues: Tokyo:Quintessence.

Nakabayashi, N., Watanabe, A. & Igarashi, K. 2004. Afm Observation Of Collapse

And Expansion Of Phosphoric Acid-Demineralized Dentin. J Biomed Material. Part A, 68, 558-65.

Nanci, A. (Ed.) 2008. Ten Cate's Oral Histology, Development, Structure, And Function: Mosby.

O'connell Ac, Marini Jc. Evaluation Of Oral Problems In An Osteogenesis Imperfecta Population. *Oral Surgery, Oral Medicine, Oral Pathology, Oral Radiology, And Endodontology* 1999; 87: 189–196.

Okamoto, Y., J. D. Heeley, I. L. Dogon, And H. Shintani. "Effects Of Phosphoric Acid And Tannic Acid On Dentine Collagen." *Journal Of Oral Rehabilitation* 18, No. 6 (1991): 507-512.

Oyarzún, Alejandro, Hermann Rathkamp, And Erik Dreyer. "Immunohistochemical And Ultrastructural Evaluation Of The Effects Of Phosphoric Acid Etching On Dentin Proteoglycans." *European Journal Of Oral Sciences* 108, No. 6 (2000): 546-554.

Paschalis E P, Burr David. Bone Mineral And Collagen Quality In Humeri Of Ovariectomized Cynomolgus Monkeys Given Rhpth(1-34) For 18 Months. Journal Of Bone And Mineral Research Volume 18, Number 4, 2003.

Pashley, D. H. 1991. Clinical Correlations Of Dentin Structure And Function. J Pros Dent, 66, 777-81.

Pashley, D. H. 1992. Smear Layer: Overview Of Structure And Function. Proceedings Of The Finnish Dental Society. Suomen Hammaslaakariseuran Toimituksia, 88 Suppl 1, 215- 24.

Pashley, D. H., Ciucchi, B., Sano, H., Carvalho, R. M. & Russell, C. M. 1995. Bond Strength Versus Dentine Structure: A Modelling Approach. Arch Oral Biol, 40, 1109-18.

Pashley, D. H., Ciucchi, B., Sano, H. & Horner, J. A. 1993. Permeability Of Dentin To Adhesive Agents. Quintessence Int, 24, 618-31.

Perdigão, Jorge, Paul Lambrechts, Bart Van Meerbeek, Ângelo R. Tomé, Guido

Vanherle, And Augusto B. Lopes. "Morphological Field Emission-Sem Study Of The Effect Of Six Phosphoric Acid Etching Agents On Human Dentin." *Dental Materials* 12, No. 4 (1996): 262-271.

Perdigao, J. & Lopes, M. 2001. The Effect Of Etching Time On Dentine Demineralisation. Quintessence Int, 32, 19-26.

Perdigão J[1], Thompson Jy, Toledano M, Osorio R: An Ultra-Morphological Characterization Of Collagen-Depleted Etched Dentin. Am J Dent 1999 Dec;12(6):308.

Pettiette Mt, Wright Jt, Trope M. Dentinogenesis Imperfecta: Endodontic Implications. *Oral Surgery, Oral Medicine, Oral Pathology, Oral Radiology, And Endodontology* 1998; 86: 733–737.

Phillips,R.W.,Andswartz,M.L.: Effect Of Fluorides On Hardness Of Tooth Enamel, J.A.D.A. 37: 1, 1948.

R.L. Smith & G.E. Sandland, "An Accurate Method Of Determining The Hardness Of Metals, With Particular Reference To Those Of A High Degree Of Hardness," *Proceedings Of The Institution Of Mechanical Engineers*, Vol. I, 1922, P 623–641.

Rauch, F. & Glorieux, F. H. 2004. Osteogenesis Imperfecta. Lancet, 363, 1377-85.

Rest, M. V. D. & Garrone, R. 1991a. Collagen Family Of Proteins. Faseb J., 5, 2814-2823.

Ritter, A. V. (2001). The effects of acetone, ethanol, hema, and air on the stiffness of human decalcified dentin matrix. *Journal of Esthetic and Restorative Dentistry, 13*(6), 388.

Sakae T, Mishima H, Kozawa Y (1988) Changes In Bovine Dentin Mineral With Sodium Hypochlorite Treatment. Journal Of Dental Research 67, 1229–34.
Sarathchandra, Pope F, Ali S. Morphometric Analysis Of Type I Collagen Fibrils In

The Osteoid Of Osteogenesis Imperfecta. *Calcified Tissue International* 1999; 65: 390–395.

Shaheen R, Alazami Am, Alshammari Mj, Faqeih E, Alhashmi N, Mousa N, Et Al. Study Of Autosomal Recessive Osteogenesis Imperfecta In Arabia Reveals A Novel Locus Defined By Tmem38b Mutation. J Med Genet. 2012;49:630-5.

Shapira, Shabtai Sapir Dmd Joseph. "Dentinogenesis Imperfecta: An Early Treatment Strategy." *Pediatric Dentistry* 23.3 (2001).

Shapiro, Jay R., Peter H. Byers, Francis H. Glorieux, And Paul Sponseller, Eds. *Osteogenesis Imperfecta: A Translational Approach To Brittle Bone Disease*. Academic Press, 2013.

Shields, E. D., Bixler, D. & El-Kafrawy, A. M. 1973. A Proposed Classification For Heritable Human Dentine Defects With A Description Of A New Entity. Arch Oral Biol, 18, 543-53.

Sillence, D. O., Rimoin, D. L. & Danks, D. M. 1979a. Clinical Variability In Osteogenesis Imperfecta-Variable Expressivity Or Genetic Heterogeneity. Birth Defects Original Article Series, 15, 113-29.

Sillence, Barlow, Garber, H. And R. (1984). Osteogenesis Imperfecta Type Ii Delineation Of The Phenotype With Reference To Genetic Heterogeneity. American Journal Of Medical Genetics, 17.

Silver, F. H., Freeman, J. W. & Seehra, G. P. 2003. Collagen Self-Assembly And The Development Of Tendon Mechanical Properties. J Biomech, 36, 1529-53.

Silver, F. H. & Landis, W. J. 2011. Deposition Of Apatite In Mineralizing Vertebrate Extracellular Matrices: A Model Of Possible Nucleation Sites On Type I Collagen. Connect Tissue Res, 52, 242-54.

Steve Weiner, Arthur Veis, Elia Beniash, Talmon Arad, Jerry W. Dillon, Boris Sabsay

& Siddiqui, F. 1999. Peritubular Dentin Formation: Crystal Organization And The Macromolecular Constituents In Human Teeth. J Struct Biol, 126, 27-41.

Sumikawa, D., Marshall, G., Gee, L. & Marshall, S. 1999. Microstructure Of Primary Tooth Dentin. Pediatr Dent, 21, 439-444.

Tagami J, Nakajima M, Shono T, Et Al. 1993. Effect Of Ageing On Dentin Bonding. Am. Dent. 6:145–147.

Takagi, Sasaki. A Probable Common Disturbance In The Early Stage Of Odontoblast Differentiation In Dentinogenesis Imperfecta Type I And Type Ii. *Journal Of Oral Pathology And Medicine* 1988; 17: 208–212.

Taketa F, Perdue Hs, O'rourke Wf, Sievert Hw, Phillips Ph. An Abrasion Method For Determining The Wear Resistence Of Teeth. J Dent Res 1957;36:739-42.

Tianda Wang, Sheng Yang, Lei Wang And Hailan Feng. Use Of Multifunctional Phosphorylated Pamam Dendrimers For Dentin Biomimetic Remineralization And Dentinal Tubule Occlusion. Department Of Prosthodontics, Peking University School And Hospital Of Stomatology, Beijing, China, Chongqing Key Laboratory Of Oral Diseases And Biomedical Sciences, College Of Stomatology, Chongqing Medical University, Chongqing, China, 2015,**5**, 11136-11144

Tidmarsh, B. G. 1981. Contents Of Human Dentine Tubules. Int Endo J, 14, 191-196.

Toledano, M., Osorio, R., Perdigao, J., Rosales, J. I., Thompson, J. Y. & Cabrerizo-Vilchez, M. A. 1999. Effect Of Acid Etching And Collagen Removal On Dentin Wettability And Roughness. J Bio Mat Res, 47, 198-203.

Totah Vp. Increase In Hardness Of Dentin On Drying. J Dent Res 1942;21:99-104.

Traub, W., Arad, T., Vetter, U. & Weiner, S. 1994. Ultrastructural Studies Of Bones

From Patients With Osteogenesis Imperfecta. Matrix Biol, 14, 337-45.

Tzaphlidou, M. 2008. Bone Architecture: Collagen Structure And Calcium/Phosphorus Maps. J Biol Phys, 34, 39-49

Valadares Er, Carneiro Tb, Santos Pm, Oliveira Ac, Zabel B. What Is New In Genetics And Osteogenesis Imperfecta Classification? Jornal De Pediatria 2014; 90: 536–541.

Van Der Rest M, Garrone R: Collagen Family Of Proteins. Federation Of American Society For Experimental Biology.1991 Oct;5(13):2814-23.

Van Dijk Fs, Nesbitt Im, Zwikstra Eh, Nikkels Pg, Piersma Sr, Fratantoni Sa, Et Al. Ppib Mutations Cause Severe Osteogenesis Imperfecta. Am J Hum Genet. 2009;85:521-7.

Van Meerbeek, B., Inokoshi, S., Braem, M., Lambrechts, P. & Vanherle, G. 1992. Morphological Aspects Of The Resin-Dentin Interdiffusion Zone With Different Dentin Adhesive Systems. J Dent Res, 71, 1530-40.

Van Meerbeek, B., Yoshida, Y., Snauwaert, J., Hellemans, L., Lambrechts, P., Vanherle, G., Wakasa, K. & Pashley, D. H. 1999. Hybridization Effectiveness Of A Two-Step Versus A Three-Step Smear Layer Removing Adhesive System Examined Correlatively By Tem And Afm. J Adhesive Dent, 1, 7-23.

Veeco (Ed.) 2000. Dimension 3100 Manual. Wallace, J. M. 2012. Applications Of Atomic Force Microscopy For The Assessment Of Nanoscale Morphological And Mechanical Properties Of Bone. Bone, 50, 420-7. 165

Wälchli C, Trueb J, Kessler B, Winterhalter K, Trueb B. **Complete Primary Structure Of Chicken Collagen Xiv**eur J Biochem, 267 (1993), Pp. 23007-23014

Wallace J, Chen Q, Fang M, Erickson B, Orr B, Holl Mb. Type I Collagen Exists As A

Distribution Of Nanoscale Morphologies In Teeth, Bones, And Tendons. *Langmuir* 2010; 26: 7349–7354.

Waltimo, J. 1996. Unusual Forms Of Collagen In Human Dentin. Matrix Biol, 15, 53-6.

Waltimo, J., Ojanotko-Harri, A. & Lukinmaa, P. L. 1996. Mild Forms Of Dentinogenesis Imperfecta In Association With Osteogenesis Imperfecta As Characterized By Light And Transmission Electron Microscopy. J Oral Pathol Med, 25, 256-64.

Wenstrup Rj, Florer Jb, Brunskill Ew, Bell Sm, Chervoneva I, Birk De. Type V Collagen Controls The Initiation Of Collagen Fibril Assembly. J Biol Chem. 2004 Dec 17;279(51):53331-7. Epub 2004 Sep 21.

Wess, T. J., Hammersley, A. P., Wess, L. & Miller, A. 1998. Molecular Packing Of Type I Collagen In Tendon. J Mol Bio, 275, 255-67.

Witkop, C. J., Jr. 1975. Hereditary Defects Of Dentin. Dent Clin North Am, 19, 25-45.
Witkop, C. J., Jr., Maclean, C. J., Schmidt, P. J. & Henry, J. L. 1966. Medical And Dental Findings In The Brandywine Isolate. Ala J Med Sci, 3, 382-403.

Wright, H.N., And Fenske, E.L.: Factors Involved In Variability In Hardness Of Tooth Structures, J. D. Res. 17: 297, 1938.

Xiao, S., Yu, C., Chou, X., Yuan, W., Wang, Y., Bu, L., Fu, G., Qian, M., Yang, J., Shi, Y., Hu, L., Han, B., Wang, Z., Huang, W., Liu, J., Chen, Z., Zhao, G. & Kong, X. 2001. Dentinogenesis Imperfecta 1 With Or Without Progressive Hearing Loss Is Associated With Distinct Mutations In Dspp. Nat Genet, 27, 201-4.

Yang, Bin, Rainer Adelung, Klaus Ludwig, Klaus Bößmann, David H. Pashley, And Matthias Kern. "Effect Of Structural Change Of Collagen Fibrils On The Durability Of Dentin Bonding." *Biomaterials* 26, No. 24 (2005): 5021-5031.